NUCLEAR SPECTROSCOPIC STUDIES WITH LITHIUM-DRIFTED GERMANIUM DETECTORS

A Thesis

Submitted to

the Faculty of Graduate Studies

University of Manitoba

In Partial Fulfillment

of the Requirements for the Degree

DOCTOR OF PHILOSOPHY

by

Robert Allan Brown

April 1968

ABSTRACT

The gamma-ray spectrum of ^{134}Cs has been studied with a 3.5 mm deep by 18 mm diameter Ge(Li) gamma-ray spectrometer. The conversion line spectrum has also been studied with the high resolution $\pi\sqrt{2}$ β-ray spectrometer at C.R.N.L. and the K-conversion coefficients of the transitions measured using a mixed source of ^{134}Cs and ^{137}Cs. Nine transitions were seen in the decay of ^{134}Cs. The present data are consistent with levels in ^{134}Ba at 0(0+), 604.6(2+), 1167.7(2+), 1400.4(4+), 1643.0(3+) and 1969.6 keV (4+). No evidence has been found for previously reported levels at 1570 and 1773 keV.

High resolution Ge(Li) detectors have been used to study the gamma-ray spectrum of 18.0 hr ^{159}Gd. Eighteen transitions were observed, two of which are reported here for the first time. The previously reported complex nature of the 617 keV transition has been examined and high resolution studies revealed a doublet structure with energies 616.5±0.3 and 617.7±0.2 keV and intensities of 2.3±0.6 x 10^{-3}% and 15.0±2.3 x 10^{-3}% per disintegration respectively. Gamma-gamma coincidence experiments were performed with large volume coaxial and thin window planar Ge(Li) detectors, using the related address technique and on-line computers. These experiments have established levels in ^{159}Tb at 58.0, 137.5, 348.1, 363.3, 580.8, 617.7, 674.3 and 854.9 keV. All of the transitions observed in the direct spectrum have been fitted into the level scheme.

The gamma-ray spectrum of ^{177}Yb has also been studied with Ge(Li) detectors. Twenty-two transitions were identified

with the decay of ^{177}Yb, seven of which have not been previously reported. Gamma-gamma coincidence experiments were performed with large volume coaxial detectors using the related address technique. The present data have established levels in ^{177}Lu with energies 121.60, 150.35, 268.73, 288.92, 451.6, 1049.5, 1149.7, 1230.7, 1241.4 and 1336.4 keV. Weak evidence has been presented for a level at 458.1 keV.

ACKNOWLEDGMENTS

The author wishes to express his sincere thanks to the directors of the research - Dr. K.I. Roulston at the University of Manitoba and Dr. G.T. Ewan at C.R.N.L. - for their constant encouragement and advice throughout the course of this work, to Dr. L.G. Elliott, G.C. Hanna and the members of the β-ray spectroscopy group at C.R.N.L. for the kind hospitality that has been accorded him while at Chalk River.

Sincere thanks must also be extended to Drs. G.I. Andersson and J. Sharpey-Schafer for supplying the computer programmes, without which this work could not have been undertaken. Helpful discussions with Dr. W.G. Gelletly are also gratefully acknowledged.

The author is greatly indebted to Mrs. J. Merritt for performing the chemical separations at C.R.N.L.

Invaluable technical assistance was given by Messrs. R.B. Walker, L.V. Smith and W.L. Perry both at C.R.N.L. and on the Deep River golf course.

For her assistance in preparing and typing the original manuscript, the author wishes to express his sincere thanks to Miss Janet Young.

The financial assistance of the National Research Council and the Faculty of Graduate Studies of the University of Manitoba is gratefully acknowledged.

CONTENTS

Chapter V

The Decay of 1.9 hr ^{177}Yb

Chapter VI

The Decay of 18 hr ^{159}Gd

LIST OF FIGURES

CHAPTER I

Semiconductor Detectors

1.1 Introduction:

Over the past few years the field of nuclear physics has witnessed the introduction of many new instrumental and experimental techniques. From the point of view of the nuclear spectroscopist the most important of these has been the development of the semiconductor detector and the subsequent improvements in the associated electronic instrumentation. These detectors have high resolution, a linear response over large energy range, a fast rising pulse from most of them, are quite small and can readily be manufactured for highly specialized geometries. They can be used for studying electrons, protons, alpha-particles, heavy charged particles and gamma-rays.

For several years the only semiconductor detectors available were p-n junction or surface barrier types and these were used mainly for the study of alpha-particles and heavy charged ions. The resolution of these detectors was typically about 15 keV for 5.5 MeV alpha-particles (McKenzie and Ewan 1961). Since the maximum depletion layer in a simple p-n junction type of diode is about 1 mm, they can be used to study protons up to about 12 MeV, deuterons up to about 16 MeV, alpha-particles up to about 48 MeV and oxygen ions up to about 200 MeV. The introduction of the lithium-drifting process in silicon by Pell (Pell 1960) made it possible to produce larger volume detectors, thereby extending the range of energies covered in heavy particle studies and also permitting their use in electron spectroscopy.

These larger volume silicon lithium-drifted detectors, Si(Li), were used to look at gamma-rays as long ago as 1962 by Mann et al (Mann 1962) who reported a resolution of 9.05 keV F.W.H.M. at 662 keV. Their big disadvantage however was the fact that the full-energy peak height was only about 2% that of the Compton edge. The first published results using the lithium drift process in germanium for gamma-ray spectroscopy are those of Freck and Wakefield (Freck 1962) who reported a resolution of about 21 keV at 662 keV, most of this width coming however from amplifier noise. The photoelectric cross section per atom exhibits a Z^5 dependence which makes germanium much more suitable for gamma-ray spectroscopy than silicon. Developments in this field progressed rapidly with reports by Webb and Williams (Webb 1963) and several papers by Tavendale and Ewan (Tavendale and Ewan 1963, Tavendale 1964a, b Ewan 1964a,b).

The development of Ge(Li) detectors to their present sophisticated state has been brought about by the work of many groups, primarily those at the Chalk River Nuclear Laboratories, the Argonne National Laboratory and the Lawrence Radiation Laboratories. The literature contains many review articles about semiconductor detectors and the reader is referred to these articles for details of both operation and fabrication techniques. Since there have been so many articles written about detectors both for gamma-ray and charged particle work, it is not possible to list all of them here. The following list in intended merely as a guide and is by no means complete: Bromley 1961,1962; Dearnaley 1963, 1966, 1967; Ewan 1964a, b, c, 1966a,b, 1968; Fowler 1966, Gibson et al 1965; Goulding 1966; Graham 1965, 1966;

Jungclassen 1965; Heath 1966; Hollander 1966; Malm 1965, 1966; Pehl 1967; Tavendale 1963, 1964 a,b, 1965a,b, 1966. No details of the construction techniques and only a few of the relevant detector characteristics will be given in this thesis.

The purpose of this thesis is to report the results of three different types of gamma-ray experiments using different kinds of Ge(Li) detectors. The experiments involve the direct measurement of gamma-ray spectra with energy and intensity determination, the determination of internal conversion coefficients using a mixed source technique and gamma-gamma coincidence studies. The remainder of this chapter is devoted to a brief description of several types of Ge(Li) detectors, their associated cryostat assembly and electronics.

1.2 Ge(Li) Spectrometers

The lithium drift process was first introduced by Pell (Pell 1960) in order to produce large sensitive volume silicon detectors and was first applied to germanium by Freck and Wakefield (Freck 1962). The process consists of evaporating a layer of lithium onto a p-doped germanium crystal and then diffusing it into the crystal to produce an n^+ layer from 100 to 200 μ deep. An electric field is then applied across the p-n junction such that it is reverse biased. The Li^+ ions, which are donors and migrate easily in germanium, are drifted under the influence of this field so that they almost perfectly compensate the acceptors in the p-type material. Thus "intrinsic" layers are produced by compensation and depths of up to 16 mm have been obtained. Fig. 1-1 shows a schematic diagram of a planar detector.

Fig. 1-1

Schematic diagram of a planar lithium-drifted Ge(Li) detector

LITHIUM-DRIFTED p-i-n JUNCTION SPECTROMETER

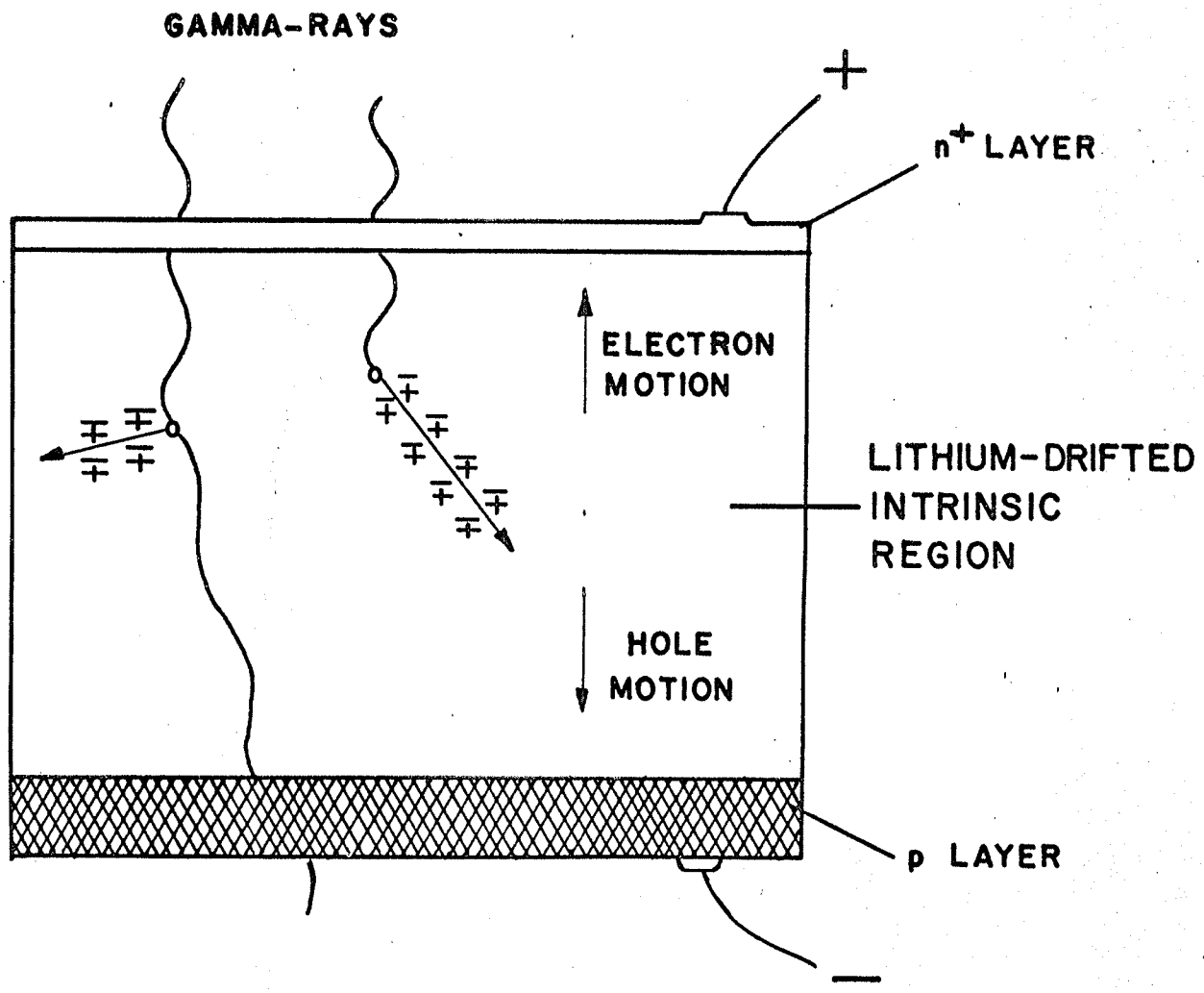

At room temperature the leakage current due to thermal agitation of carriers across the band gap (0.67 ev in germanium) prohibits the use of these drifted crystals as spectrometers. Also, at room temperature, the mobility of Li^+ ions is extremely high and unless crystals are cooled, a loss of compensation is observed. For these reasons, and the fact that liquid nitrogen is readily obtainable, the detectors are operated at liquid nitrogen temperatures (77°K) where leakage currents of 10^{-10} and 10^{-11} amperes are not uncommon.

A gamma-ray can interact with the detector in three ways.

1) Photoelectric Interaction

The gamma-ray interacts with a K-electron ejecting it from the K shell with energy $E_\gamma - E_K$, where E_K is the binding energy of the K-electron. This electron subsequently loses energy by the production of carriers. The x-rays produced by the re-arrangement of the orbital electrons filling the K shell vacancy are also absorbed by the detector, giving a total pulse corresponding to the full energy E_γ.

2) Compton Interaction

The incoming gamma-ray undergoes a Compton collision losing only part of its energy. The scattered gamma-ray may subsequently escape from the crystal or it may interact with it. The Compton scattered electron again loses its energy by carrier production.

3) Pair Production

In the vicinity of a nucleus, a gamma-ray with energy greater than 1022 keV may annihilate to produce an electron-positron pair. The electron loses energy by creation of more electron

hole pairs. The positron also produces electron-hole pairs until it comes to rest, after which it annihilates with another electron producing two 511 keV gamma-rays. If both quanta escape a "double escape" peak is observed with energy (E_γ - 1022)keV while if one escapes a "single escape" peak with energy (E_γ - 511)keV is observed

The relative probabilities of these processes are shown in Fig. 1-2 which shows the variation of photoelectric, Compton and pair production cross sections with energy. The values of the cross sections shown are from the tables by Storm et al (Storm 1958). The solid lines represent the values for germanium while the dashed lines are the corresponding curves for silicon. The photoelectric cross section varies roughly as Z^5 and for germanium is about 40 times that of silicon at 500 keV. The Compton scattering cross section, as given by Klein and Nishina, varies directly as Z so that the ratio of $\sigma_{photoelectric}/\ \sigma_{Compton}$ varies as Z^4 again making germanium preferable to silicon; the fraction being $(^{32}/_{14})^4 \approx 27$. This factor however is derived from consideration of single-absorption processes only. The probability of multiple processes (reabsorption of Compton scattered gamma-rays) makes this factor even larger. For a $30cm^3$ coaxial detector, approximately 80% of the full energy pulses for a 1 MeV gamma-ray come from multiple processes (Malm 1966). Above 1.5 MeV the pair production cross section is greater than the photoelectric cross section and increases with increasing energy. The pair production cross section varies as Z^2 again indicating the preference for germanium over silicon for gamma-ray spectroscopy.

The energy resolution of a Ge(Li) detector system depends upon several factors the most important of which are

Fig. 1-2

Photoelectric, Compton and pair production absorption cross sections for germanium and silicon.

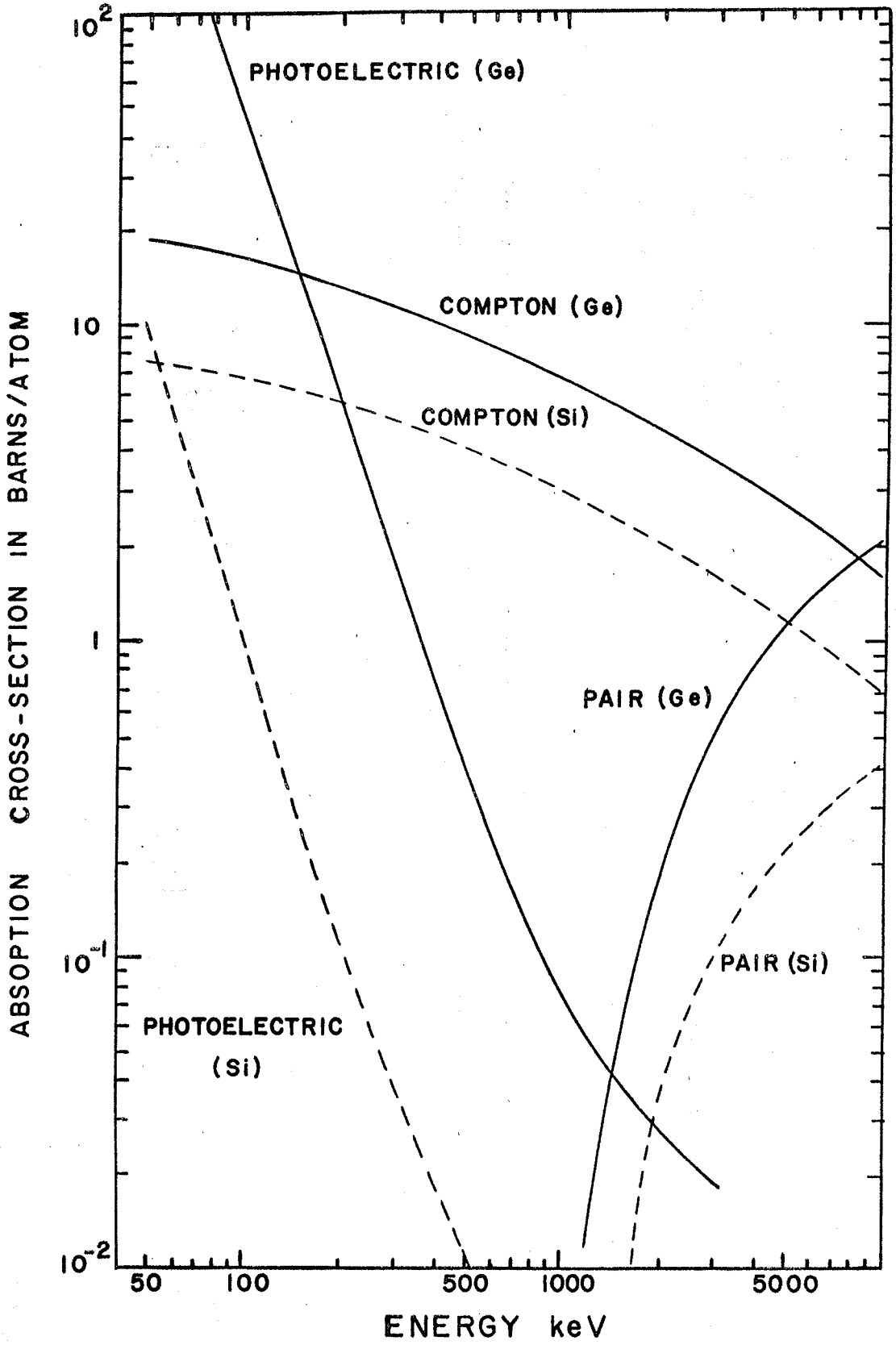
PHOTOELECTRIC (Ge)
COMPTON (Ge)
COMPTON (Si)
PAIR (Ge)
PAIR (Si)
PHOTOELECTRIC
(Si)
ABSOPTION CROSS-SECTION IN BARNS/ATOM
ENERGY keV
10^2
10
1
10^{-1}
10^{-2}
50
100
500
1000
5000

preamplifier and amplifier noise (which will be discussed in section 1.5), detector leakage current noise, collection efficiency and statistical fluctuations in the production and collection of electron-hole pairs. The last of these provides the fundamental limitation to the detector resolution.

If all of the energy lost by the gamma-ray went into the production of electron-hole pairs there would be no fluctuation at all in the number produced. However if the probability of producing electron-hole pairs was small in comparison to the other methods of energy loss eg. thermal heating of the lattice, optical phonon collisions etc. then a Poisson distribution would be expected. The R.M.S. fluctuation would then be

$$\langle n \rangle = \sqrt{N} = \sqrt{\frac{E}{\xi}}$$

where E = energy deposited in the detector,

ξ = average energy required to produce an electron-hole pair, and the F.W.H.M. = $2.35\langle n \rangle$. In the case of semiconductors the observed fluctuations lie between these extremes. The observed root-mean-square deviation is expressed as $\sqrt{F \times N}$ where F is known as the Fano factor. Recent measurements by Mann (Mann 1966) and Heath (Heath 1966) have shown that the Fano factor for germanium is about 0.16. This Fano factor implies that the optimum resolution to be expected at 1MeV is about 1.6 keV.

Apart from the electronic factors which affect the resolution, there are properties of the detectors themselves such as leakage currents, trapping effects and charge collection efficiency. These effects are more apparent for high energy gamma-rays where the fractional energy resolution is better than at low energies. Trapping effects show up as a tail on the low energy

side of the full-energy peak. Charge collection efficiency depends upon the reverse bias across the detector and trapping is reduced by increasing the bias (Tavendale 1965a). However, if the bias is increased too far, the leakage current can become too high and the line width is dominated by that contribution.

The preceding is a very brief review of some of the characteristics common to all types of Ge(Li) detectors. For more details the reader is referred to the references listed in sec. 1.1.

1.3 Types of Ge(Li) Detectors

Planar Detectors

The first type of Ge(Li) detector produced was the planar detector which has been described briefly in sec. 1.2. These detectors originally had depletion depths of typically 2 or 3 mm, low photopeak efficiency and large Compton distributions. Since the Compton distribution serves no useful purpose in gamma-ray spectroscopic measurements, it is desirable to reduce it as much as possible relative to the photopeak height. This can be done by increasing the size of the depletion region and hence the active volume. The photoelectric absorption is increased because of the increased depth, and the probability of multiple interactions is also increased thereby reducing the size of the Compton distribution. Fig. 1-3 compares the intrinsic full energy peak efficiency of several Ge(Li) detectors and also shows the corresponding curve for a 3" x 3" NaI(Tl) detector. Some of the curves shown are for the coaxial type of detectors discussed in the next section.

The planar detectors mentioned sofar have an n^+ layer whose thickness can be anything from about 100 μ upwards. This dead layer presents serious attentuation problems when dealing with

Fig. 1-3

Comparison of efficiency curves for different sizes of Ge(Li) detectors.

A.E.C.L. Ref. # A-3210-G

GERMANIUM LITHIUM DRIFT p-i-n DETECTOR EFFICIENCIES

EFFICIENCIES FROM ⊙ CALIBRATED ^{60}Co SOURCE
× ^{226}Ra SOURCE
\+ ^{207}Bi SOURCE
▲ ^{226}Ra SOURCE (DOUBLE ESCAPE)

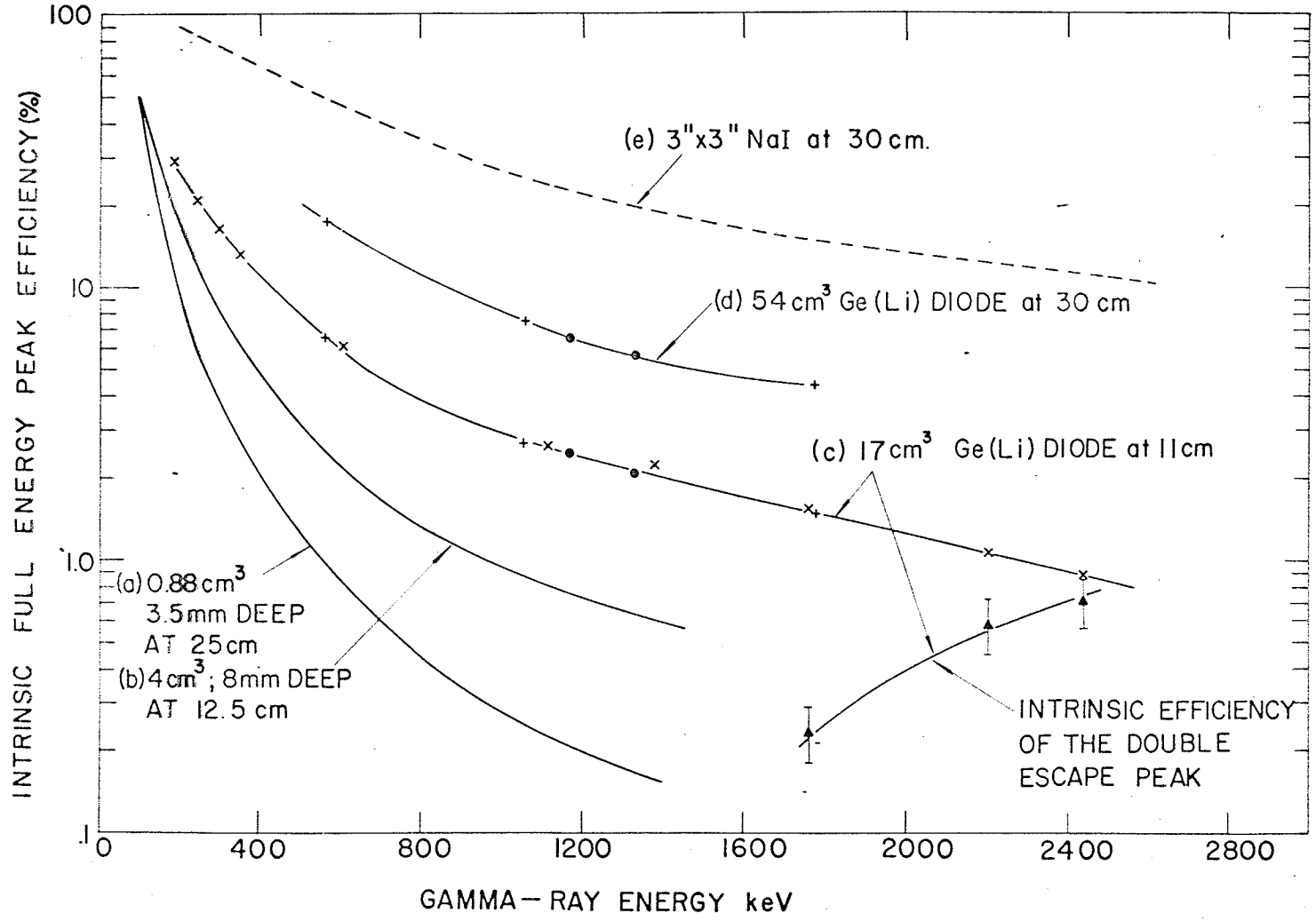

low energy gamma-rays. In order to remove this dead layer, the lithium can be drifted right through the p-type material and a surface barrier or diffused p^+ layer can be formed at the back surface. Window thicknesses of about 0.5 μ have been reported by Pehl et al (Pehl 1966).

The available germanium crystals suitable for making gamma-ray detectors vary in quality. Some of the better crystals have been drifted at C.R.N.L. up to depths of 11mm. This means that the finished detectors have active volumes of up to 9 cm^3 (Malm 1965) when prepared from slices cut from the ingot perpendicular to the direction of growth and drifted from one of these cut faces towards the other. It was because of this restriction in the volume that the "coaxial" detector was developed.

Coaxial Detectors

The first stage in the development of large volume Ge(Li) detectors was the so-called "single open-ended coaxial" detector (Tavendale 1965b). This detector was made by evaporating lithium onto all but one side of the germanium ingot and diffusing the lithium in to form an n^+ region on all five sides. The p contact was then made to the centre of the uncoated side and the drifting was performed in a similar manner to that used for planar detectors.

A detailed study of the shape of the depletion region in these detectors has been made by Malm and Fowler (Malm 1965). Several diodes of this kind were fabricated at C.R.N.L. the largest having an active volume of 54 cm^3. Malm (Malm 1966) has studied the shape of the depletion region of this detector by collimated gamma-ray beam scans and Fig. 1-4 shows the results of this study. The core tapering is due to the significant IR voltage drop along the length of the undrifted p-type core during

Fig. 1-4

Curves resulting from scanning a large single open-ended coaxial diode with a beam of collimated 320 keV gamma-rays at the positions shown. An approximate cross section through the center of the diode derived from the scans is shown.

A.E.C.L. Ref. # A-3209-F

GERMANIUM LITHIUM – DRIFT p-i-n DETECTOR No GLCIR

COAXIAL 54 cm^3 VOL

COLLIMATED γ – RAY BEAM SCANS

USING ^{51}Cr (320 keV) SOURCE

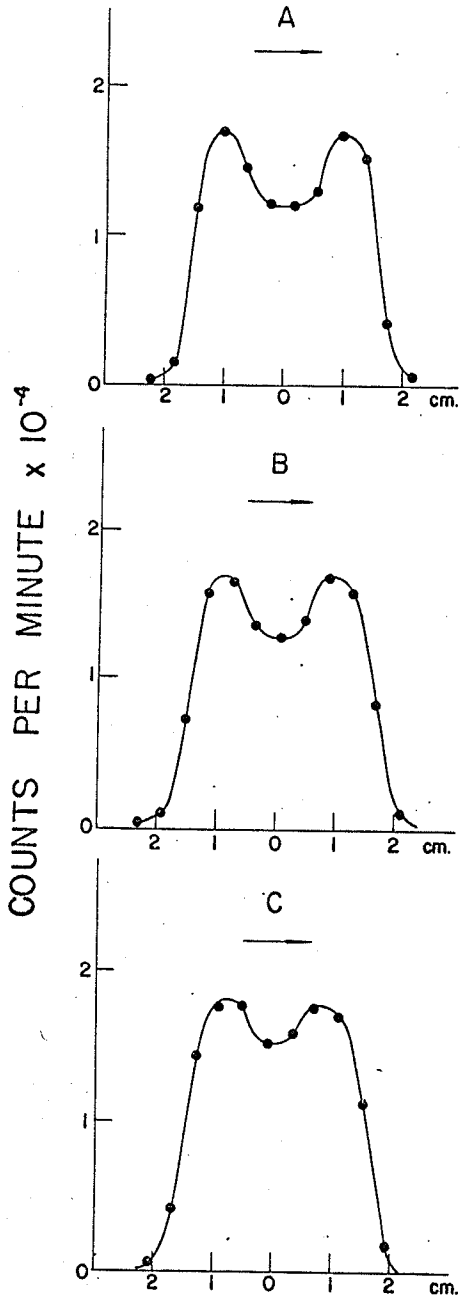

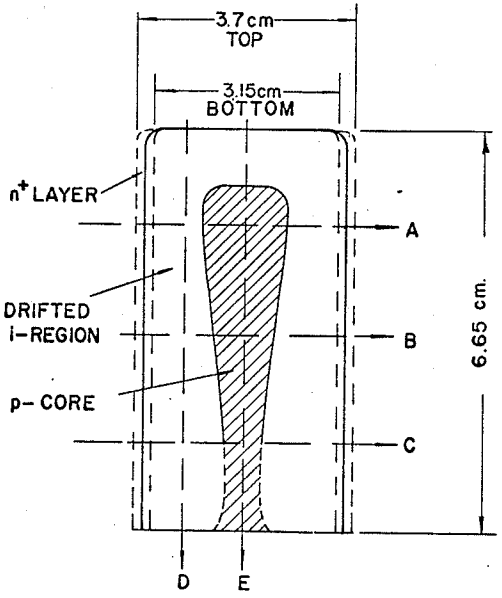

APPROXIMATE CROSS-SECTION THROUGH CENTRE

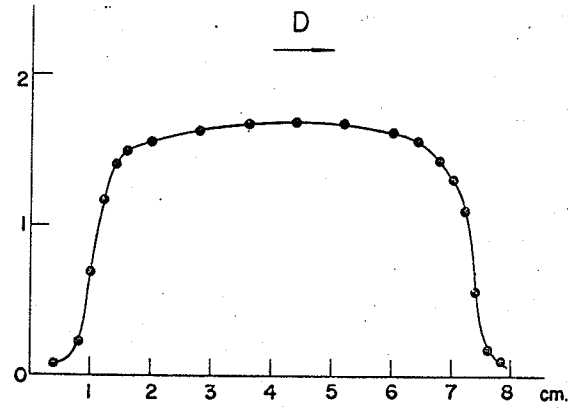

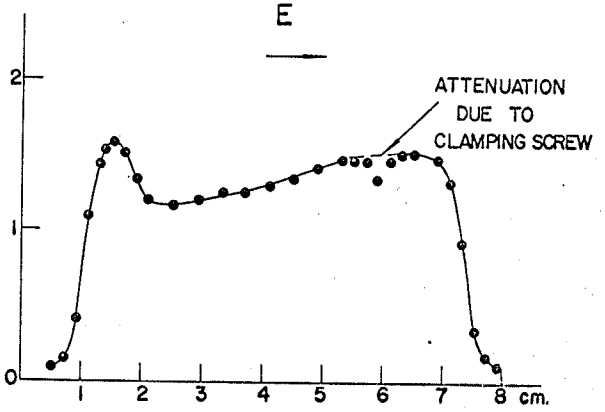

the high power drift. As the drift proceeds reducing the area of the core, the effect becomes more and more pronounced. This non-uniform shape of the core presents no great problem when only direct gamma-ray spectra are to be investigated but it does give rise to serious timing problems when coincidence experiments are performed. The timing characteristics of Ge(Li) detectors will be discussed in Chap. IV.

The next stage in the fabrication of large volume detectors was the "double open-ended coaxial" and the cylindrical "true coaxial" detector. These detectors are produced by evaporating lithium onto the outside surface of the ingot and diffusing as before. The p contacts are then made to the centre of both ends and the lithium is drifted in radially. Detectors produced in this manner have only a slight variation in width of the inactive core (Malm 1966), probably due to small differences in the p-type impurity concentration through the crystal or to small temperature differences during the drift. The timing characteristics of these detectors are again discussed in Chap. IV.

1.4 Detector Cryostat

Each company which manufactures Ge(Li) detectors has its own design of cryostat and its own type of pumping system. Since the detectors used for the experiments at C.R.N.L. were manufactured there it is worthwhile describing a typical detector mounting arrangement used for these experiments. There are slight variations with each detector but the following description might be described as the basic arrangement. All but one of the detectors used a "chicken feeder" assembly, the exception being GLC6X which used a "dip-stick" arrangement (Chasman 1965). All the detectors

used at C.R.N.L. were unencapsulated. The vacuum in each cryostat was maintained with a 1 ℓ/sec vac-ion pump. The power supply for these pumps consisted of series of batteries, giving the necessary 3 kV, which facilitated movement of the entire cryostat assembly.

Fig. 1.5 shows a photograph of the detector mount on the "chicken-feeder" assembly. The long pipe in the upper right hand corner encloses the vacuum which in turn surrounds a hollow cold finger containing liquid nitrogen. The length of this cold finger is dictated by the geometry necessary for the experiment being performed. The assembly shown here was designed to fit into an anti-Compton shield and was approximately 18" long. The copper box which sits vertically above the cold finger in the center of the photograph contains the main section of the preamplifier. The high voltage filter box is an RC integrating circuit, with a 10 sec time constant, which provides a slow build-up of the bias in order to safeguard the field effect transistors (henceforth abbreviated to F.E.T.'s).

The germanium diode sits in the open space in the lower left hand corner of the photograph. The front and sides of the detector are shielded with aluminum foil (not shown on the sides in the photograph) in order to prevent condensation on the detector surface of any oil which might enter during the initial pumping down of the system. The detector is D.C. coupled to the input of the preamplifier and the signal is taken from the detector through a contact in the lucite disc. Since the aluminum mount, holding the detector, is floated at high voltage, it is insulated from the cold finger by a boron nitride disc. This acts as a good thermal conductor and a good electrical insulator.

Fig. 1-5

Photograph of the cryostat assembly used with the Ge(Li) detectors at C.R.N.L.

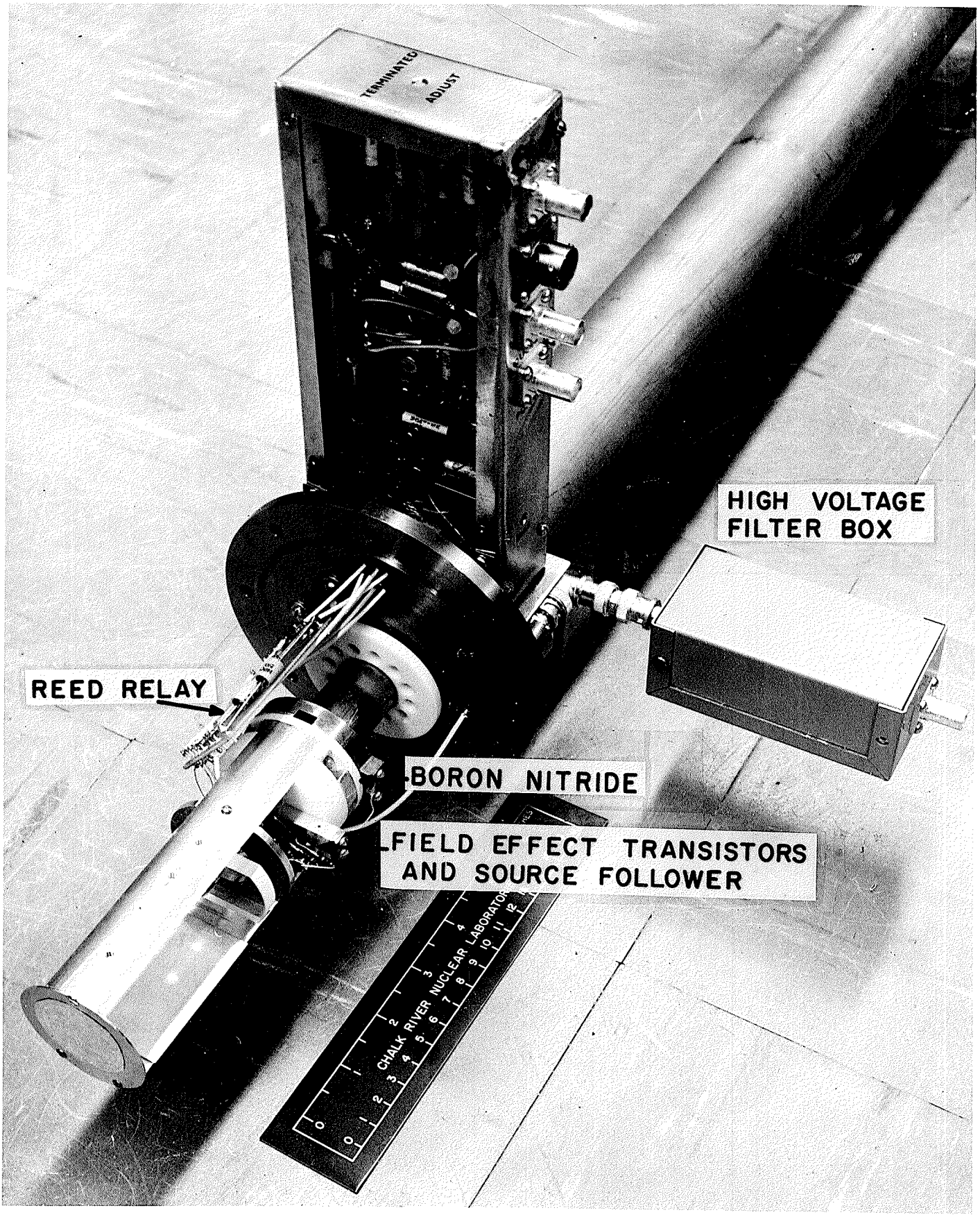
TERMINATED
ADJUST
HIGH VOLTAGE
FILTER BOX
REED RELAY
BORON NITRIDE
FIELD EFFECT TRANSISTORS
AND SOURCE FOLLOWER
CHALK RIVER NUCLEAR LABORATORIES

The F.E.T.'s are mounted on a copper block which is attached to the cold finger by a teflon disc. The optimum operating temperature for the F.E.T.'s is about 120° to 130°K. This temperature is maintained by connecting the copper block to the cold finger by a thin piece of copper wire, so chosen that the power dissipated by the F.E.T.'s and the heat conduction along the wire give the correct operating temperature. The board mounted above the cold finger has on it the feedback resistor and capacitor, electrical connections from the main preamplifier section to the F.E.T.'s and a reed relay. This reed relay can be closed by a magnet held outside the outer aluminum cap. It is used to ground the inputs of the F.E.T.'s in order to prevent damage while the detector is being "cleaned up" (Tavendale 1964a).

1.5 Low Noise Preamplifier

The statistical factors discussed in sec 1.2 represent the fundamental limit of the resolution obtainable with Ge(Li) detectors. There are however several sources of noise present which prevent the reaching of this resolution. Some of these are described below.

1) Detector leakage current noise is assumed to be pure shot noise which arises from the thermal generation of electron-hole pairs in the depletion layer.
2) Detector series resistance noise is due to resistance in the connections to the sensitive volume of the detector.
3) The input current noise is due to fluctuations in the input current to the first amplifying device in the system.
4) The parallel resistance noise arises from any resistors

shunting the input circuit eg. detector load, input biasing resistor in the first stage and any resistor across the feed back capacitor in the charge sensitive preamplifier.

5) The noise developed in the first amplifying device produces a voltage noise source which can be represented by Johnson noise in a resistor.

6) Surface leakage currents at the periphery of the junction produce severe low frequency noise in many detectors.

7) "Flicker noise" caused by fluctuations in the plate current of a vacuum tube or other amplifying device. This type of noise is dominantly in the low frequency part of the spectrum.

A study of these noise sources and the various types of pulse shaping networks necessary to give a good signal to noise ratio has been made by Goulding (Goulding 1965). Recently Heath et al (Heath 1966) have published a paper on the instrumental requirements for gamma-ray spectroscopy, and Blankenship and Nowlin (Blankenship 1966) have produced some new concepts in nuclear pulse amplifier design.

The charge pulse produced in the detector is amplified and fed into a pulse shaper which rejects as much noise while retaining as much signal as possible. A charge sensitive configuration of the preamplifier is used since to first approximation it gives an output signal size which is independent of the detector and stray capacities which appear from its input to ground. The early preamplifiers used for this type of work (Ewan 1964a) used two 7788 tubes in cascode followed by a 7308 tube as a long-tailed

pair. This preamplifier gave a noise contribution of 1.7 keV with a slope-input capacitance curve of about 0.04 keV/pf.

The recent improvements in field effect transistors have allowed these devices to replace vacuum tubes. A low noise charge sensitive preamplifier using paralleled F.E.T.'s has been designed by Smith and Cline (Smith 1966). Their investigations showed that the noise-capacity slope was proportional to $\sqrt{\frac{T}{\tau_o\, n\, g_m}}$ where

T = absolute temperature, n = number of paralleled F.E.T.'s,
τ_o = time constant of equal integrating and differentiating network and
g_m = transconductance of each F.E.T. Thus by using four paralleled F.E.T.'s and by cooling to 140°K (this was found to be the optimum operating temperature) they were able to produce a slope of 0.017 keV/pf compared with 0.030 keV/pf for a single F.E.T. The noise with zero detector capacitance however was found to vary as $\sqrt{n}$ so that the initial noise increases as the number of F.E.T.'s increases. The number of F.E.T.'s used in the input stage of the preamplifier is therefore governed by the capacitance of the detector being used. With the F.E.T.'s cooled to 140°K Smith and Cline were able to get 0.36 keV(Ge) + 0.030 keV/pf with a single F.E.T. and 0.62 keV(Ge) + 0.017 keV/pf with four paralleled F.E.T.'s.

If the detector is DC coupled to the preamplifier an improvement in resolution results. This is due to the removal of stray capacitance caused by the distributed capacitance of the load resistor and coupling capacitor to ground, and the division of the input signal between the coupling capacitor and the input capacitance of the F.E.T.'s.

The preamplifier circuit used with the detectors at C.R.N.L. for the experiments reported in this thesis is shown in Fig. 1-5. The number of F.E.T.'s in the input stage depends

Fig. 1-6

Circuit diagram for the low noise preamplifier.

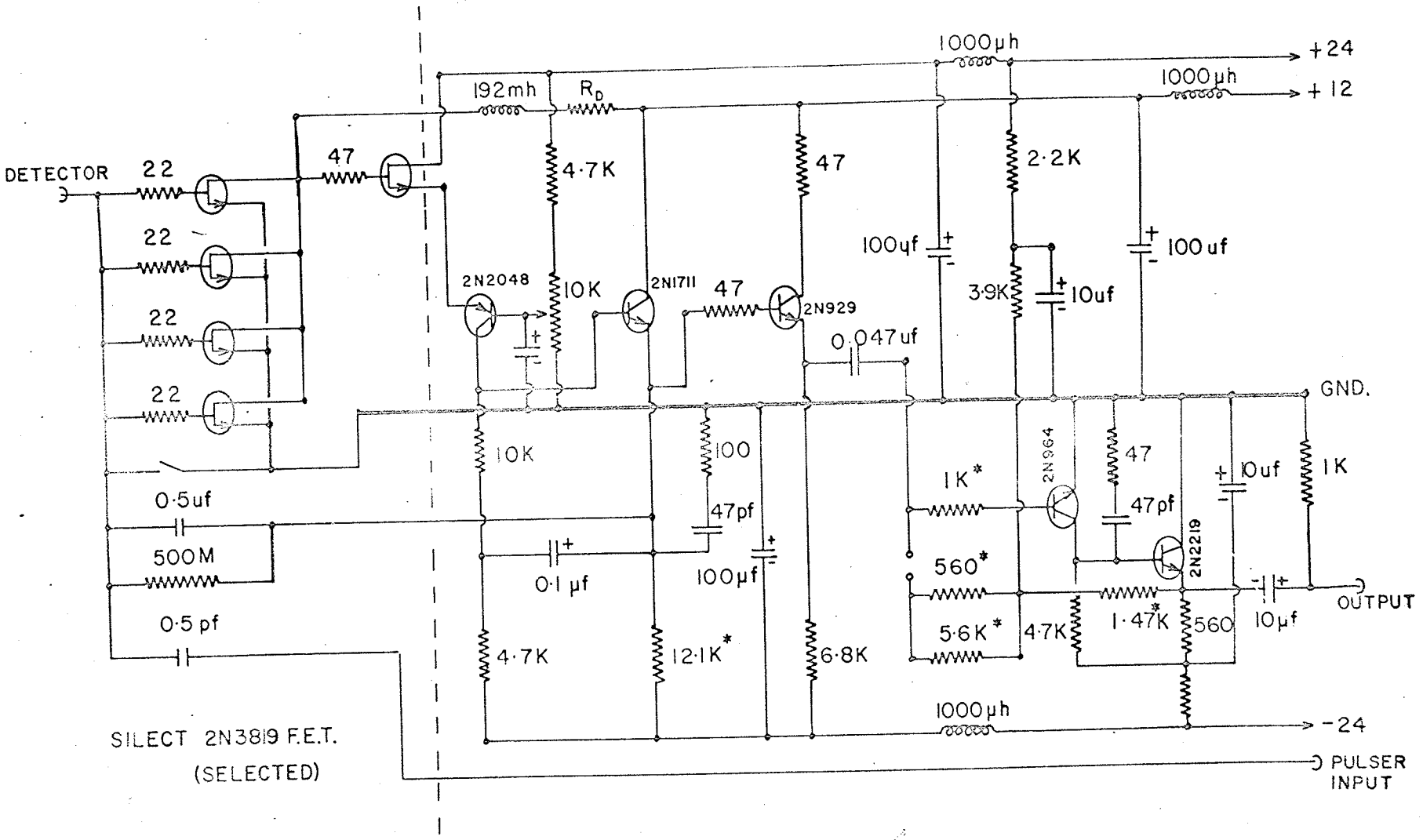
DETECTOR
22
22
22
22
47
192mh
R_D
4·7K
2N2048
10K
2N1711
47
2N929
47
0·047uf
1000µh
+24
1000µh
+12
100µf
2·2K
3·9K
10uf
100 uf
GND.
10K
100
47pf
100µf
0·1 µf
0·5uf
500M
0·5 pf
4·7K
12·1K*
6·8K
1K*
560*
5·6K*
4·7K
2N964
47
47pf
2N2219
1·47K*
560
10uf
1K
10µf
OUTPUT
1000µh
-24
PULSER INPUT
SILECT 2N3819 F.E.T.
(SELECTED)

upon the capacitance of the detector being used. Both of the large volume coaxial detectors had a capacitance of about 40 to 50 pf and so four paralleled F.E.T.'s were used, whereas the high resolution detector GA6 used only one F.E.T. The circuit is based on that of Smith and Cline (Smith 1966), having a grounded source F.E.T. amplifier and source follower as the first stage followed by a grounded base amplifier and emitter follower. The source follower (F.E.T. equivalent of emitter follower) allows the front end of the preamplifier to be separated from the main section by several feet without deterioration of resolution. The last two transistors constitute a driver stage which is capable of transmitting the preamplifier signal over large distances to the main amplifier.

CHAPTER II

Direct Gamma-Ray Spectra

2.1 Gamma-Ray Peak Shape

In the formulation of an energy level scheme two of the most important gamma-ray properties which can be measured with germanium detectors are the energies and relative intensities of the transitions. Both of these quantities are directly comparable with nuclear theory and for this reason their precise determination is extremely important. However in order to measure the relative intensities to any degreee of accuracy, it is necessary to establish some consistent criteria for the measurement of the photopeak area.

The shape of the photoelectric peak in a Ge(Li) detector is roughly Gaussian with a low energy exponential tail due to incomplete charge collection within the detector. The charge collection efficiency can be improved by increasing the detector bias. This however can only be done within limits since it causes a rise in detector leakage current which in turn produces a deterioration of the resolution. Another factor which affects the peak shape is the counting rate. This however is due to the electronics and can be reduced by careful design of the preamplifier and amplifier system (Goulding 1967, Blankenship 1966).

In order to calculate the intensity of a gamma-ray, the area of the photopeak must be determined. An absolute area need not be defined as long as some consistent set of rules is used to define the area. If the photopeak was sitting on a level background, there would be no difficulty in defining a uniform peak area. However this is not the situation with the photopeaks in Ge(Li) spectra. The

region between the Compton edge and the photopeak tends to be filled in by partial re-absorption of Compton scattered gamma-rays so that the background on the low energy side of the photopeak may be an order of magnitude higher than on the high energy side. The problem then arises as to what background should be used.

In a typical gamma-ray spectrum a variety of intensities appears ranging from very weak to extremely strong. For a peak sitting on a large Compton distribution, the commonly accepted background level is a smooth line joining the Compton distribution on the low energy side of the photopeak with that on the high energy side. Clearly, if one then wishes to measure the intensity of this transition relative to that of a much stronger transition which is not sitting on a large Compton distribution, some criterion must be adopted for drawing a background under this peak which will reproduce the same area had this second peak been superimposed upon a large Compton distribution.

This problem has been studied in detail by Haverfield (Haverfield 1966). He tried several different shapes for the background and concluded that for best reproducibility, the following criterion should be used. If the photopeak region is drawn up on linear graph paper, then the background line is obtained by joining the point of maximum radius of curvature on the low energy side to the base on the high energy side of the peak. By then including only those points greater than 1% of the peak height, Haverfield was able to reproduce to within 1 to 1½% the area of this same peak when it was superimposed on a large Compton distribution.

For the gamma-ray intensities calculated in this thesis, the above criterion was used. Since only relative intensities were of interest, it makes little difference whether the 1%, 2% or

5% level is chosen as long as that same value is used for determining the area of all the peaks in the given spectrum.

Fig. 2-1 illustrates another effect which can change the shape of the photopeak, this one however being observed only with "double open-ended coaxial" detectors. The lower portion of Fig. 2-1 shows the gamma-ray spectrum of an ^{241}Am source, positioned at the side of the detector as illustrated in the lower insert. In this spectrum the usual Gaussian shape with low energy tail is seen along with a flat plateau arising from 0° to 180° Compton scattered gamma-rays. When the source is placed directly in front of the detector, as shown in the insert in the upper half of the figure, a distinct shoulder appears on the low energy side of the peak. This can be explained by Compton scattering of gamma-rays from the inactive core into the active volume of the detector. For an initial photon energy of 60 keV, the energy of a gamma-ray Compton scattered at 90° to the incident direction is 53 keV. Since the "half-distance" (the amount of material necessary to reduce the incident flux by one half) in germanium for 60 keV gamma-rays is about 650μ, the predominant angles of scattering from the inactive core are in the forward direction. Scattering in this region would therefore produce a shoulder on the low energy side of the photopeak of up to 7 or 8 keV. This is consistent with the data shown in Fig. 2-1. When the source was moved further back from the detector, the size of the shoulder decreased in accordance with the decrease in solid angle subtended by the inactive core.

Fig. 2-1

Spectra showing scattering of low energy gamma-rays from the inactive core in a double open-ended coaxial detector.

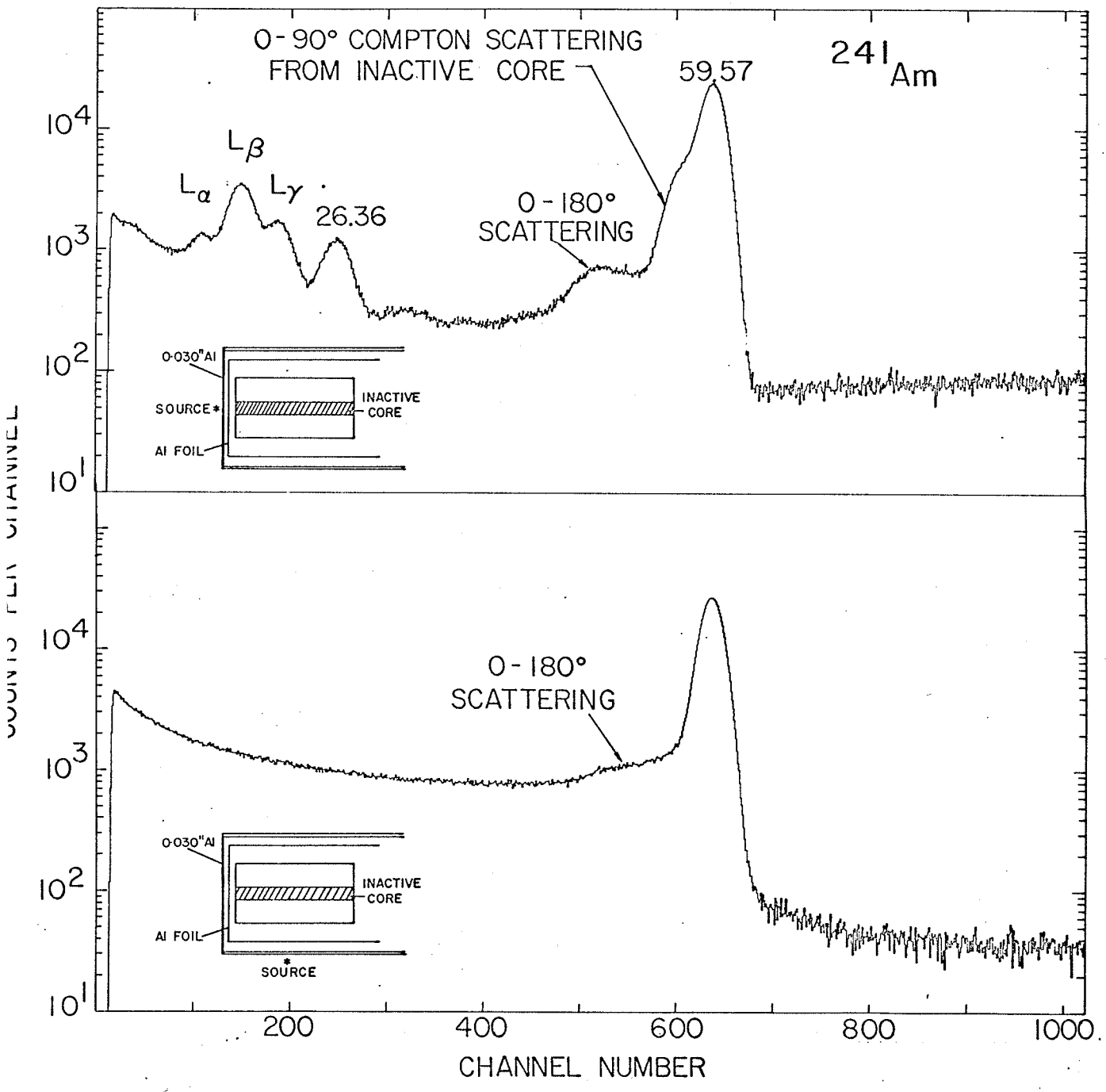
0-90° COMPTON SCATTERING
FROM INACTIVE CORE
59.57
241Am
Lβ
Lα
Lγ
26.36
0-180°
SCATTERING
0·030"Al
SOURCE*
INACTIVE
CORE
Al FOIL
0-180°
SCATTERING
0·030"Al
INACTIVE
CORE
Al FOIL
SOURCE
10⁴
10³
10²
10¹
200
400
600
800
1000
CHANNEL NUMBER

2.2 Efficiency Calibration

In order to calculate the relative intensities of gamma-rays a relative photopeak efficiency curve must be obtained for the detector assembly used. The intrinsic efficiency of a detector is defined as that fraction of gamma-rays striking the detector which are detected in the pulse height spectrum. To calculate the intrinsic photopeak efficiency the ratio of the number of events under the photopeak to the total area of the pulse height spectrum must also be determined. The intrinsic photopeak efficiency is then the product of this photofraction and the intrinsic efficiency.

Theoretical calculations of these two functions have been made for germanium, (Wanio 1965, Castro Faria 1966) but only for a few specialized detector shapes. The germanium ingots used for detector manufacturing come from several sources and the shape of the ingots varies greatly from one manufacturer to the next. In most cases it is therefore necessary to use some other and better method to determine the efficiency curve.

The method used in these experiments involved the use of sources with more than one gamma-ray, the relative intensities of which were accurately known. The sources used for this depended upon the energy region of interest. From about 100 to 2000 keV these were ^{226}Ra and ^{207}Bi since the intensities of the strong transitions in these isotopes are known to about 10%. In order to get more points on the curve a set of eight commercially available (I.A.E.A.) standard sources was used. These were ^{241}Am, ^{57}Co, ^{54}Mn, ^{203}Hg, ^{22}Na, ^{137}Cs, ^{60}Co, and ^{88}Y, the absolute source strengths of which were known to within 1 or 2%. This also permitted the absolute efficiency curve to be calculated for the particular detector assembly

and source position used.

The physical construction of the IAEA* standards consisted of radioactive material sandwiched between two thin polyethylene discs. In some cases the position of the active material could not been seen, so an autoradiograph was made. This enabled accurate positioning of the sources in front of the detector for the efficiency calibration.

Figs. 2-2, 2-3, 2-4, and 2-5 show the photopeak efficiency curves for two of the detectors used in this work (G9C2 and GA6). Fig. 2-2 shows the curve for the 5.0 mm planar detector GA6. The ordinate of the graph is the relative efficiency multiplied by the square of the gamma-ray energy. Theoretical calculations for small volume detectors (Wanio 1965) indicate that the efficiency curve should follow roughly an $E_\gamma^{-2.5}$ dependency between about 100 and 500 keV and roughly $E_\gamma^{-1.5}$ between 500 keV and 3 MeV. Multiplication by an E_γ^2 factor provides a convenient scale and permits greater accuracy in curve reading than the log-log plot used by some groups.

For larger volume detectors, multiple processes increase the photopeak efficiency giving a different energy dependence to the efficiency curve. Fig. 2-3 shows the efficiency curve for G9C2 (44 cm^3 coaxial detector) and as can be seen the region from 500 to 1800 keV follows roughly a linear energy relationship.

With the exception of the special thin-window detectors (sec. 1.3), the efficiency of a planar detector drops off sharply for gamma-ray energies less than 100 keV due to absorption in the n^+ dead layer. Fig. 2-4 shows the efficiency curve obtained for GA6 in this region using ^{203}Hg, ^{188}Re, ^{57}Co and ^{160}Tb sources.

---

* International Atomic Energy Agency Kartner Ring II

A-1010 Vienna

Fig. 2-2

Relative photopeak efficiency curvefor planar detector GA6 covering the range from 200keV to 1800keV.

3374-G

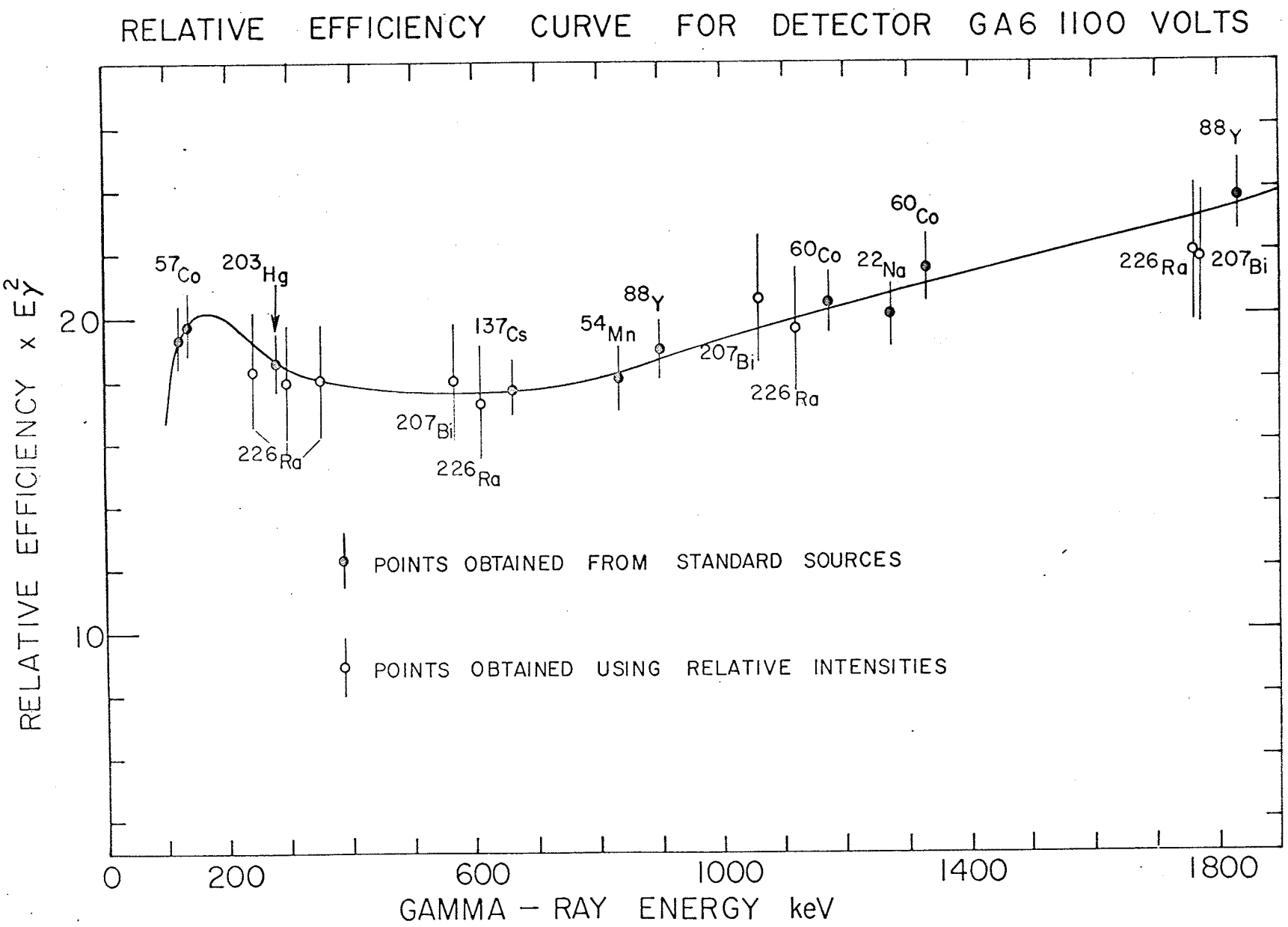
RELATIVE EFFICIENCY CURVE FOR DETECTOR GA6 1100 VOLTS
RELATIVE EFFICIENCY x Eγ²
20
10
0
200
600
1000
1400
1800
GAMMA – RAY ENERGY keV
57Co
203Hg
226Ra
207Bi
137Cs
226Ra
54Mn
88Y
207Bi
60Co
226Ra
60Co
22Na
226Ra
207Bi
88Y
POINTS OBTAINED FROM STANDARD SOURCES
POINTS OBTAINED USING RELATIVE INTENSITIES

Fig. 2-3

Relative photopeak efficiency curve for coaxial detector G9C2 covering the energy range from 200keV to 1800keV.

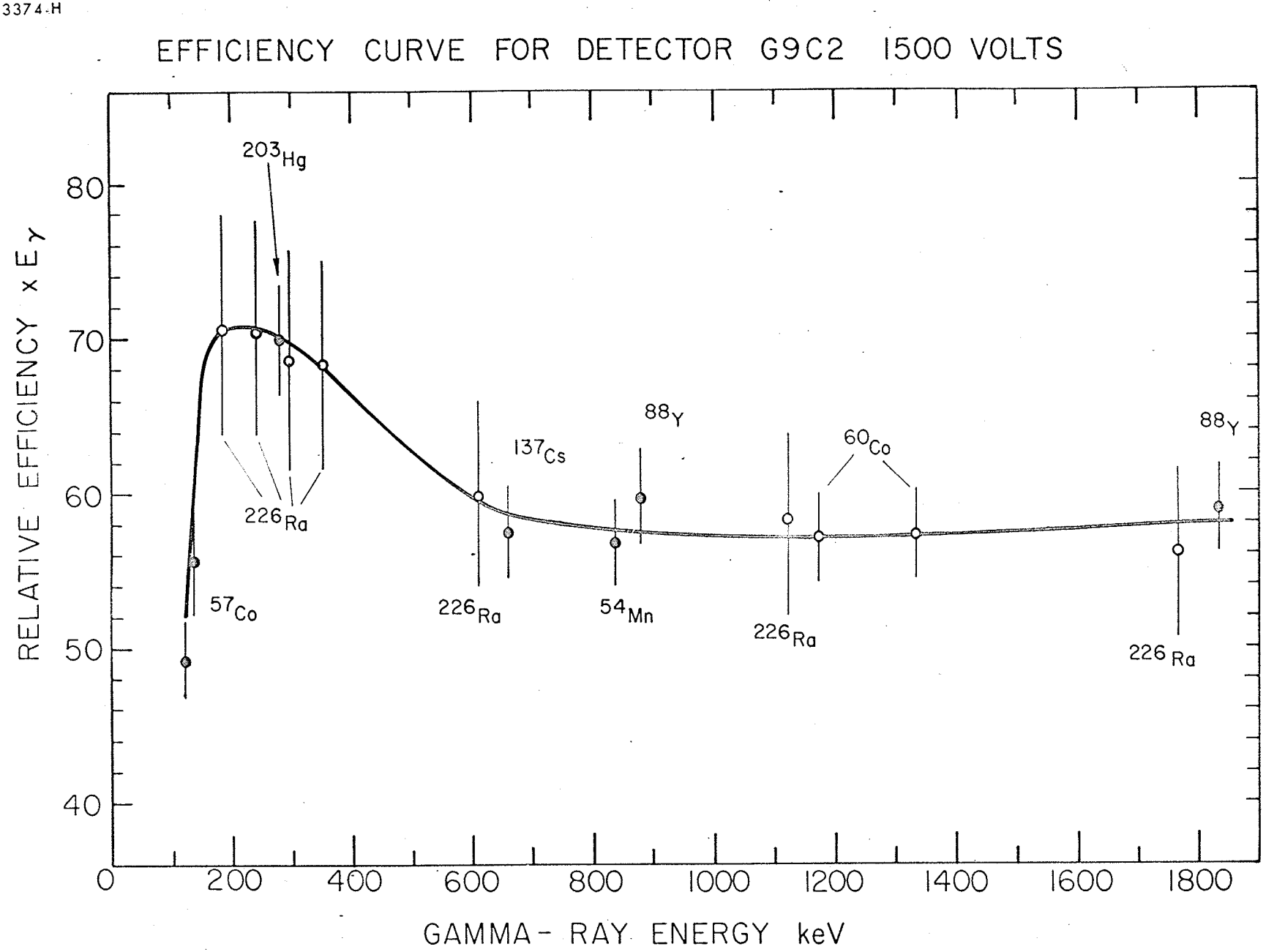
EFFICIENCY CURVE FOR DETECTOR G9C2 1500 VOLTS
RELATIVE EFFICIENCY x E_γ
GAMMA - RAY ENERGY keV
80
70
60
50
40
0
200
400
600
800
1000
1200
1400
1600
1800
^{203}Hg
^{226}Ra
^{57}Co
^{137}Cs
^{226}Ra
^{88}Y
^{54}Mn
^{60}Co
^{226}Ra
^{88}Y
^{226}Ra

TABLE 2 - I

Relative Intensity Standards used for region below 300 keV.

Isotope	Photon Energy (keV)	Relative Intensity
^{241}Am	59.543	100
	26.35	7.0
^{57}Co	136.3	13
	122.0	100
	14.4	11
^{188}Re	155.0	100
	71.4 Os K_β	6.6
	63.0 Os K_α	24.2
^{203}Hg	279.2	100
	82.6 Tl K_β	3.44
	72.9 Tl K_α	11.9
^{160}Tb	86.8	100
	51.1 Dy K_β	28.8
	46.0 Dy K_α	116

Table 2-I lists the relative intensities of the x-rays and gamma-rays as given by Haverfield (Haverfield 1966) that were used in this region. Also shown in Fig. 2-4 are the photoelectric cross section for germanium, the total absorption cross section for 0.1 cm Al and 10 mg/cm^2 Au and for a 0.7 mm layer of germanium. Detector No. GA6 was originally an encapsulated R.C.A. detector, the encapsulation of which was subsequently removed. When this detector was manufactured, it was common practise to evaporate a thin layer of gold onto the surface to provide good electrical contact. For this reason a correction has been applied for the absorption in the gold layer. The Al absorption occurs in the front face of the cryostat. The solid line drawn through the points in Fig. 2-4 is a suitably normalized combination of the photoelectric cross section, Au and Al absorption curves along with the absorption curve for a 0.7 mm layer of germanium. Several different thicknesses were tried for this last curve with 0.7 mm giving the best fit.

Fig. 2-5 shows the efficiency curve obtained for detector No. G9C2 for the region below 300 keV. Since this is a double open-ended coaxial detector, the dramatic drop off with efficiency below about 90 keV is surprising. The steepness of the initial drop off indicates that there is a dead layer of germanium about 0.7 or 0.8 mm deep. If this were the case however, the x-rays of ^{160}Tb and the 26.35 keV gamma-ray in ^{241}Am would not be seen with the experimentally observed intensity. The cause of this peculiar curve below 90 keV is not understood at the present time. It could be due to a very uneven core or a mesa effect on the front surface (from the many etchings the detector has had) giving rise to a poor

Fig. 2-4

Relative photpeak efficiency curve for detector GA6 below 300keV. Also shown are the photoelectric cross section for germanium and absorption cross sections for 0.1cm. Al and10mg/cm^2 Au.

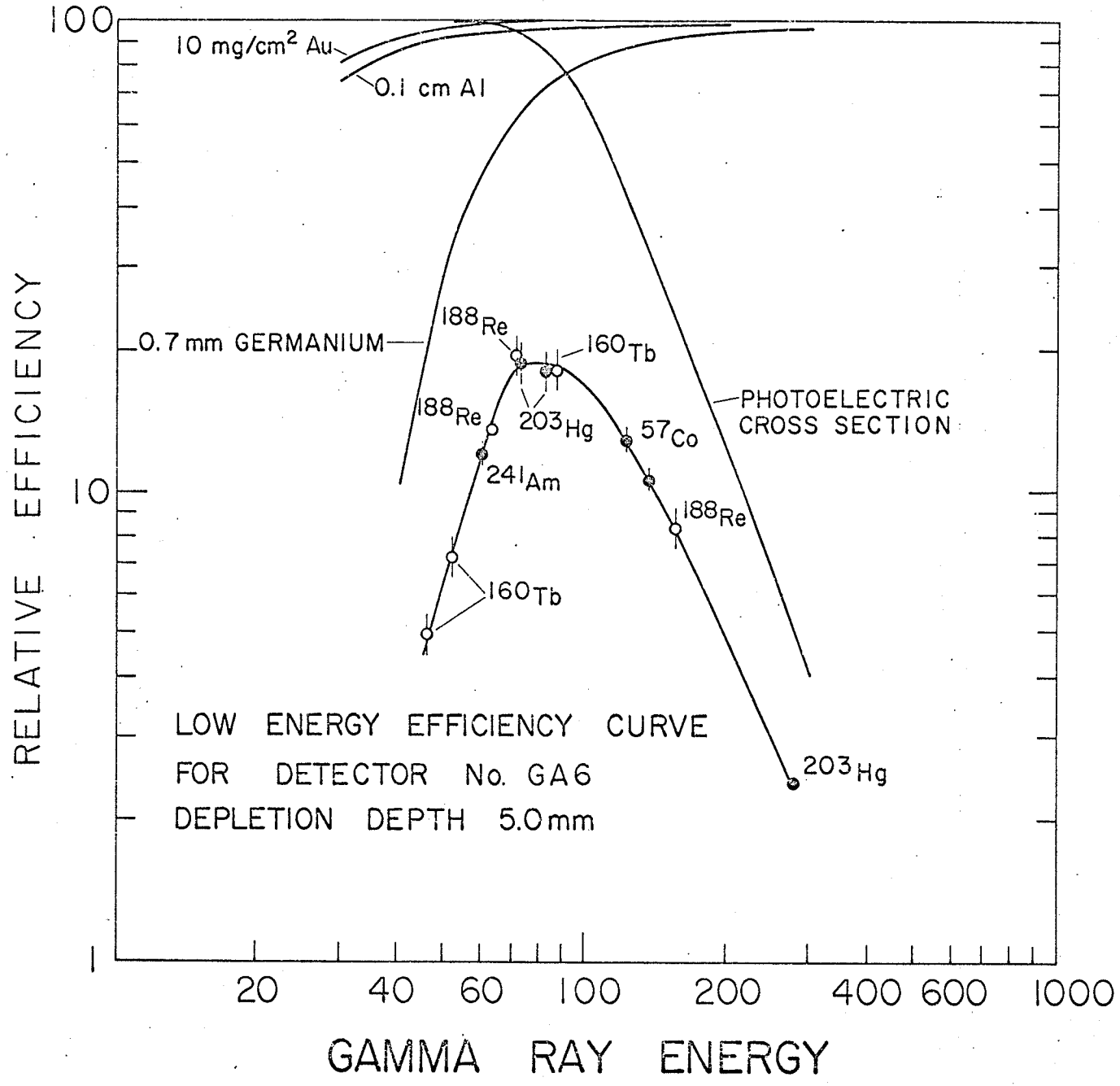
100
10
1
RELATIVE EFFICIENCY
10 mg/cm² Au
0.1 cm Al
0.7 mm GERMANIUM
PHOTOELECTRIC CROSS SECTION
188Re
160Tb
188Re
203Hg
57Co
241Am
188Re
160Tb
203Hg
LOW ENERGY EFFICIENCY CURVE
FOR DETECTOR No. GA6
DEPLETION DEPTH 5.0mm
20
40
60
100
200
400
600
1000
GAMMA RAY ENERGY

Fig. 2-5

Relative photopeak efficiency curve for G9C2 below 300keV.

74-J

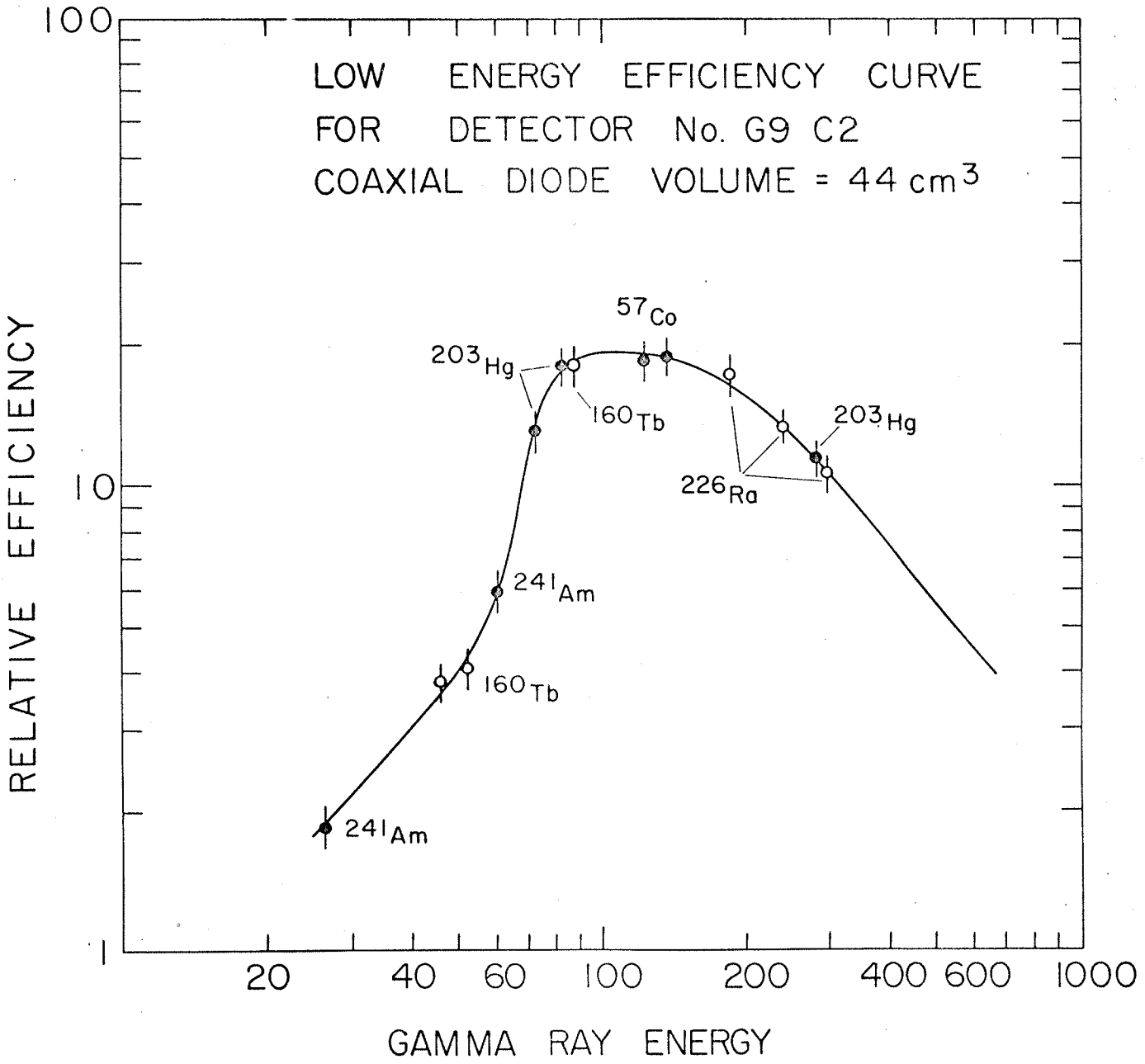
LOW ENERGY EFFICIENCY CURVE
FOR DETECTOR No. G9 C2
COAXIAL DIODE VOLUME = 44 cm3
RELATIVE EFFICIENCY
GAMMA RAY ENERGY
100
10
1
20
40
60
100
200
400
600
1000
57Co
203Hg
160Tb
203Hg
226Ra
241Am
160Tb
241Am

electric field distribution at the front end of the diode. Collimated gamma-ray scans are underway at the present time in order to determine the cause of this effect.

2.3 Pulse Height Analysis

Before discussing the energy measurement of gamma-rays, a brief description of the pulse height analyser system should be given. Pulses from the Ge(Li) detector were fed, by means of the preamplifier described in section 1.5, to a Tennelec TC200 linear amplifier. The unit, in addition to amplifying the signal, shaped the pulse in order to give an optimum signal to noise ratio. These shaped pulses were then fed to a pulse height analyser.

Two types of analysers were used for the experiments on ^{159}Gd and ^{177}Yb. One of these, a Nuclear Data 3300 system, was a conventional type of analyser with a 4096 channel A.D.C. and a 4096 channel memory. Because of this large memory, no biased amplifiers were used with this system.

The other data collection system employed a PDP-8 digital computer. The linear amplifier pulses were further shaped by a Tennelec TC250 biased amplifier to give unipolar rectangular pulses required by the A.D.C.'s in the PDP-8 computer. The biased amplifier was also necessary since the size of the PDP-8 memory limited the data region to 1024 channels. The encoded pulses were then stored in the computer memory by means of a programme. The PDP-8 system allowed more manipulation of the collected data while in the memory (eg. integration, background subtraction) than the Nuclear Data 3300 system.

2.4 Energy Measurement

The positioning of gamma-rays in a complex decay scheme is greatly facilitated if the energies of these transitions are accurately known. There are often cases where the energy separation between two pairs of levels is very nearly the same and only a precise determination of the gamma-ray energy can indicate between which pair the transition fits.

The accuracy with which a gamma-ray can be measured depends upon several things -- the ability to define the peak position, the availability of standard sources relative to which the transition energy can be measured and the non linearity of the detector system used. With the multi-channel analysers in common use today (1000 to 4000 channels), it is possible to spread the photopeak over several channels, and with good statistics, it is possible to define the peak "position" to within about 1/10 of a channel.

There are two methods which are commonly used to define the position of a peak -- the center point of the line drawn at the half maximum height or the "top peak center" method. The latter method is an extension of the former whereby horizontal lines are drawn at several heights and the center points of these lines are joined by a straight line. This line is then extended until it cuts the top of the peak and this point is used to define the peak position. Either method may be used although the "top peak center" method is usually used when the peak is not symmetric, as is the case with Ge(Li) photopeaks. Whichever method is used must be followed consistently throughout the experiment.

There are many gamma-rays with accurately known energies which may be used as standards and an extensive compilation of these

has been made recently by Marion (Marion 1968). In general, the accuracy with which an unknown gamma-ray can be measured depends upon how far it is from the standard line. This is a direct consequence of the system non-linearity and means that several standards must be used for each spectrum taken.

The non-linearity of the detection system may arise from the preamplifier, the amplifier, biased amplifier if one is used, or from the A.D.C. of the multi-channel analyser being used to collect the data. The system non-linearity may also be a function of the counting rate. The linearity of biased amplifiers is known to be dependent upon the counting rate and in some cases A.D.C.'s may also exhibit this effect. Large amounts of money and effort may be invested in attempts to improve this situation but ultimately the non-linearity of the system must still be measured. The following method was used for the experiments on ^{177}Yb and ^{159}Gd reported in this thesis.

Pulses from a precision pulse generator were fed into the preamplifier input so that they were shaped and amplified by the same electronic system as the pulses from the Ge(Li) detector. The setting of the potentiometer on the pulse generator was incremented in equal steps to cover the entire memory of the multichannel analyser. When the positions of these peaks had been determined, the equation of a straight line was fitted to the amplitude of two of them. The deviation from linearity of the other peak positions was then plotted against channel number, the result of which were curves similar to those shown in Fig. 2-6. Large deviations occur at the ends of both A.D.C.'s and the system used with the PDP-8 exhibited a much larger deviation over the whole range than did the

Fig. 2-6

System non-linearity measurements.

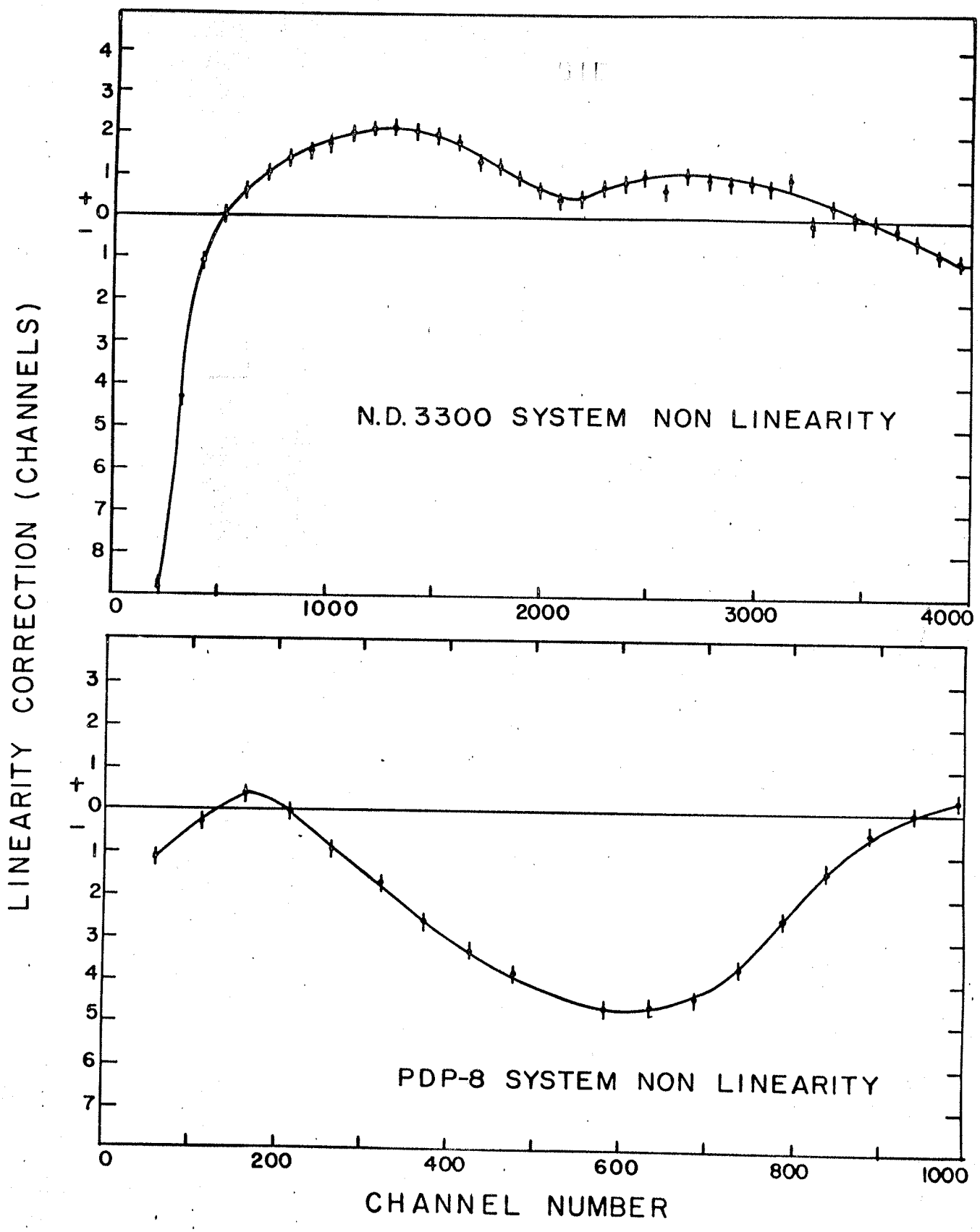
N.D. 3300 SYSTEM NON LINEARITY
PDP-8 SYSTEM NON LINEARITY
LINEARITY CORRECTION (CHANNELS)
CHANNEL NUMBER
+
-
0
1
2
3
4
5
6
7
8
0
1000
2000
3000
4000
200
400
600
800

Nuclear Data 3300 system. The A.D.C.'s used with the PDP-8 system preferred unipolar rectangular pulses and these were produced from the Tennelec TC250 biased amplifier. While it was unnecessary to use the biased amplifier with the N.D. 3300 system, it was used for the comparison with the PDP-8 system shown in Fig. 2-6.

The usual procedure followed in these experiments was to record the unknown spectrum simultaneously with several standard sources as well as signals from the pulse generator. The combination of standard sources and pulse generator provided the non-linearity curve and energy calibration from which the unknown energies were calculated. The energies of weak gamma-rays which were masked by either the standards or by the pulser can then be calculated on subsequent runs using the other gamma-rays as internal standards.

The importance of simultaneous energy calibration cannot be over emphasized if accurate energy measurements are desired. If the deviation from linearity is a smoothly varying function, it is possible, under certain circumstances and with care, to measure energies to better than 100 eV.

CHAPTER III

Decay Scheme Studies of ^{134}Cs

3.1 Introduction:

The de-excitation of a nucleus from low lying states takes place dominantly by means of electromagnetic transitions. These transitions are of two main types:

(a) Emission of a gamma-ray

(b) Emission of an electron following internal conversion of a gamma-ray.

These processes of de-excitation are competitive and for given initial and final states the ratio of process b to a is defined as the "internal conversion coefficient." The process of internal conversion is the conversion of nuclear excitation energy into kinetic energy through the direct electromagnetic interaction between the electrons and the nucleons. Since there are several electron orbitals, the internal conversion coefficient (I.C.C.) for a particular shell or subshell i is defined by

$$\alpha_i = \frac{Ne(i)}{N_\gamma}$$

where Ne(i) is the number of electrons ejected from the i^{th} shell and N_γ is the number of unconverted gamma-rays.

For a detailed discussion of the theory of internal conversion the reader is referred to the literature (Rose 1951, 1958; Sliv and Band 1956,1965) or to a review article by Rose (1965). It will suffice at this time to point out some of the relevant features and to illustrate the importance of I.C.C. measurement to gamma-ray spectroscopy.

For transitions between two nuclear states with spins and parities J_i, J_f and Π_i, Π_f respectively the amount of angular momentum which can be carried away by the gamma-ray or internal conversion electron is restricted to

$$|J_i - J_f| \leq L \leq J_i + J_f \text{ with } \quad \frac{\Pi i}{\Pi f} = (-1)^L \text{ for EL radiation}$$
$$= (-1)^{L-1} \text{ for ML radiation}$$

From the theory of multipole radiations (Moszkowski, 1966) it can be shown that the relative intensities of multipoles L and L + 2 is such that the L + 2 contribution can usually be neglected. The parity selection rule prohibits the mixing of L and L + 1 multipolarities of the same character but does allow mixing of characters, for example magnetic 2^L-pole with electric 2^{L+1}pole. (M1,E2 mixture)

Time dependent perturbation theory must be used to calculate the rate of internal conversion. The result from such a calculation gives

$$N_e = \frac{1}{2J_i+1} \sum_{m_f,m_i} S_e \frac{2\Pi}{\hbar} |\langle \Psi_f \psi_f | H' | \Psi_i \psi_i \rangle|^2 \rho_E$$

(See Preston Chap.11) where Ψ_f, Ψ_i and ψ_f, ψ_i are respectively the wave functions for the final and initial states of the nucleons and electrons. S_e represents summations and averages over final and initial electron states. ρ_E is the density of final states and H' is the Hamiltonian for the interaction of the electrons and nucleons. Let us consider, for the moment, electric multipole transitions. If one uses the approximate form of the interaction Hamiltonian given by Preston (eq. 11-22 Preston), the above expression for N_e is found to depend upon the squares of two

$$\langle f|\Theta^{E}_{l,m}|i\rangle \quad \text{and} \quad \langle \psi_f | r_e^{-(\lambda+1)} Y_\lambda^m(\theta_e, \phi_e) | \psi_i \rangle$$

where $\Theta_{l,m}$ is the electric multipole operator. The first matrix element contains the dependence of the internal conversion process upon nuclear parameters. The gamma-ray transition probability N_γ for the emission of a photon of energy hw and angular momentum λ,μ is given by

$$N_{\gamma i \to f}(\sigma,\lambda,\mu) = \frac{8\pi\ (\lambda+1)}{\lambda\ (2\lambda+1)} \quad 2\ \frac{k^{2}+1}{h} |\langle f|\Theta^{E}_{\lambda\ \mu}|i\rangle|^{2}$$

When the I.C.C. N_e/N_γ is calculated the matrix elements involving the electric multipole operator cancel out.

In order to calculate the I.C.C. for magnetic multipole transitions, the proper form of the interaction Hamiltonian must be used (eg. 11-13 Preston). The result of the calculation for N_e then involves matrix elements with the magnetic multipole operator which again cancel out when the ratio N_e/N_γ is formed.

The second matrix element and the other factors involved in N_e are dependent upon the electronic states only. It should be noted that this latter matrix element is very dependent upon the value of λ and it is this feature which makes I.C.C. measurements so important in gamma-ray spectroscopy. This matrix element is also a function of the Z of an atom. For transition energies large compared to the binding energy of the electrons the following trends occur. The I.C.C. decreases as the shell gets further removed from the nucleus, decreases as the transition energy increases, increases as the Z and the L values increase.

The main purpose of this chapter is to report the results of a study of the decay of ^{134}Cs and the measurements of K-I.C.C. using a method involving the conversion electron to gamma-ray ratio. This method involves mixing a standard source, in which the conversion coefficient of a particular transition is accurately known, with the

work ^{137}Cs was mixed with ^{134}Cs and the conversion coefficient of the 605 keV transition was measured from

$$\alpha_k\ (605) = \frac{I_k\ (605)}{I_k\ (662)} \times \frac{I_\gamma\ (662)}{I_\gamma\ (605)}\ \alpha_k\ (662)$$

The conversion electron and gamma-ray spectra were then normalized using this value and the other conversion coefficients calculated.

3.2 Decay of ^{134}Cs

The decay of 2.1 yr. ^{134}Cs to ^{134}Ba has been studied by many workers but there is lack of agreement on the level scheme of ^{134}Ba. This is principally due to the existence of a complex gamma-ray spectrum with several closely-spaced gamma rays which could not be resolved by NaI spectrometers. Much of the present information on the gamma-ray spectrum had been deduced from sum coincidence spectra, but recently Schriber and Hogg (Schriber 1963) who made a detailed study using this method, have shown that several of the transitions previously reported are due to misinterpretation of the sum coincidence spectra. The development of the Ge(Li) gamma-ray spectrometer now makes it possible to study gamma-ray spectra at much higher resolution than with NaI spectrometers, and hence enables the gamma-rays from ^{134}Cs to be resolved directly.

In another recent paper on the beta decay of ^{134}Cs, Van Wijngaarden and Connor (Van Wijngaarden 1964) observed that the K-conversion coefficients of two high energy E2 transitions were about 30% lower than the theoretical values. As comparison of experimental conversion coefficients with theoretical values is often used to determine multipolarities of gamma transitions, it is important to check this reported discrepancy. The high reso-

lution of the Ge(Li) gamma-ray spectrometers (Tavendale 1963, 1964a, Ewan 1964a) is also useful in determining conversion coefficients as it now makes possible the use of the mixed source technique in complex decay schemes.

This chapter reports the results of energy and relative intensity measurements of the gamma rays from ^{134}Cs using a Ge(Li) gamma-ray spectrometer. The K-conversion lines of these transitions have been studied using the Chalk River high resolution $\pi\sqrt{2}$ β-ray spectrometer. (Graham, 1960). The K-conversion coefficients of the gamma transitions have also been measured, relative to the accurately known value of the K-conversion coefficient of the 662 keV transition observed in the decay of ^{137}Cs (Merritt 1965) using a mixed source of ^{134}Cs and ^{137}Cs.

3.3 Experimental Apparatus and Procedure

The ^{134}Cs source was supplied by the Commercial Products Division of AECL. It had been produced by a four month radiation of ^{133}Cs in a flux of 2×10^{14} neutrons/cm^2/sec in the NRU reactor at Chalk River. For studies with the Ge(Li) detector ≈10μC was deposited on a 2.5 cm diameter copper disc. For conversion electron studies, sources were prepared by vacuum sublimation onto an aluminum backing through a slot 1.25 cm long and 3 mm wide. The composite source was prepared by mixing ^{134}Cs and ^{137}Cs and subliming the mixture onto an aluminum backing.

The gamma-ray spectrum was studied with a Ge(Li) detector 3.5 mm deep and 18 mm in diameter prepared by Dr. A. J. Tavendale at Chalk River. Details of the construction of the detector (Tavendale 1964a), the experimental arrangement and the

variation of the photopeak efficiency with energy have been given elsewhere. (Ewan 1964a). In order to resolve the 796 and 802 keV gamma-rays a smaller detector manufactured by RCA Victor Ltd. * was used. It was possible to obtain slightly better resolution with this detector because of its lower capacitance.

The internal conversion spectrum was studied at about 0.15% resolution in the Chalk River high resolution $\pi\sqrt{2}$ β-ray spectrometer. Only those regions were surveyed where the K-conversion lines of the gamma rays seen with the Ge(Li) detector occurred.

3.4 Gamma-Ray Spectrum

The gamma-ray spectra observed in the Ge(Li) detectors are shown in Figs. 3-1 and 3-2. These spectra were recorded on a 400 channel pulse-height analyser preceded by a biased amplifier. A description of the electronics has been given elsewhere (Ewan 1964).

The gamma-ray spectrum from 75 keV up to 375 keV is shown in Fig. 3-1a. No gamma-rays were observed in this region. There are four gamma-rays in the region from 375 to 625 keV, as shown in Fig. 3-1b, with energies 475, 563, 569 and 605 keV respectively. No distinct peak had previously been recorded at 475 keV with sodium iodide crystals, and the other three peaks had appeared as a broad peak at 600 keV.

Fig. 3-2a shows the region from 550 to 850 keV. The improvement in resolution of the 563-569 keV doublet over that shown in Fig. 3-1b was achieved by using a lower counting rate and automatic gain stabilization with the pulse-height analysis

---

* RCA Victor Ltd., 1001 Lenoir St., Montreal, P.Q., Canada.

Fig. 3-1

(a) Low energy region of ^{134}Cs gamma-ray spectrum observed with 3.5mm x 18mm diameter Ge(Li) detector.

(b) ^{134}Cs gamma-ray spectrum from 375keV to 625keV.

A.E.C.L. Ref. # A-3077–D

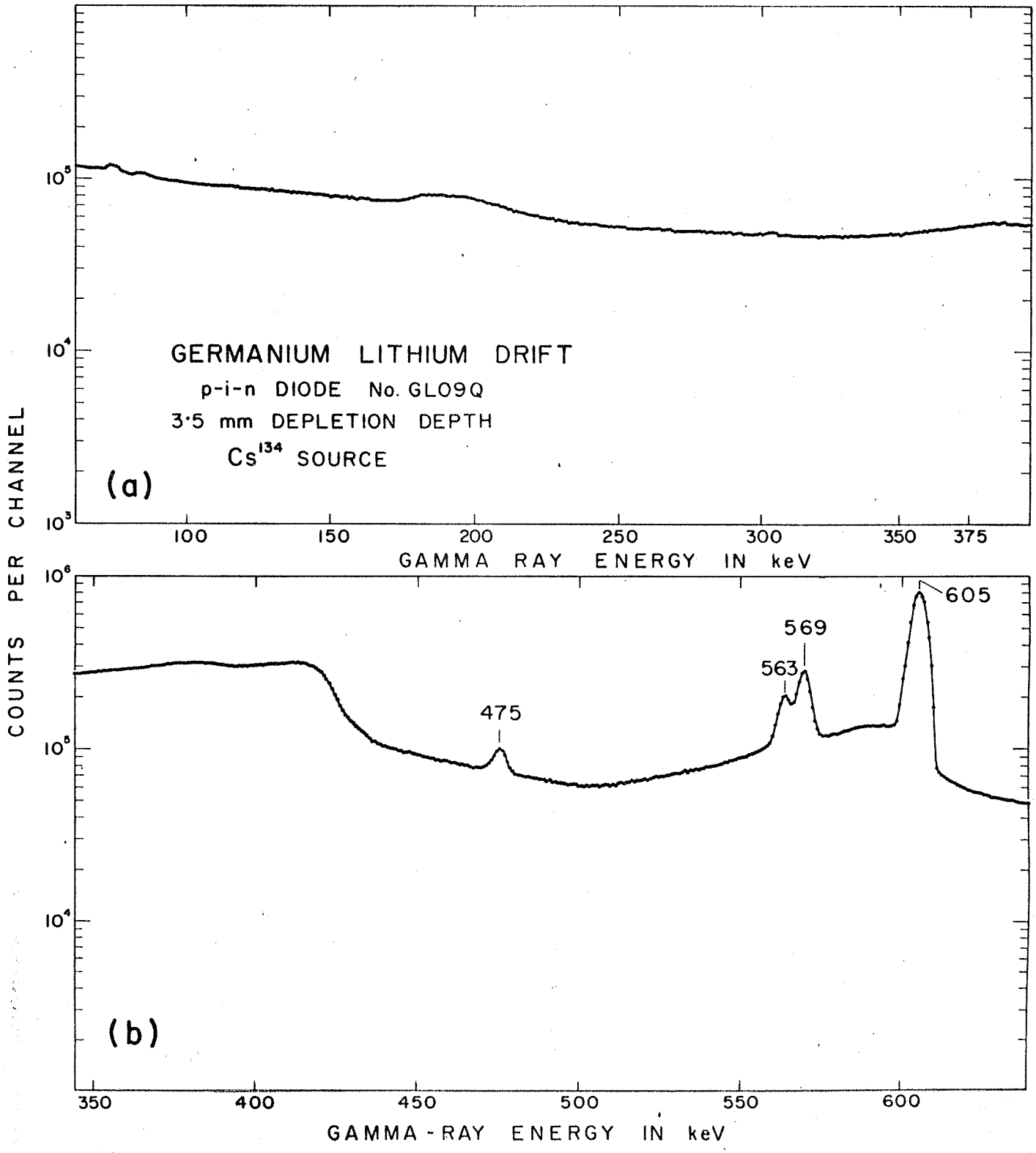

Fig. 3-2

(a) ^{134}Cs gamma-ray spectrum from 550keV to 850keV. The improved resolution of the 563-569 keV doublet from Fig. 3-1b is due to lower counting rate and automatic gain stabilization in the pulse-height system.

(b) High energy region of ^{134}Cs gamma-ray spectrum with 0.64cm lead between the source and deteetor.

A.E.C.L. Ref. # A-3114-G

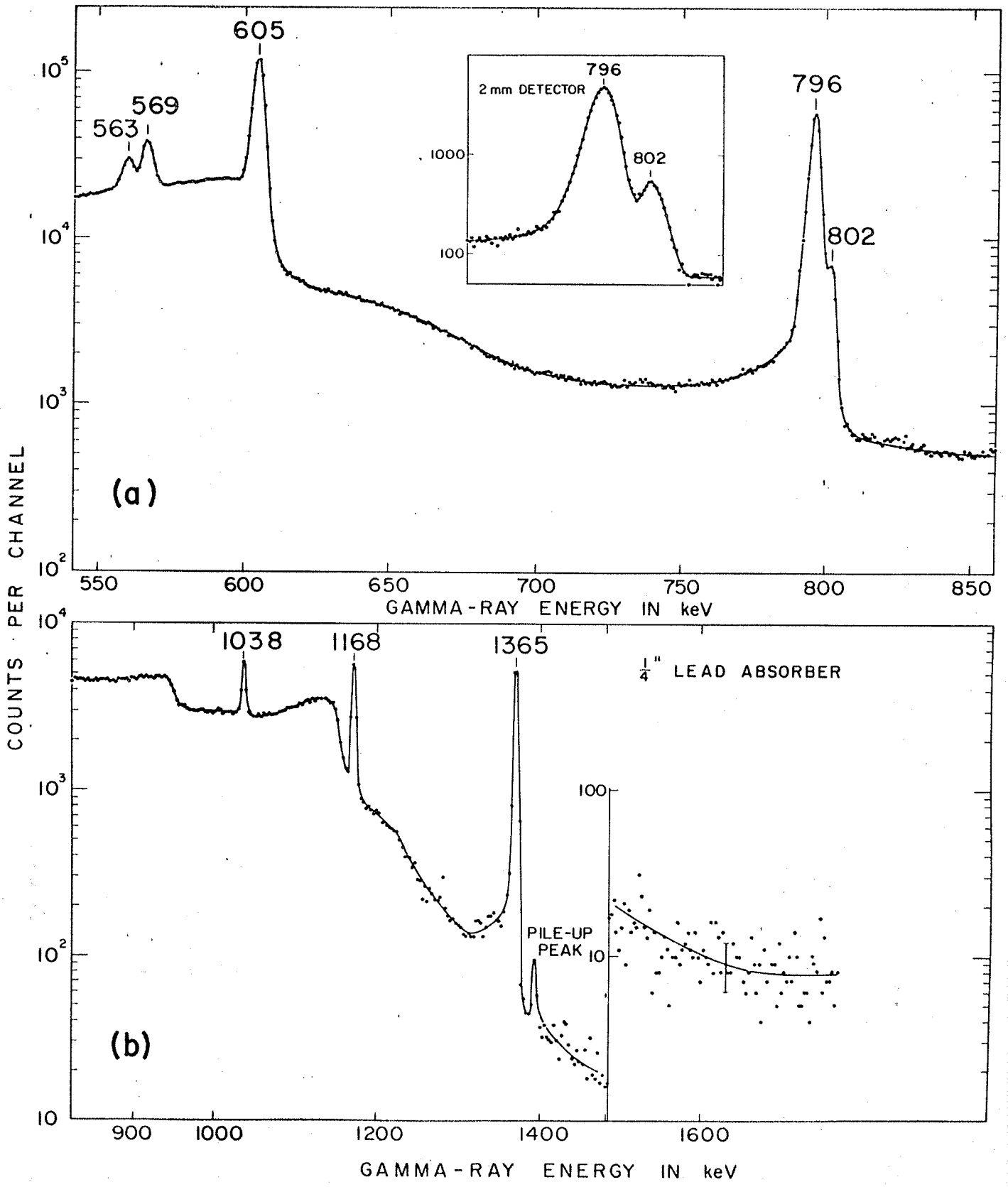

system(Patwardhan 1964). The inset shows the 796-802 keV doublet, as recorded by the RCA detector with 2.0 mm depletion depth and 0.8 cm^2 cross-sectional area.

The high energy portion of the spectrum is shown in Fig. 3-2b. Gamma-rays with energies 1038, 1168 and 1365 keV respectively can be seen along with a peak at 1401 keV. This spectrum was taken with ½ inch of lead between the source and detector. The attentuation of the 1401 keV peak relative to the 1365 keV peak, when lead absorber was added, indicated that it was pile-up due to the 796 keV and 605 keV gamma rays which are in coincidence. A limit on the possible intensity of a gamma ray of 1401 keV or higher energy is $<2 \times 10^{-4}$ per disintegration.

Table 3-I gives the values of the intensities obtained in the present work. The calculations are based on the efficiency curve given by Ewan and Tavendale (Ewan 1964a) for this detector which has an estimated accuracy of ±5%.

In calculating the intensity of the 605 keV γ-ray the subtraction of background is difficult, as the Compton edges of the 796 and 802 keV γ-rays fall directly under the peak. The Compton distributions for these γ-rays was estimated by measuring the shape of the spectrum obtained from the 834 keV γ-ray from a ^{54}Mn source and allowing for the difference in energy. The background subtracted from the 605 keV peak in Fig. 3-2a was similar to the one shown later as a broken line in Fig. 3-4 .

The intensity measurements are estimated to be accurate to ~ 10% with the exception of the 802 keV γ-ray. The higher estimate of the error in this case is caused by the difficulty in resolving the 796-802 doublet. In Table 3-I the results are also compared

Table 3-I

GAMMA-RAY SPECTRUM OF ^{134}Cs

Energy (keV)	Relative Intensities				
	Present Work	Ref.(a)	Ref.(b)	Ref.(c)	Ref.(d)
475.3	1.54 ± 0.15	2.5 ± 0.5	1.3	1.2	<1
563.1	8.52 ± 0.8	10 ± 3		9	) 27.4 ± 3)
569.2	14.6 ± 1.4	18 ± 3		13	)
604.6	100 ± 5	100	100	100	100 ± 5
795.8	90 ± 9	) 101.4 ± 3)	) 92)	) 92)	) 103 ± 5)
801.8	9.0 ± 1.5	)	)	)	)
1038.4	1.06± 0.10	1.16±0.04	1.5	1.1	1.32±0.13
1167.7	1.99± 0.17	2.26±0.08	2.2	2.7	2.34±0.23
1365.0	3.46± 0.30	3.79±0.15	3.3	3.6	3.67±0.36

(a) B.S. DZHELEPOV et al., Izvest. Akad. Nauk. SSSR, Ser. Fiz. 23, 826 (1959).

(b) R.K. GIRGIS and R. VAN LIESHOUT, Nucl. Phys. 12, 672 (1959).

(c) P.N. TREHAN, Thesis, Louisiana State University (1960). Quoted in Nuclear Data Sheets.

(d) W. VAN WIJNGAARDEN and R.D. CONNOR, Can. J. Phys. 42, 504 (1964).

with those obtained by other workers. For the purpose of this comparison the intensity of the 605 keV transition has been arbitrarily set equal to 100 and the other intensities have been normalized to this value.

There is no evidence for the γ-rays at 960, 1401 and 1570 keV reported by some previous workers. A limit on the possible intensity per disintegration of a 1401 keV γ-ray is < 0.02% and for a 1570 keV γ-ray < 0.01%. The limit on the possible intensity of a 960 keV γ-ray is somewhat higher as it occurs near the Compton edge of the 1168 keV γ-ray. It is estimated to be < 0.1% per disintegration. This information supports the conclusion of Schriber and Hogg (Schriber 1963) and of Van Wijngaarden and Connor (Van Wijngaarden 1964) that there is no evidence for levels at 1570 and 1770 keV.

3.5 K-Conversion Coefficients

Values obtained for conversion coefficients in ^{134}Ba have shown large variations and in some cases have differed considerably from the theoretical values calculated by Rose and by Sliv and Band (Rose 1958, Sliv 1956). Van Wijngaarden and Connor (Van Wijngaarden 1964) have reported departures ~ 30% from theoretical values for the high energy E2 transition, their values lying below the theoretical ones. Because of these discrepancies, it was decided to investigate the conversion line spectra as well as the γ-ray spectra.

A study of the conversion lines was made using the high resolution $\pi\sqrt{2}$ β-ray spectrometer (Graham 1960). Portions of the spectra obtained are shown in Fig. 3-3 . The low energy region was recorded with the baffles set at 0.15% resolution; for the high

Fig. 3-3

Conversion line spectra of ^{134}Cs observed with the Chalk River $\pi\sqrt{2}$ beta-ray spectrometer. The upper half of the figure was recorded at a resolution of 0.15% while the lower was recorded at 0.20%. The high energy region is the aggregate of three separate runs.

A.E.C.L. Ref. # A-3114-F

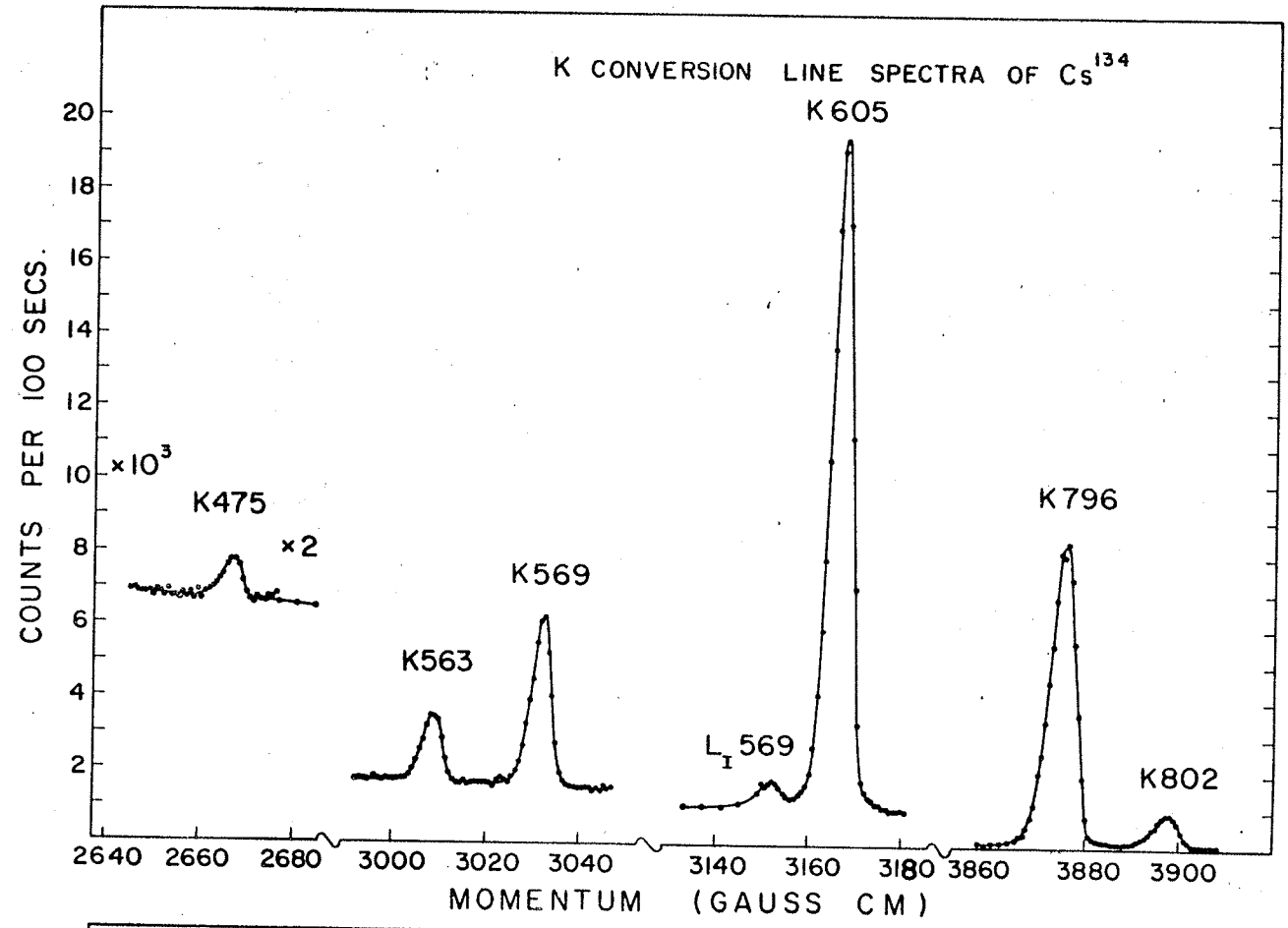

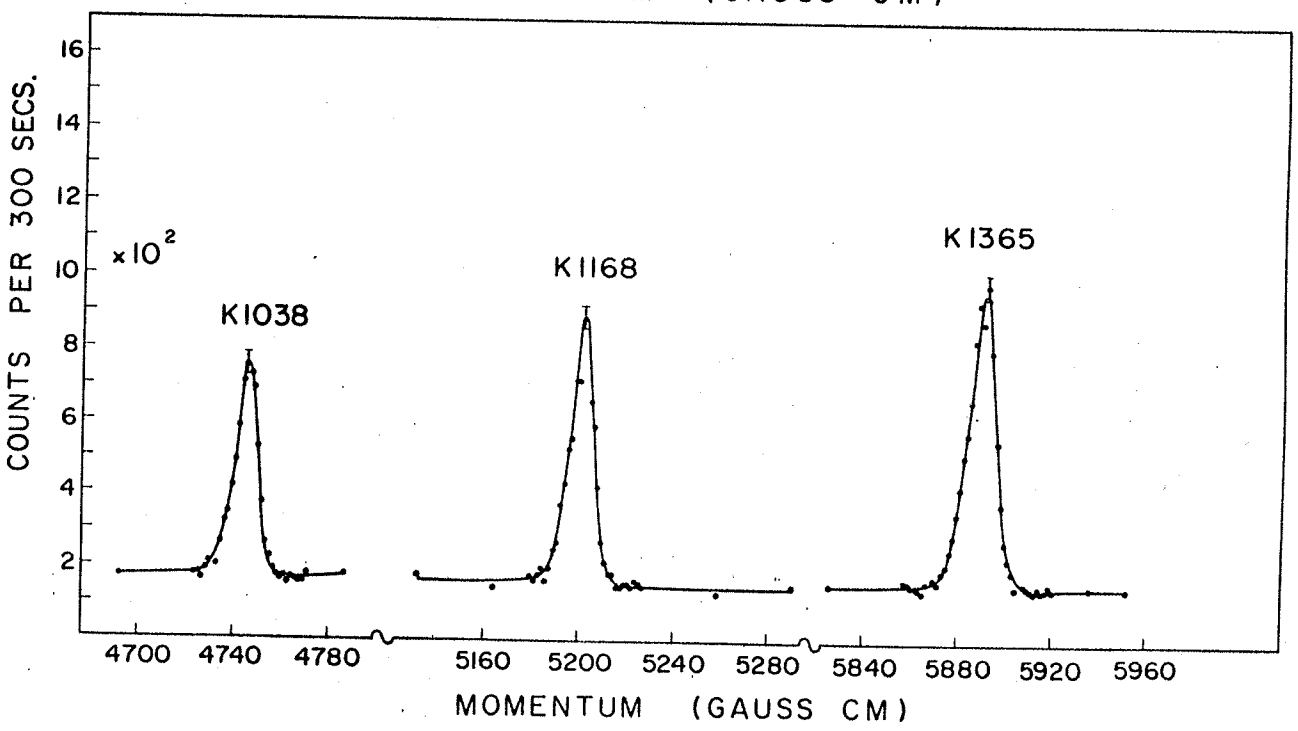

energy region a stronger source and a baffle setting of 0.20% resolution were used. The high energy region is a composite of three separate runs. It should be noted that we studied only those regions of the conversion spectra where K-conversion lines were indicated by the γ-ray spectra from the Ge(Li) detector. The relative intensities of the K-conversion lines are given in column 3 of Table 3-II . The intensity of the K-605 line is corrected for the small contribution from the M-569 conversion line which lies beneath this peak.

In order to normalize the conversion line intensities to the γ-ray intensities the conversion coefficient for the 605 keV transition from ^{134}Cs was measured using the mixed source technique. This technique is particularly suited to the high resolution of the Ge(Li) detectors since it can now be used in complex decay schemes. A composite source of ^{134}Cs and ^{137}Cs was prepared. The relative γ-ray intensities of the 605 keV and 662 keV transitions were measured with the Ge(Li) spectrometer and the relative K-conversion line intensities were measured in the $\pi\sqrt{2}$ β-ray spectrometer. The spectra used for this purpose are shown in Fig. 3-4 . The intensity of the K-605 line was corrected for contributions from the tail of L-569 and for the M-569 lines which lay below the K-605 peak. These results give the ratios $I_{\gamma-605}/I_{\gamma-662}$ and I_{K-605}/I_{K-662}. Since the K-conversion coefficient of the 662 keV γ-ray from ^{137}Cs is known, that of the 605 keV transition from ^{134}Cs can be deduced using the relation,

$$\alpha_K(605) = \frac{I_{K-605}}{I_{K-662}} \cdot \frac{I_{\gamma-662}}{I_{\gamma-605}} \cdot \alpha_K(662)$$

Fig. 3-4

The upper half of the figure shows part of the gamma-ray spectrum of the mixed ^{134}Cs and ^{137}Cs sourceobserved with the Ge(Li) detector.

The lower half of the figure shows part of the conversion line spectrum of the same source observed with the $\pi\sqrt{2}$ beta-ray spectrometer.

A.E.C.L. Ref. # A-3078–G

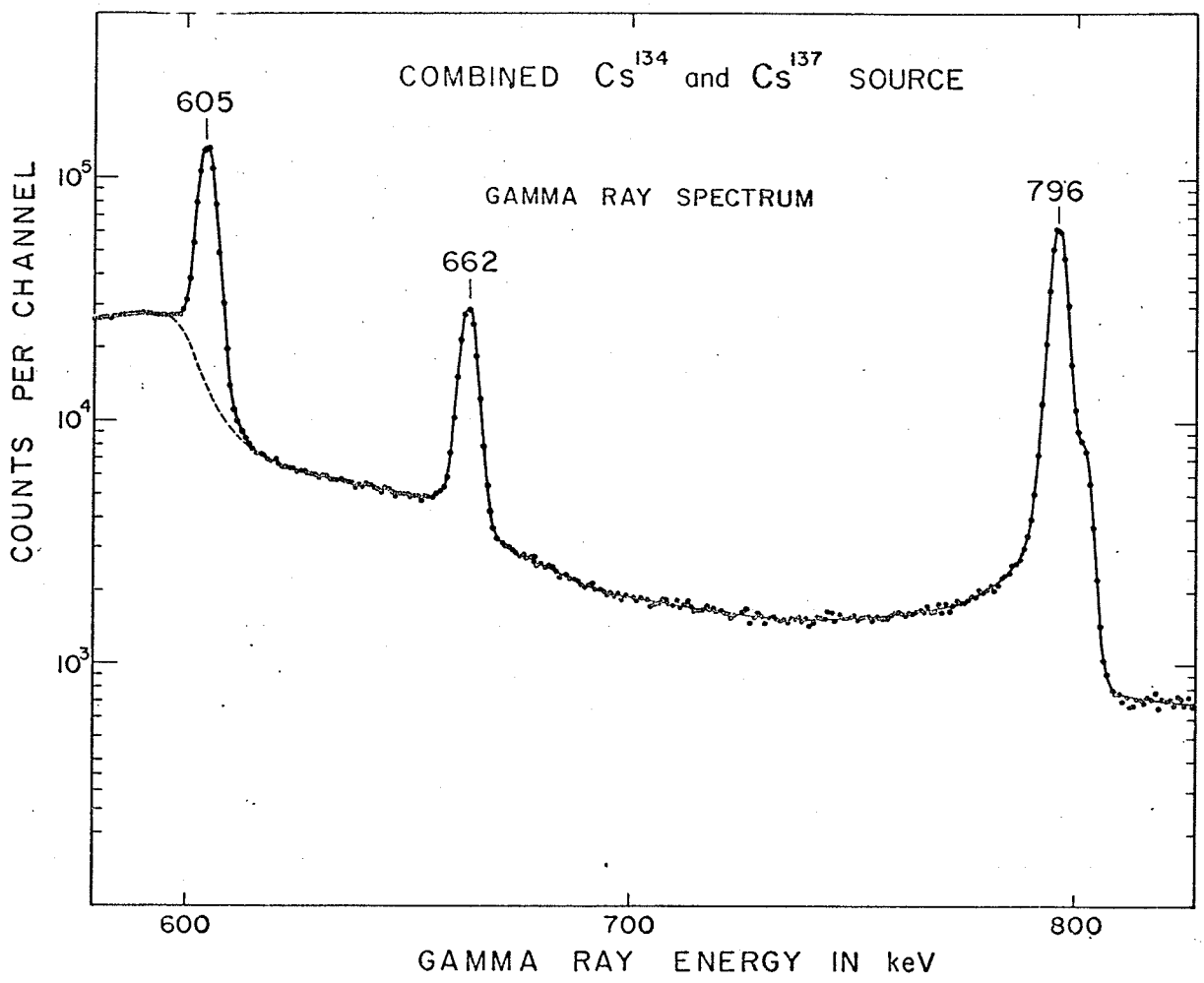

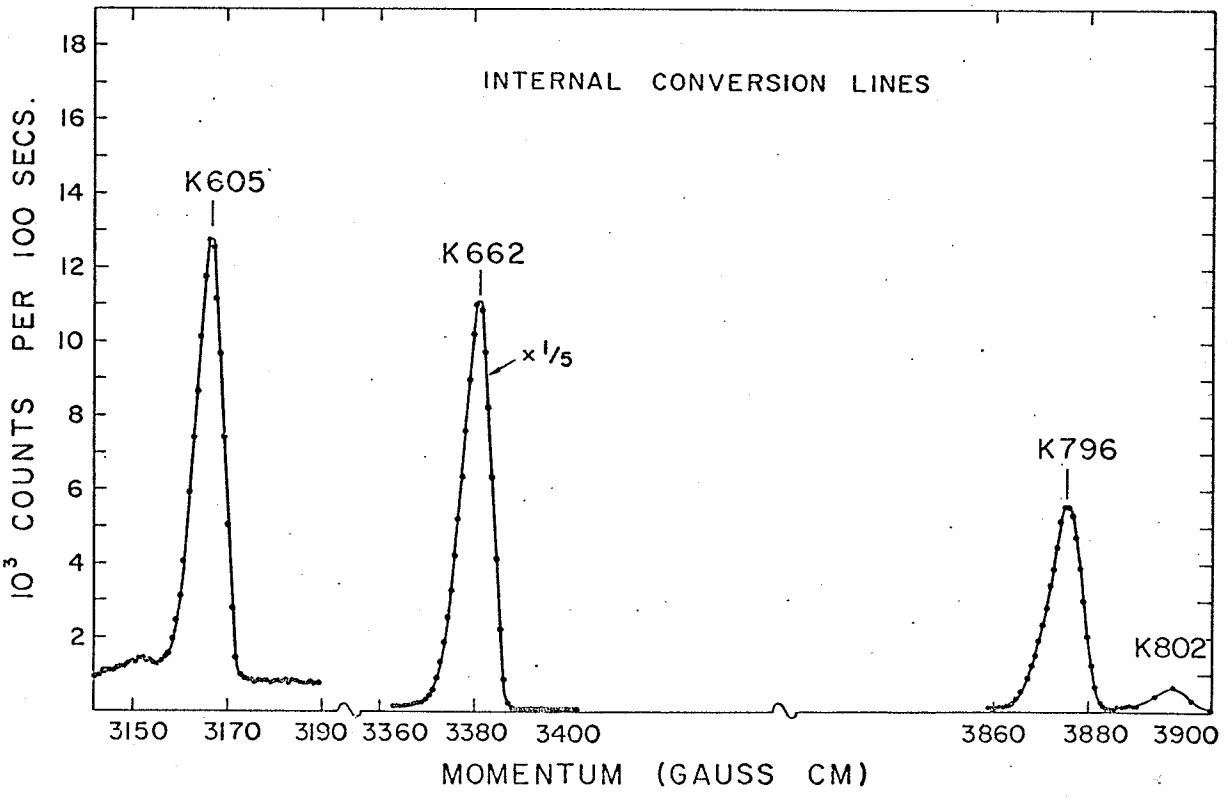

Table 3-II

PROPERTIES OF GAMMA TRANSITIONS IN ^{134}Ba

Gamma-Ray Energy (keV)	Gamma-Ray Intensity % per Dis.	K-Conversion Line[a] Intensity per 10^4 Dis.	α_K Experimental	α_K Theoretical[b] E2	α_K Theoretical[b] M1	Assigned Multipolarity
			$\times 10^{-3}$	$\times 10^{-3}$		
475.26±0.10	1.5±0.15	1.41 ± 0.06	9.40 ± 1.0	9.48	12.9	E2
563.11±0.12	8.3±0.8	4.65 ± 0.2	5.60 ± 0.6	5.99	8.50	E2
569.24±0.12	14.2±1.4	11.62 ± 0.5	8.18 ± 0.9	5.77	8.23	M1
604.64±0.12	97.5	47.3 ± 1.0	4.85 ± 0.2[c]	5.00	7.11	E2
795.80±0.16	87.8±9	21.6 ± 0.8	2.46 ± 0.3	2.61	3.68	E2
801.80±0.16	8.8±1.5	2.26 ± 0.1	2.57 ± 0.4	2.56	3.60	E2
1038.46±0.20	1.03±0.1	0.167±0.009	1.62 ± 0.18	1.44	1.92	M1+E2
1167.65±0.25	1.94±0.15	0.204±0.010	1.05 ± 0.10	1.12	1.52	E2
1364.97±0.28	3.37±0.30	0.241±0.010	0.72 ± 0.07	0.82	1.07	E2

(a) Conversion line intensity scale normalized to gamma-ray scale using experimental value of α_K for γ-604.64.

(b) Values interpolated from tables of Sliv and Band.

(c) Direct measurement relative to α_K of 661.6 γ-ray from ^{137}Cs.

The value of $\alpha_K(662)$ has recently been accurately measured by Merritt and Taylor (Merritt 1965) to be 0.0894 ± 0.0010. Using this value our results give an experimental value for the K-conversion coefficient of the 605 keV transition of (4.85 ± 0.2) x 10^{-3}.

Table 3-II summarizes the properties of the γ-ray transitions observed in the decay of ^{134}Cs. The measured values of the γ-ray energies from the present work are listed in column 1. These were measured from the conversion line spectra recorded with a $\pi\sqrt{2}$ β-ray spectrometer using as a reference the value obtained by Graham et al (Graham 1960) for the 662 keV γ-ray in ^{137}Cs. We estimate that the accuracy of the energy measurements is 1 part in 5000. Column 2 lists the values obtained for the γ-ray intensities normalized to a value of 97.5 for the 605 keV γ-ray. This normalization gives values in percent per disintegration by making the total intensity of transitions feeding the ground state equal to 100. Previous experiments have shown that there is no β-feed to the ground state (Van Wijngaarden 1964). Column 3 lists the K-conversion line intensities. These have been normalized to give the experimental K-conversion coefficients for the 605 keV γ-ray and so are also per disintegration. The experimental K-conversion coefficients are shown in column 5 and 6. The multipolarity assigned to each of these transitions is shown in the last column.

3.6 Results

In Fig. 3-5 the experimental measurements of the K-conversion coefficients are compared with the theoretical values of Sliv and Band. In order to obtain a convenient scale all values have been

Fig. 3-5

Comparison of the experimental values of K-conversion coefficients with the theoretical values of Sliv and Band for M1 and E2 transitions.

A.E.C.L. Ref. # A-3107-H

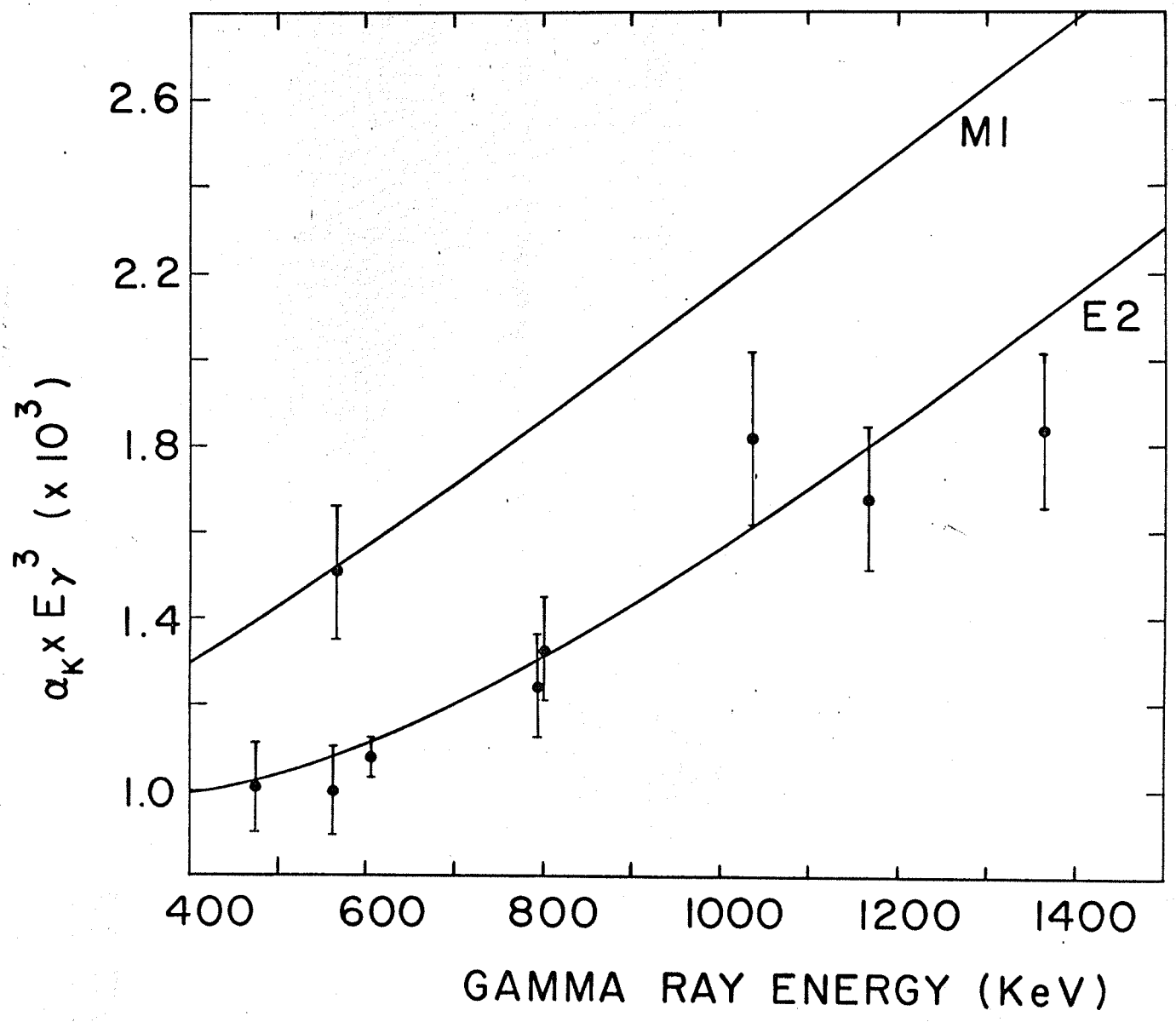

multiplied by E_γ^3. The 569 keV transition is dominantly M1, the 1038 keV transition probably an M1+E2 admixture, and all other transitions dominantly E2. For the E2 transitions there is reasonable agreement, within the experimental accuracy, between the experimental and the theoretical values, although in general the experimental values tend to be slightly lower than the theoretical values. The greatest discrepancy is (12 ± 10)% for the 1365 keV γ-transition. The α_k for the 1168 keV transition, while somewhat low, is in better agreement with theory than previously reported measurements (see Van Wijngaarden 1964).

The most accurate measurement is the value of (4.85 ± 0.2) x 10^{-3} for the 605 keV (2+ → 0+) transition which was determined by the mixed source technique, and so is relative to the accurate value of the K-conversion coefficient of the 662 keV transition from ^{137}Cs. This conversion coefficient has also recently been measured by Hankla et al and Zganjar et al at Vanderbilt University using the internal-external conversion method. Their values (Hankla 1963, Zganjar 1962) of (4.65 ± 0.3) x 10^{-3} and (5.0 ± 0.2) x 10^{-3} are in good agreement with the present result.

3.7 Level Scheme

Fig. 3-6 shows the disintegration scheme of ^{134}Cs consistent with the results of the present experiments and the β-spectra observed by Van Wijngaarden and Connor (Van Wijngaarden 1964). The β-feeds shown in Fig. 3-6 are calculated by intensity balance of transitions feeding and de-exciting the levels. They agree within the experimental error with those observed by Van Wijngaarden and Connor. There is no evidence for the levels at

Fig. 3-6

Level scheme of ^{134}Ba observed in the beta-decay of ^{134}Cs.

A.E.C.L. Ref. # A-3107-G

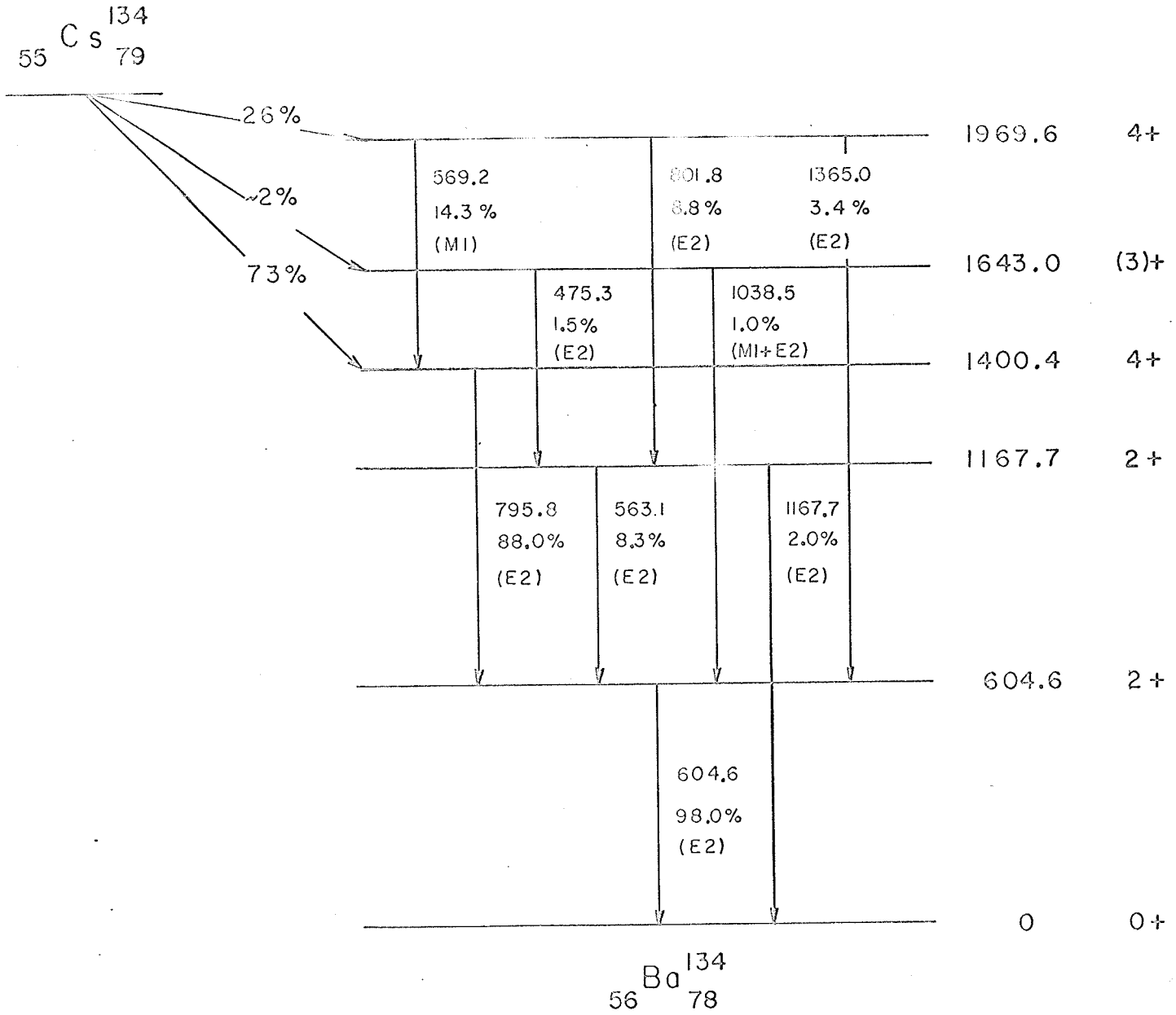

1570 and 1770 keV suggested by some previous workers. This agrees with the analysis of Schriber and Hogg. (Schriber 1963) The level at 1643 keV had been given a tentative spin assignment of 3+ based on the probable M1 + E2 character of the 1038 keV transition.

In the time since these results were published (January 1965) other groups have investigated this isotope (Comite 1965, Bashandy 1966) and their results are not in agreement with the present work. More recently however Abdul-Malek and Naumann (Abdul-Malek 1968) have re-investigated the decay of ^{134}Cs with a Ge(Li) detector and a six-gap orange spectrometer. Table 3-III compares their results with those obtained in the present work and shows them to be in good agreement.

Angular correlation studies of the transitions de-exciting the 1643 keV level have been reported by Hsu and Emery (Hsu 1968). Their values for the A_2 and A_4 coefficients for the two cascades are

$\gamma 475 - \gamma 1168 \quad A_2 = -0.255 \pm 0.075 \quad A_4 = -0.15 \pm 0.11$

$\gamma 1038 - \gamma 605 \quad A_2 = 0.101 \pm 0.002 \quad A_4 = 0.006 \pm 0.003$

These values together with the multipolarity assignments reported in the present work establish the spin of the 1643 keV level as 3+ in agreement with the previously postulated value.

Also shown in Table 3-III are the results of a recent investigation of this isotope by Raeside et al (Raeside 1967). In addition to studying the gamma-ray spectrum with a Ge(Li) detector and performing Ge(Li) - NaI(Tl) coincidence experiments, this group examined the low energy region with a 2m curved-crystal spectrometer. The results of the curved-crystal studies revealed two hitherto unseen gamma-rays with energies 242.694 ± 0.041 and

COMPARISON OF RELATIVE INTENSITIES OF GAMMA-RAY TRANSITIONS IN ^{134}Ba

GAMMA-RAY ENERGY (keV)		*RELATIVE INTENSITIES % per disintegration		
PRESENT WORK	RAESIDE	PRESENT WORK	ABDUL-MALEK	RAESIDE
	242.694±0.041			0.02±0.01*
	325.512±0.095			0.02±0.01*
475.26±0.10	475.355±0.038	1.5±0.15	1.4±0.2	1.51±0.16
563.11+0.12	563.325±0.041	8.3±0.8	8.7±1.0	8.96±0.84
569.24±0.12	569.371±0.047	14.2±1.4	15.0±1.6	15.81±1.1
604.64±0.12	604.774±0.027	97.5	98.0	98.04
795.80+0.16	795.806±0.050	87.8±9	88.4±9.1	87.79±6.6
801.80±0.16	801.86±0.28	8.8±1.5	9.2±1.0	8.94±0.8
1038.46±0.20	1038.61±0.49	1.03±0.1	1.1±0.6	1.02±0.08
1167.65±0.25	1167.99±0.39	1.94±0.15	1.9±0.2	1.96±0.22
1364.97±0.28	1365.08±0.32	3.37±0.30	3.3±0.3	3.25±0.32

* Obtained from curved-crystal studies.

326.512 ± 0.095 keV. The intensity of each transition is given as 0.02 ± 0.01% per disintegration which explains why they were not seen in the present work. Both gamma-rays have been fitted into the level scheme presented herein with the higher energy one fitting between the 1970(4+) and 1643(3+) keV levels and the lower one between the 1643(3+) and 1400(4+) keV levels.

3.8 Discussion

In 1961 Sheline et al (Sheline 1961) proposed that in addition to the already well established regions of nuclear deformation in the periodic table, there should exist a region of deformed nuclei among the neutron deficient rare-earth elements. Marshalek et al (Marshalek 1963) have performed theoretical calculations over large regions of the nuclear periodic table to determine the deformation of and the energy difference between spherical and deformed nuclei as a function of nucleon numbers. They concluded that a deformed region should exist with N and Z between 50 and 82 and on the basis of the experiments by Sheline et al (Sheline 1961) on ^{126}Ba, ^{128}Ba and ^{130}Ba, which were performed in conjunction with this theoretical work, concluded that these Ba nuclei were deformed.

Preliminary results of Gerschel et al (Gerschel 1964) confirmed Sheline's results on the first excited 2+ states and in addition reported 4+ and 6+ states in ^{126}Ba and ^{128}Ba which were interpreted as rotational states. More recent experiments by Clarkson et al (Clarkson 1967) on ^{124}Ba and ^{126}Ba have confirmed the rotational nature of the levels in these isotopes. Gerschel also points out that the region from ^{130}Ba up to singly magic ^{138}Ba should form a transition region from deformed

to nearly spherical nuclei. The levels of these isotopes should therefore be expected to exhibit vibrational characteristics.

The recent results of Gerschel et al (Gerschel 1965) on the decay of ^{130}La and ^{132}La, into ^{130}Ba and ^{132}Ba respectively, lend support to this contention. Their results indicate that both of these isotopes have second excited 2+ states at about 2.2 times the energy of the first 2+ state. In addition 3- states are indicated in agreement with the systematics of octupole vibrations in this region (Hansen 1963). A comparison of the low lying levels in the even-even Ba isotopes is given in Fig. 3-7. The level schemes were taken from the references discussed in this section.

The level scheme shown for ^{134}Ba is based upon the present work and the ^{134}La studies of Julian and Jha (Julian 1967). A 780 keV gamma-ray had been reported in the ^{134}La studies of Ricci et al (Ricci 1965) and in the preliminary results of Julian and Jha (Julian 1964). This gamma-ray was originally thought to de-excite a 0+ level at 1365 keV to the 605 keV level but further studies by the latter authors showed that this transition belonged to the ^{135}Ce contaminant in their source (Julian 1968). Julian's results also show that the log ft. values calculated for the transitions to the higher excited states in ^{134}Ba indicate allowed transitions. This would exclude the interpretation of the 2335 keV level as the 3- state as proposed by Ricci et al (Ricci 1965).

The decay scheme shown for ^{136}Ba is based upon the work of Reising and Pate (Reising 1965) and Julian (Julian 1968). Reising interprets the first 2+ and 4+ states as arising from the one-phonon

Fig. 3-7

Comparison of the low lying energy levels in the even-even barium isotopes.

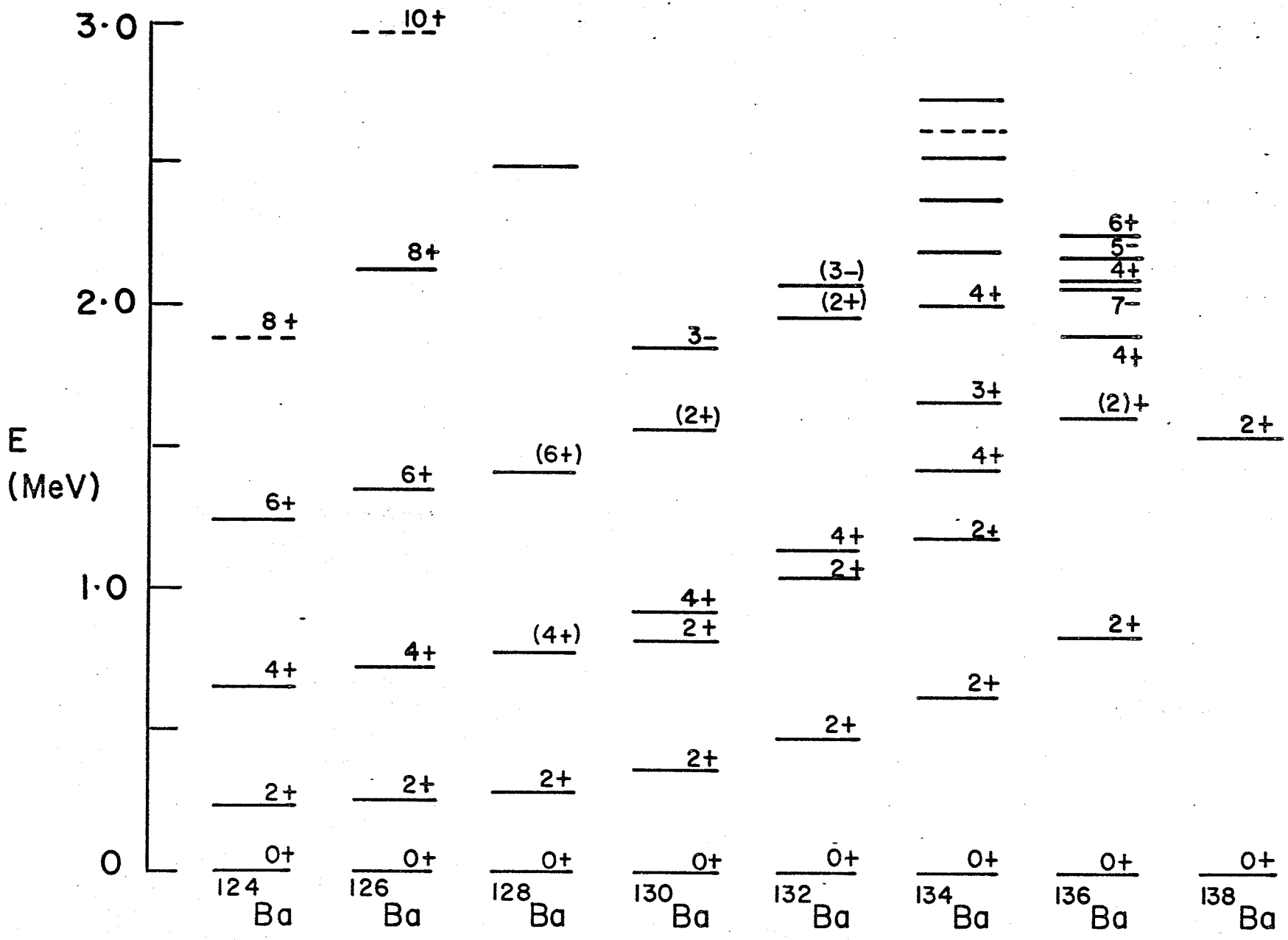
3·0
2·0
1·0
0
E
(MeV)
10+
8+
8+
6+
6+
(6+)
6+
4+
4+
(4+)
4+
2+
2+
2+
0+
0+
0+
0+
124 Ba
126 Ba
128 Ba
3-
(2+)
4+
2+
2+
130 Ba
(3-)
(2+)
4+
2+
2+
0+
132 Ba
4+
3+
4+
2+
2+
0+
134 Ba
6+
5-
4+
7-
4+
(2)+
2+
0+
136 Ba
2+
0+
138 Ba

and two-phonon vibrational states respectively. The (2)+ level at 1579 keV is seen in the decay of ^{136}La and it seems plausible to interpret this as the 2+ state arising from the two-phonon vibrations. The other levels appear to be of quasi-particle nature and can be explained by shell model predictions (Reising 1965).

Since the low lying levels in the nuclei surrounding ^{134}Ba can be interpreted as being of a vibrational nature it seems natural to interpret the levels in ^{134}Ba similarly. The first excited 2+ level is then identified with the one-phonon vibration, the second 2+ and the 4+ levels with the two-phonon vibration. As pointed out by Julian (Julian 1967), the first 2+ state cannot be described as a pure harmonic oscillator state since two-phonon transitions are forbidden and the 1168 keV transition is quite strong. Further investigation of the high energy region is necessary before anything definite can be said about the nature of the high lying states.

In the transition region between rotational and vibrational nuclei it is also possible to interpret level schemes on the basis of the Davydov and Fillipov (Davydov 1958) asymmetric rotor model. In Table 3-IV the relative spacings of the levels in ^{134}Ba are compared with those predicted by the asymmetric rotor model for a value of $\gamma \simeq 30^{o}$. The agreement is reasonably good except for the second 4+ state which occurs at too low an energy. The dominantly M1 character of the 570 keV transition from this level to the first 4+ state at 1400 keV also indicates that it is probably not a pure asymmetric rotor state.

The experimental ratios for both the 2+ and 3+ levels

are slightly lower than the predicted value. Das Gupta and Gunye (Das Gupta 1964) have considered the generalized Davydov theory (Davydov 1961) and applied their calculations to ^{192}Pt. This theory uses only collective co-ordinates and therefore the predictions depend principally upon the shape of the nucleus and not on the individual particle states. The shape of ^{134}Ba might be expected to be similar to ^{192}Pt, as there are 78 neutrons in ^{134}Ba and 78 protons in ^{192}Pt and about 12% of the other particles (or holes) are outside the nearest closed shell. The results of Das Gupta and Gunye for $\gamma = 30^{o}$ are compared with the experimental data for ^{134}Ba. This gives slightly better agreement than the pure asymmetric rotor model. No attempt has been made to optimize the parameters in Das Gupta and Gunye's paper. For ^{134}Ba they would probably differ slightly from those applicable to ^{192}Pt.

Table 3-IV

COMPARISON OF LEVEL SCHEME OF ^{134}Ba WITH THEORETICAL PREDICTIONS

	$E_{2+'}/E_{2+}$	E_{4+}/E_{2+}	E_{3+}/E_{2+}	$E_{4+'}/E_{4+}$	$\frac{B(E2;\ 2+' \rightarrow 0+)}{B(E2;\ 2+' \rightarrow 2+)}$
Experimental	1.95	2.32	2.72	3.25	~ 0.006
Asymmetric Rotor ($\gamma = 30^{o}$)	2.00	2.67	3.00	5.66	0
Das Gupta and Gunye	2.04	2.48	2.81		0

CHAPTER IV

Gamma-Gamma Coincidence Experiments

4.1 Introduction:

Coincidence experiments have many applications (e.g. measurements of lifetimes, angular correlations, etc.) but only two of these applications will be made use of in this thesis -- the fitting of gamma-rays into a decay scheme and the intensity measurement of weak transitions. With NaI(Tl) spectrometers the poor resolution not only masked weak gamma-rays but also closely spaced doublets. Coincidence experiments were needed to identify such transitions.

The introduction of the Ge(Li) detector has illustrated the complexity of many decay schemes by revealing hitherto unseen gamma-rays so the need for coincidence experiments is greater than ever. Until recently the small volume and low efficiency of planar detectors limited coincidence experiments to one Ge(Li) detector and one NaI(Tl) detector. However the introduction of large volume coaxial diodes now permits the use of Ge(Li) detectors on both sides of the experiment. The decision as to whether a NaI(Tl)-Ge(Li) or Ge(Li)-Ge(Li) system should be used depends upon the experiment in question. There are undoubtedly many cases where the former system is adequate and in some cases even preferable. There are also however many cases in which the spectrum is too complex to allow NaI(Tl) detectors to be used. It is in these cases that the Ge(Li)-Ge(Li) system provides a powerful and indispensible tool.

The following sections of this chapter describe some of the timing characteristics of Ge(Li) detectors and the coincidence technique used for the experiments discussed in Chapter V and VI.

4.2 Timing Characteristics of Ge(Li) Detectors

Pulses from NaI(Tl) spectrometers are particularily suited for coincidence studies since the pulse shape is constant and determined by the decay time of the crystal. This however is not the case with Ge(Li) detectors since the rise time of the pulse depends upon the time taken to collect the electrons and holes. Several papers have been written on the subject (Graham et al, 1966, Strauss et al, 1966, Ewan et al, 1966a) so only a brief review of the timing characteristics will be given here. Fig. 4-1 to 4-5 are taken from the papers by Graham and Ewan.

The pulse shape from lithium-drifted detectors depends upon several things including the depth of the detector, the electric field distribution, the mobilities of electron and holes and the position at which the electrons and holes are produced (Goulding, 1965). Fig. 4-1 gives a very simplified representation of the situation. The upper left hand diagram shows a schematic of a planar detector, with the + and - signs indicating three different positions in which electrons and holes can be produced. For simplicity the mobilities of both carriers are taken to be the same. If the electron hole pairs are produced at the center of the detector, then the time taken to collect the charge will be approximately one half of that taken when they are produced close to either the p or n side of the diode. These two rise times correspond to the solid lines shown in the diagram in the lower left of Fig. 4-1 (Ewan et al 1966a) For electron-hole pairs produced elsewhere in the detector, the rise of the pulse starts off rapidly, until one carrier is collected, and then builds up with a rise time

Fig. 4-1

The left-hand side illustrates schematically the pulse shape from events occurring at different positions in a planar detector. The right-hand side shows the timing distribution observed with an RCA 5mm detector using leading edge timing. The apparatus is shown schematically in the upper right.

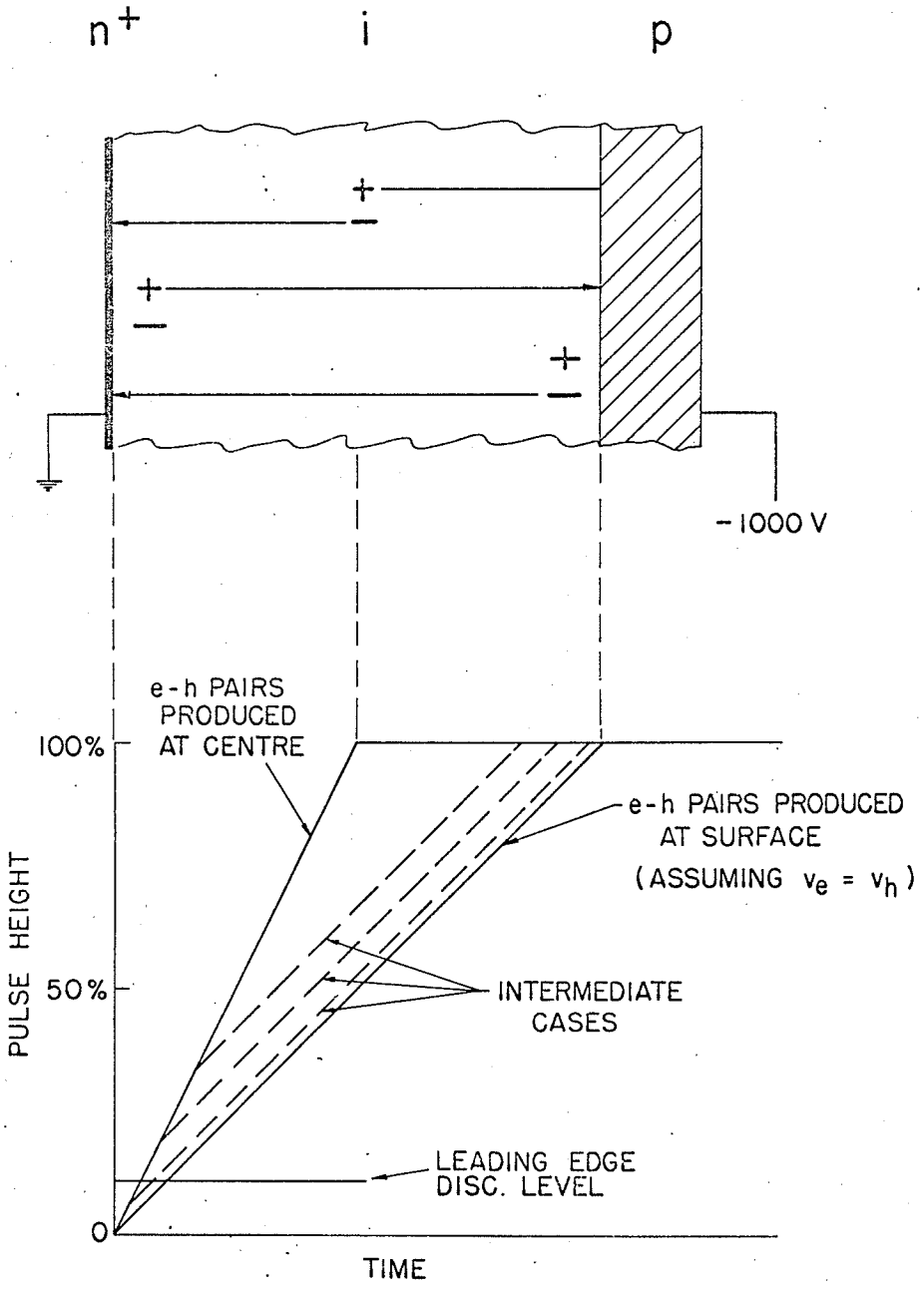
n+
i
p
+
−
+
−
+
−
−1000 V
e-h PAIRS PRODUCED AT CENTRE
100%
e-h PAIRS PRODUCED AT SURFACE
(ASSUMING $v_e = v_h$)
INTERMEDIATE CASES
50%
LEADING EDGE DISC. LEVEL
0
PULSE HEIGHT
TIME

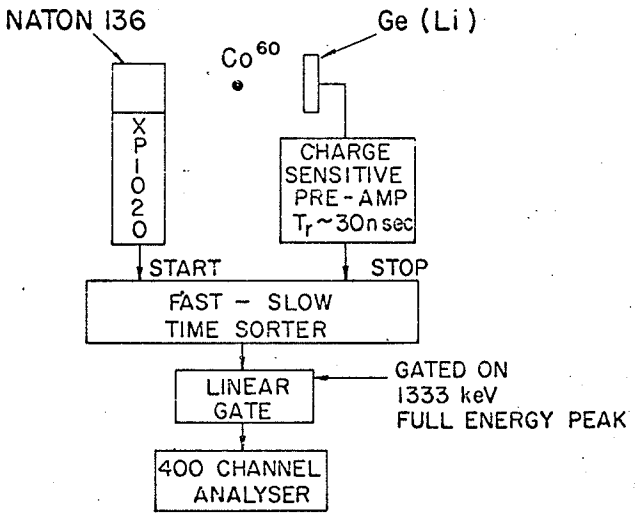
NATON 136
Co60
Ge (Li)
XP1020
CHARGE SENSITIVE PRE-AMP
T_r ~30n sec
START
STOP
FAST – SLOW TIME SORTER
LINEAR GATE
GATED ON 1333 keV FULL ENERGY PEAK
400 CHANNEL ANALYSER

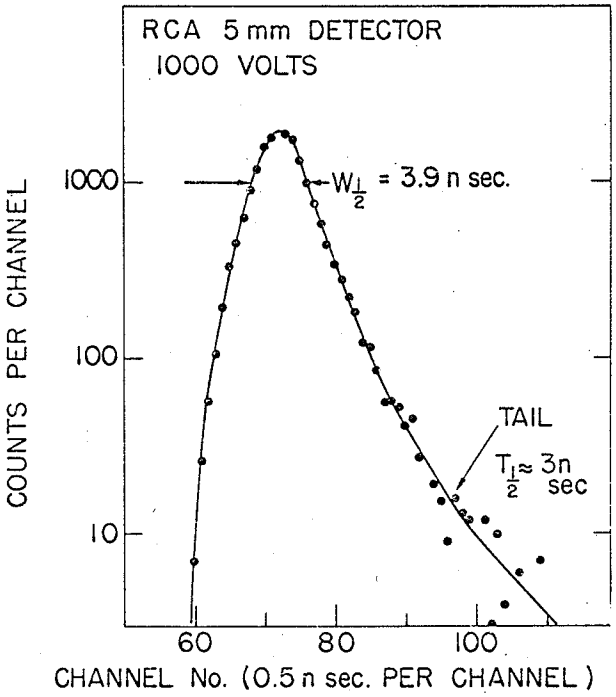
RCA 5 mm DETECTOR
1000 VOLTS
1000
100
10
$W_{\frac{1}{2}}$ = 3.9 n sec.
TAIL
$T_{\frac{1}{2}} \approx$ 3n sec
COUNTS PER CHANNEL
60
80
100
CHANNEL No. (0.5 n sec. PER CHANNEL)

equivalent to the transit time of the other carrier.

In actual fact the situation is considerably more complicated since the carriers do not have the same mobility. The velocities of electrons and holes depends upon the electric field strength until fields of > 2000 V/cm are reached, at which stage they approach a saturation velocity of ~ 1.5×10^7 cm/sec (Prior 1960, Goulding 1966). The electric fields in detectors are also not uniform and this together with trapping, recombination and multiple interactions causes a spread in rise times.

It is quite common in NaI(Tl) work to use a cross-over pick off (C.O.P.O) unit to derive the time pulse. This timing signal corresponds to the time taken to reach one half of full pulse height. The large spread in times required to reach this level in Ge(Li) detectors makes this method unsuitable so leading edge timing must be used. Even with the discriminator set as low as possible there still arises the problem of "walk" with pulse height. Some pulses trigger the discriminator later than others and a tail appears on the time distribution. A typical example of a prompt timing distribution from ^{60}Co gamma-rays is shown in the lower right hand corner of Fig. 4-1 (Ewan et al 1966) with a schematic diagram of the equipment used to obtain it shown above. As can be seen from the diagram, the full width at half maximum is 3.9 nsec but there is also a tail with a slope of ~ 3 nsec. The tail limits the life-time that can be measured from the slope of the time distribution.

As already mentioned, both the size of the detector and the field across it affect the pulse rise time and hence the resolution curve. Full widths at half maximum from ~ 2 nsec for

Fig. 4-2

Measurement of charge collection times in Ge(Li) coaxial detectors at 77 K. A schematic diagram of the apparatus used for the measurements is shown on the left of the figure. Oscilloscope traces corresponding to the full-energy 511 keV peak are shown on the right for two different source positions.

A.E.C.L. Ref. # A-3209-H

CHARGE COLLECTION TIME IN Ge(Li) COAXIAL DETECTORS

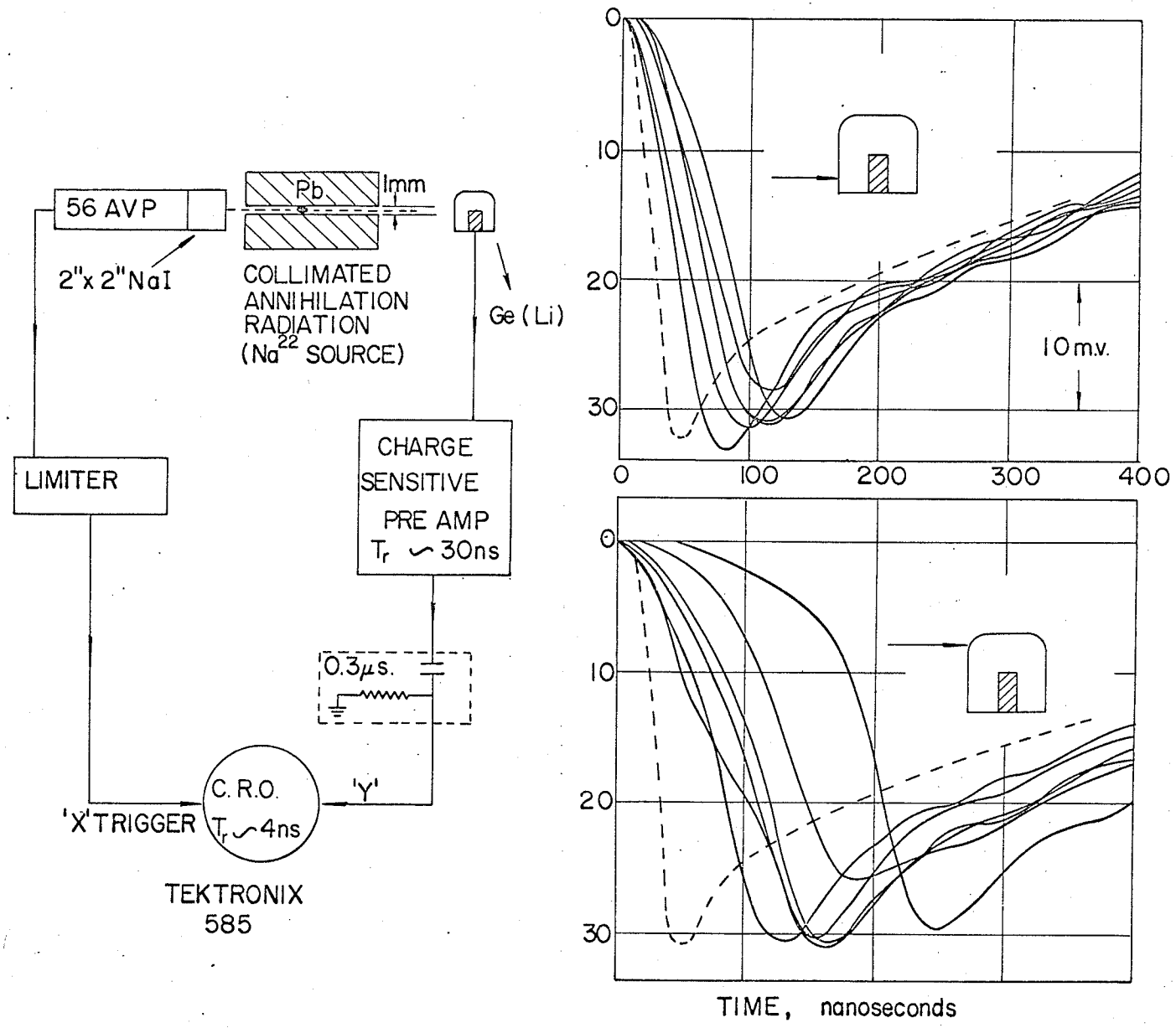

a 2 mm detector (Pigneret et al 1966) to 6.0 nsec for a 10 mm deep detector (Ewan et al 1966a) have been reported.

The small volume and low efficiency of the planar detector however limits its use in coincidence studies. As a result larger volume coaxial detectors were developed as already mentioned in Chap. I. The first of these detectors developed had one closed end and one open end. Detailed studies of the depletion depths of these detectors have been made by Malm (Malm et al 1966).

The electric fields produced in these detectors are very non uniform and as a result, the pulse rise time is very dependent upon where the gamma-ray interacts with the detector. This variation in pulse rise time with position is illustrated in Fig. 4-2 (Graham et al 1966). A positon emitting source ^{22}Na was placed between two lead blocks to produce a narrow (1 mm wide) beam of 511 keV gamma-rays. An oscilloscope was triggered by one of the annihilation quanta detected in a NaI(Tl) detector and the output pulses from the Ge(Li) detector were displayed. The only pulses shown in the diagram are those corresponding to the full-energy peak.

The pulse shapes were observed at several positions across the detector with the beam of gamma-rays aimed at the coaxial region (upper right hand diagram). The rise time (10% to 90% of maximum pulse size) can be seen to be ~ 50-80 nsec. The dashed line shows the rise time of a mercury pulser. When the beam is shone into the closed end region, as shown in the lower diagram, the pulse rise time is seen to be longer and there is considerable variation in the pulse shape.

Fig. 4-3 (Graham et al 1966) shows the variation in

Fig. 4-3

Dependence of time spectra as a function of axial position of the source in a coaxial Ge(Li) detector having sharp edges and a radial depletion depth of about 7mm.

A.E.C.L. Ref. # A-3229-A

POSITION DEPENDENT TIME SPECTRA IN COAXIAL DETECTORS

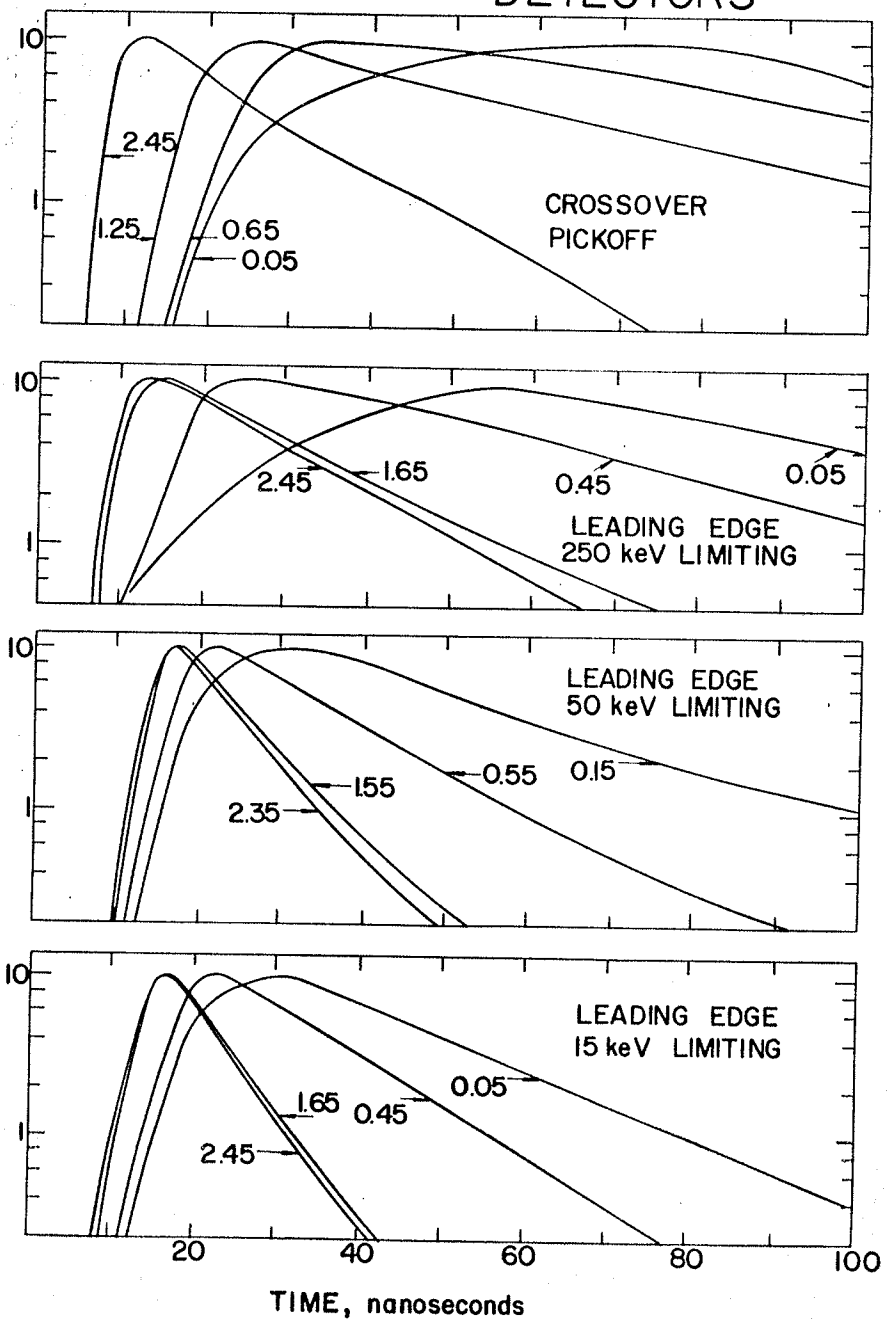

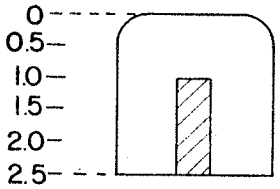

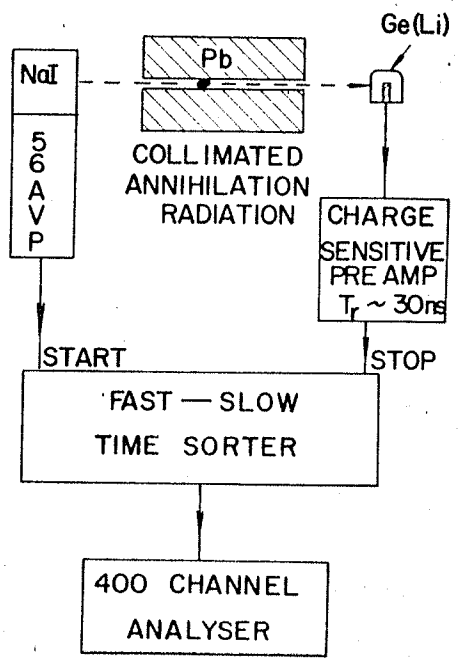

time spectra with position. The upper curve was taken using cross-over pick off timing while the lower three used leading edge timing with the discriminator set at different levels. It is apparent from these figures that there is a large spread in F.W.H.M. with position but that leading edge timing produces a much smaller variation than cross-over pick off. These detectors are therefore only useful for coincidence experiments where resolving times of $2\tau \sim 50$ nsec are acceptable.

The next step in the development of large volume detectors was the cylindrical coaxial detector with both ends open. An example of the time spectra obtained from such a detector is shown in Fig. 4-4. The curve on the left shows a full width at half maximum of 9 nsec and a full width at one tenth maximum of 19 nsec. This should be compared to the curve on the right obtained with cross-over pick off timing which shows a full width at one tenth maximum of 39 nsec. (Malm 1966)

The timing experiments discussed so far have involved one Ge(Li) detector and one NaI(Tl). The large volume coaxial diodes make it feasible to use Ge(Li) detectors on both sides of the coincidence arrangement. Time spectra with two Ge(Li) detectors have been reported by Ewan (Ewan 1966a) and an example is shown in Fig. 4-5. This curve was obtained using two cylindrical double open-ended coaxial detectors which were both gated on the 511 keV full-energy peaks. One of the detectors had a depletion depth of 9.5 mm while the other was only 7.5 mm deep. Sec. 4.5 of this thesis illustrates one of the timing problems which can arise when two of these detectors with unequal depletion depths are used in a coincidence experiment.

Fig. 4-4

A comparison of time distributions using leading-edge and cross-over pickoff triggering.

A.E.C.L. Ref. # A-3260-B

TIME DISTRIBUTIONS FOR Ge(Li) COAXIAL DIODE No. GLC6X
BIAS = 1000 VOLTS

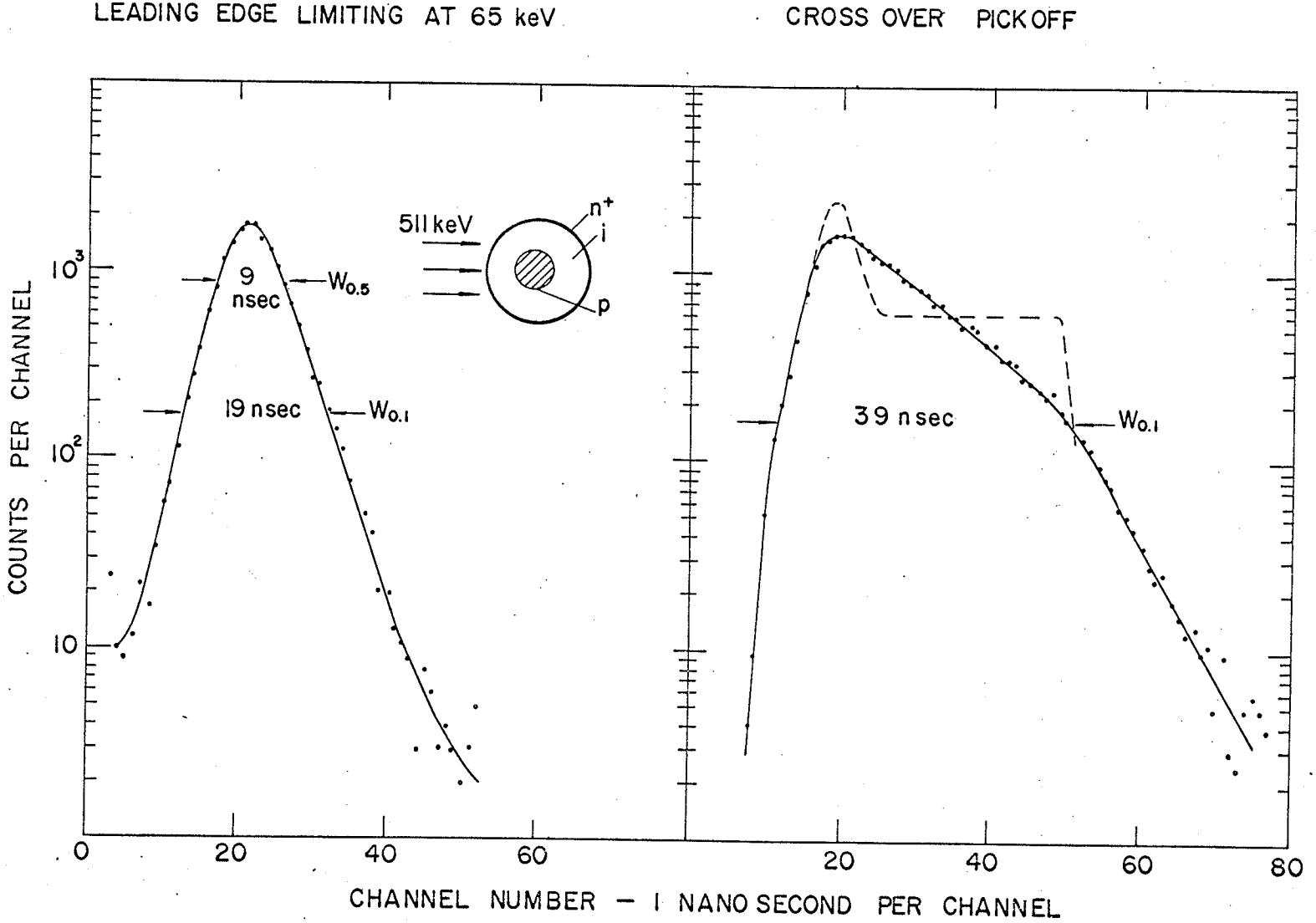

Fig. 4-5

Time resolution curve observed with two coaxial Ge(Li) detectors. A ^{22}Na source was used and the side channels selected the 511 keV full-energy peaks.

A.E.C.L. Ref. # A-3279-F

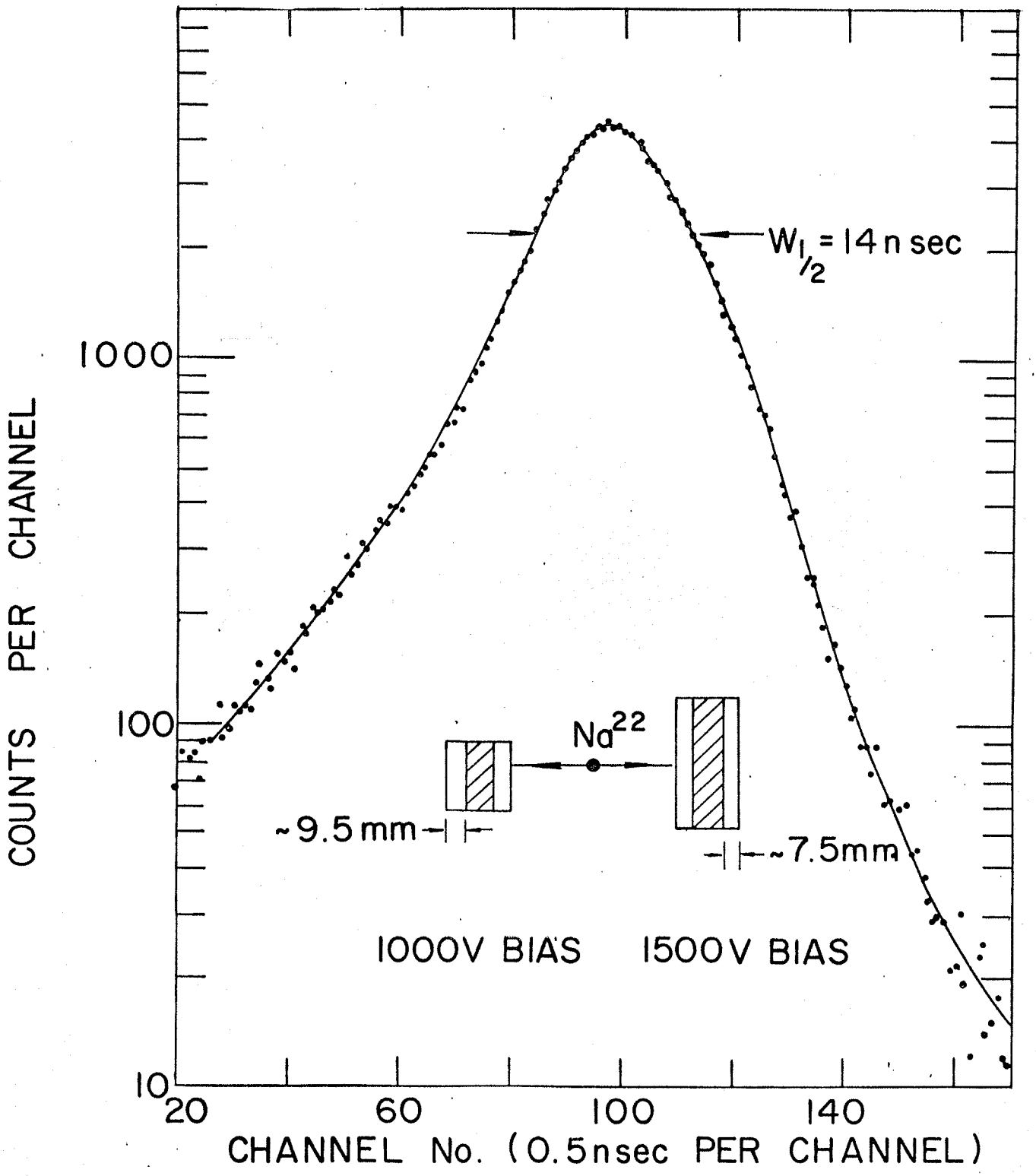

From this brief review of timing characteristics it is evident that the best timing resolution comes from planar diodes.

The type of Ge(Li) detector used in a particular experiment is governed to a large extent by the nucleus under investigation. If the decay scheme is such that low energy gamma rays are in coincidence with high energy ones, then it would be very advantageous to use a thin window planar detector ~ 1 cm deep on one side of the coincidence experiment and a large volume coaxial diode on the other side. However if the coincident gamma rays are all of high energy then large volume coaxial detectors should be used on both sides of the experiment. If long resolving times can be tolerated (50-100 nsec) then single open ended detectors are adequate. However if faster resolving times are needed, then double open-ended diodes must be used.

4.3 Coincidence Apparatus

A block schematic of the apparatus used for the gamma-gamma coincidence experiments reported in this thesis is shown in Fig. 4-6. With the exception of the linear amplifier and biased amplifier, which were manufactured by Tennelec and the preamplifier which was built at C.R.N.L., the equipment was all supplied by Ortec.

The detectors used in these experiments were produced at C.R.N.L. by the counter development section. Two of them were double open ended coaxially drifted Ge(Li) detectors, one having an active volume of 44 cc and the other an active volume

Fig. 4-6

Block schematic of the electronic equipment used for the gamma-gamma coincidence experiments.

3379-D

COINCIDENCE SYSTEM

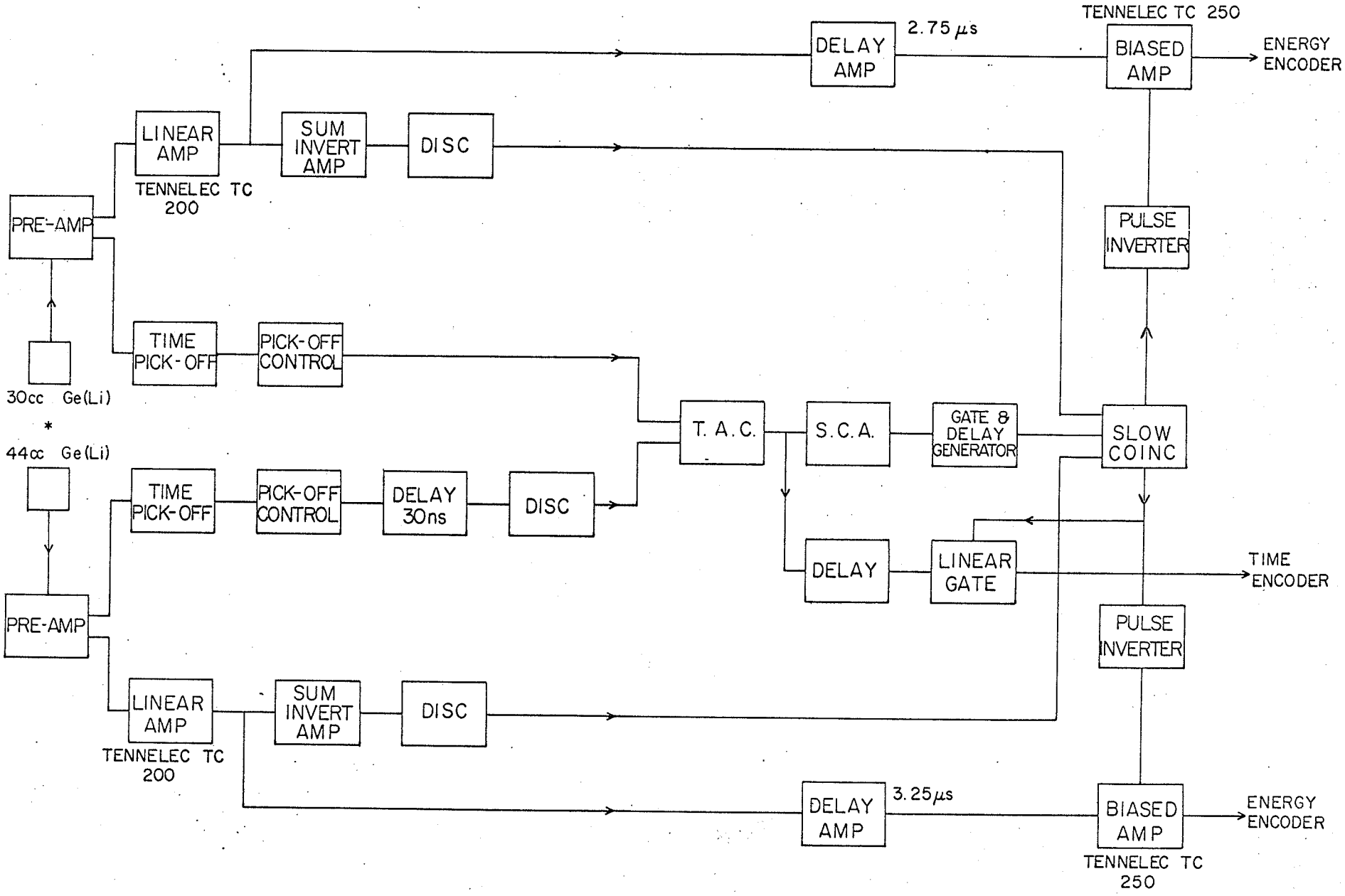

of 30 cc. The 44 cc diode (code number G9C2) was 63 mm long with an external diameter of 31.5 mm and a dead core 7 mm in diameter. The resolution of this detector has been measured to be 2.75 keV on the 1173 keV photopeak in ^{60}Co, using low counting rates, and has a photopeak to Compton ratio of approximately 20:1 at this energy. An example of its performance is shown in Fig. 4-7. The 30 cc detector (code no. GLC6X) had a resolution of 5 keV at the same energy. All of the diodes were operated at liquid nitrogen temperature in essentially the same kind of cryostat as described in Chap. I. The preamplifier has already been described in that section so nothing further will be said about it here.

As can be seen from Fig. 4-6, the system used was essentially a fast-slow type of coincidence arrangement. Pulses from each preamplifier were split two ways, one to produce a linear signal for energy analysis and the other to produce a timing pulse for the fast coincidence unit. The "linear output" was fed to a linear amplifier (Tennelec TC200) where amplification and pulse shaping were performed. Two outputs were then taken from this amplifier. One of these was delayed and sent into a biased amplifier and stretcher (Tennelec TC250). This unit was used to produce unipolar rectangular shaped pulses for the encoders in the computers. It was gated by a signal from the slow coincidence unit (Ortec model 409) so that only specially selected events were passed to the computer for analysis. The other output from the linear amplifier was fed into a 'sum-invert' amplifier (Ortec model 433 used here only as an inverter) and then into a discriminator (Ortec model 420). This discriminator fed pulses

Fig. 4-7

The upper portion of the figure shows the ^{60}Co gamma-ray spectrum observed with coaxial detector G9C2.

The lower portion shows an expanded view of the two photopeaks and the insert shows the dimensions of the detector.

A.E.C.L. Ref. # A-3364-B

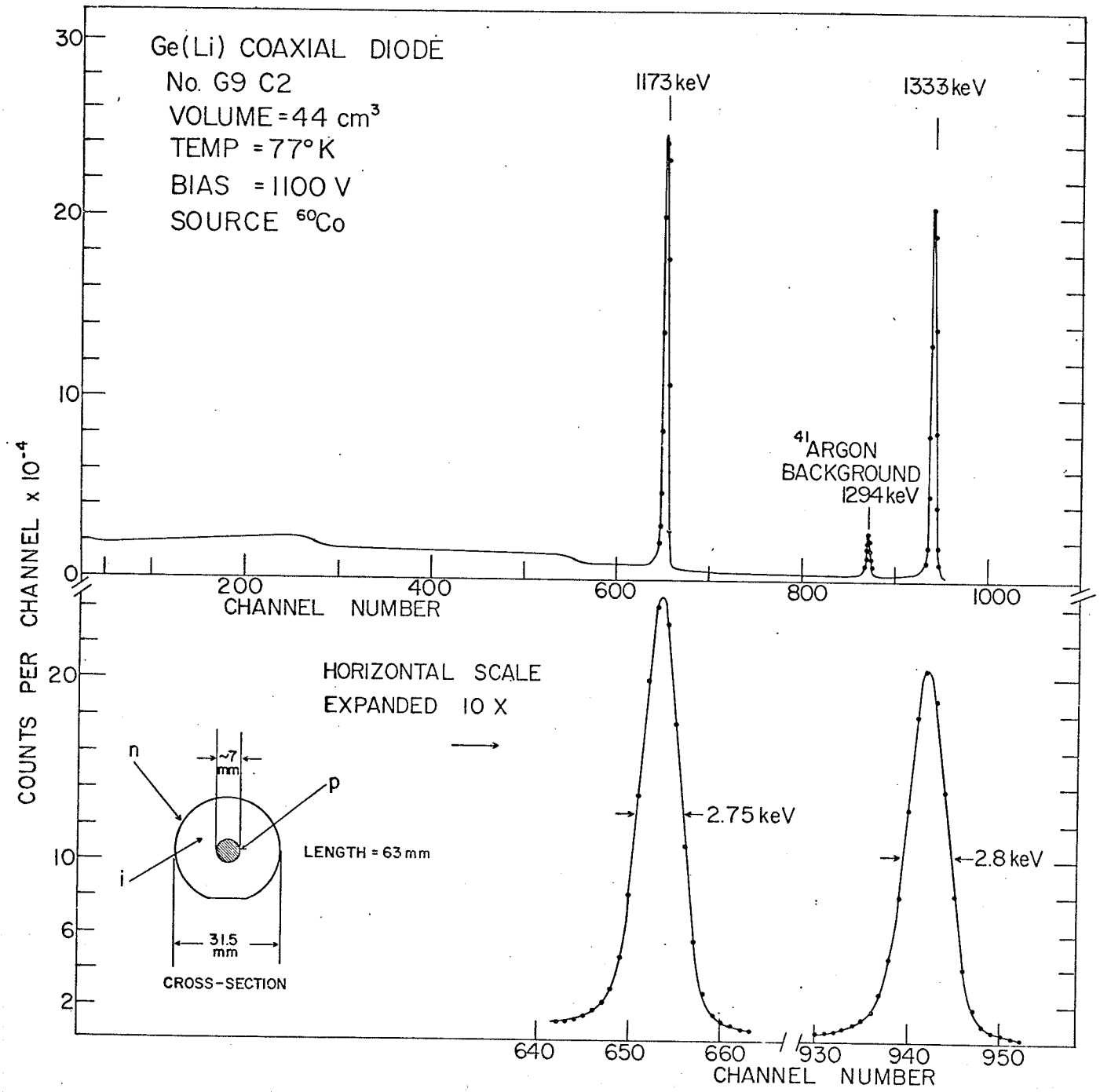

to one of the slow coincidence inputs whenever the incoming pulse was above a certain minimum.

The other pulse from the preamplifier was fed into a time pickoff unit (Ortec model 260) and then into a time pickoff control unit (Ortec model 403) which was used to set the level at which timing pulses were produced. The output pulses from this unit were fast rising tunnel diode pulses (~ 5.0 nsec) which were then used as "start" and "stop" pulses for a time to amplitude converter (Ortec model 437). Time delays were inserted as required to match up the delays through the preamplifier and time pickoff units. The time to amplitude converter (T.A.C.) was used as the fast coincidence part of the system.

The T.A.C. output was split and one output was fed to a single channel analyser (S.C.A.) (Ortec model 420). When the data were collected on the PDP-8 computer, this S.C.A. was used to set the time window on the T.A.C. output. Its output was subsequently sent through a gate and delay generator (Ortec model 416) in order to provide a suitably delayed pulse for the third input to the slow coincidence unit. When the PDP-1 was used to collect the data, the S.C.A. was used in the integral mode to give a slow coincidence input for any pulse above a required level. The other output from the T.A.C. was delayed and sent through a linear gate (Ortec model 409) which was gated from the slow coincidence unit. Thus in the PDP-1 mode of operation, three pulses were sent to the computer, two of which had met certain energy requirements and the third contained the time relationship between them. In the PDP-8 mode only the energy pulses were fed

to the computer the time relationship between them having been preselected by the S.C.A. on the T.A.C. output.

4.4 Fast Counting Rate Effects

It is inevitable that somewhere in the amplifier-preamplifier system there must be AC coupling betweeen stages. To optimize the signal to noise ratio single RC shaped pulses are preferable to double differentiated pulses produced either by RC or delay line shaping. When an exponentially decaying pulse is fed to a differentiating circuit, the output pulse has a fall time determined by the differentiator but also has a long undershoot, the time constant of which is determined by the decay time of the original pulse. When fast counting rates are used, this undershoot leads to "pile-up" problems and, as a result, a loss in resolution. Under overload conditions, this undershoot can be severe enough to saturate the amplifier during a large portion of the under shoot leading to excessive dead time.

With the low photopeak efficiency of even large volume Ge(Li) detectors, it is necessary to use high counting rates (15,000-20,000/sec) in order to give reasonable counting rates in coincidence experiments. Detailed studies of the requirements for nuclear pulse amplifiers have been made by several groups and their results appear in the literature (Blankenship and Nowlin 1966, Goulding 1967). A method commonly used to eliminate the undershoot from RC clipped pulses is the "pole-zero" technique and the amplifiers used in the coincidence experiments reported in this thesis were modified in this way. Fig. 4-8 illustrates schematically the technique and the pertinent mathematics is

Fig. 4-8

Mathematical description of a pole-zero compensation network. The upper half shows the pulse shape with no pole-zero compensation while the lower half illustrates the cancellation network.

NO POLE-ZERO COMPENSATION

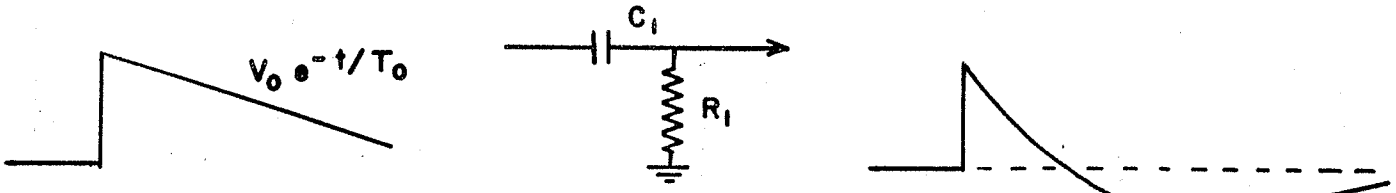

INPUT PULSE SHAPE x TRANSFER FUNCTION = OUTPUT WAVEFORM

$$V_0 e^{-t/T_0} \quad x \quad G(t) \quad = \quad V_1(t)$$

$$\frac{V_0}{(S + 1/T_0)} \; x \; \frac{S}{(S + 1/R_1 C_1)} \quad = \quad V_1(s) \qquad \text{LAPLACE TRANSFORM}$$

$$\frac{V_0}{T_0 - T_1} \left[T_0 e^{-t/T_1} - T_1 e^{-t/T_0} \right] = V_1(t) \quad \text{WITH} \quad T_1 = R_1 C_1$$

POLE ZERO CANCELLATION

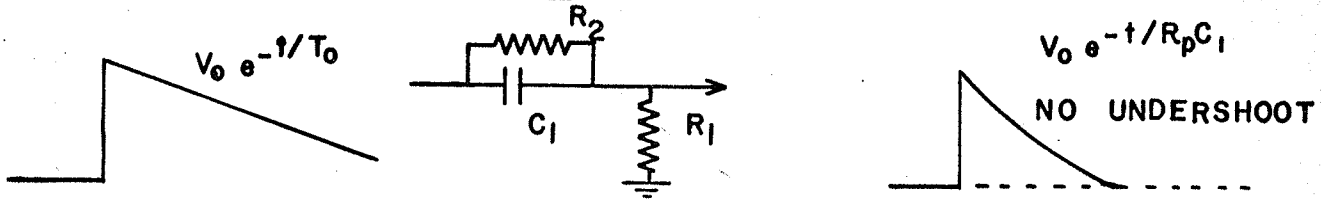

$$V_0 e^{-t/T_0} \quad x \quad G(t) \quad = \quad V_1(t)$$

$$\frac{V_0}{S + 1/T_0} \; x \; \frac{S + 1/R_2 C_1}{S + \dfrac{R_1 + R_2}{R_1 R_2 C_1}} \quad = \quad V_1(S) \qquad \text{LAPLACE TRANSFORM}$$

POLE-ZERO CANCELLATION BY SETTING $S + 1/T_0 = S + 1/R_2 C_1$

$$\frac{V_0}{S + \dfrac{R_1 + R_2}{R_1 R_2 C_1}} = \frac{V_0}{S + \dfrac{1}{R_p C_1}} = V_1(S) \qquad R_p = \frac{R_1 R_2}{R_1 + R_2}$$

$$V_0 e^{-t/R_p C_1} = V_1(t)$$

included in the diagram. Effectively what happens is a portion of the incoming pulse is fed across the capacitor by the resistor and added on to the differentiated pulse cancelling out the undershoot. This method is applicable only when the DC voltages on either side of the capacitor are the same or very nearly the same and when single time constants are used for pulse shaping. The combination of the bleeder resistance and the coupling capacitance must have the same time constant as the incoming pulse.

The preamplifiers were AC coupled to the main amplifiers and no pole-zero compensation was used at these points. In order to overcome baseline shift at high rates, it was necessary to use double RC pulse shaping in the main amplifier. The best resolution at high counting rates was obtained by using double RC pulse shaping and "adjusting" the pole zero compensation. A deterioration was observed in resolution from 2.75 keV, with slow counting rates and single RC pulses, to about 4.0 keV with high rates (~ 25,000 cps) and this modified pole-zero compensation.

4.5 Related Address Technique

In gamma-gamma coincidence experiments using NaI(Tl) detectors the standard procedure for many years has been to set a window with a single channel analyser on a full energy peak in one detector and use a multichannel analyser to record all the events in coincidence with that gamma-ray from the other detector. The accuracy with which this type of experiment could be performed was determined largely by the stability of the window. With the fairly wide photo-peaks from a NaI(Tl) spectrometer and the improvement in electronics over the last

decade, good stability can be achieved quite readily. However with the advent of Ge(Li) detectors the picture has changed somewhat. Provided the experiments are being done with one NaI(Tl) detector and one Ge(Li) detector, and the windows are set on the NaI(Tl) side, then no difficulties arise. If the windows are to be set on the Ge(Li) side then the narrowness of the Ge(Li) peaks makes the requirements on stability all the more severe.

Another drawback with the above type of system is the limitation on the number of windows that can be set at the one time. In order to determine the events coincident with the Compton distribution under the photopeak, it is necessary to move the window just off the photopeak and repeat the experiment. It is also necessary to repeat the run again in order to measure the accidental coincidences, which can be appreciable if the counting rates are high. All of this is very time consuming and if the radioactive source under study has a short half life, the corrections to the data can be quite complicated.

If two Ge(Li) detectors are used, the low detection efficiency means that long runs are needed for each of the above measurements. This in turn means that the results are extremely sensitive to the overall stability of the system. In view of these requirements it seems desirable to have a system which records all of the above information simultaneously. The introduction of small digital computers for on-line experiments in recent years has provided the necessary tool for such a system. The system used in the coincidence experiments reported herein is referred to as the "Related Address Technique" and a description of this technique follows.

Two types of computers were used for these experiments, a PDP-8 and a PDP-1 both manufactured by Digital Equipment Corp. The PDP-8, to which the author had ready access, was limited by the small memory (4096 channels), so whenever possible, the PDP-1 was borrowed from the Tandem Accelerator group at C.R.N.L.

A block schematic of the system is shown in Fig. 4-9. Let us suppose that we have a coincidence event. The pulses from both detectors are fed from the biased amplifiers to the encoders in the PDP-1. The ADC's then encode these pulses and produce two addresses for this coincident event. The output from the T.A.C. is fed to a third encoder and another address is produced corresponding to the time relationship between the two events. These three addresses are then stored sequentially in a memory buffer unit viz. address of event E1 from side A, address of event E2 from side B and address of event T from the T.A.C. In actual fact the programme for the PDP-1 recorded groups of four addresses but in these experiments the fourth address was left blank. When 80 coincident events had been analysed and stored in the memory buffer, the contents of this buffer were then transferred to magnetic tape and the buffer was cleared. In order to avoid losses during transfer time two buffers were used, the second one collecting while the first was being transferred. Thus the magnetic tape consisted of a series of blocks with 80 groups of four addresses.

By using this technique of recording all the coincident events simultaneously as well as their time relationship, the actual experiment is performed after all the data have been collected. The experimenter can then decide which gamma-rays he wants to set windows on.

Fig. 4-9

Schematic diagram of the "Related Address Technique" used for the gamma-gamma coincidence experiments.

3365-K

RELATED ADDRESS TECHNIQUE

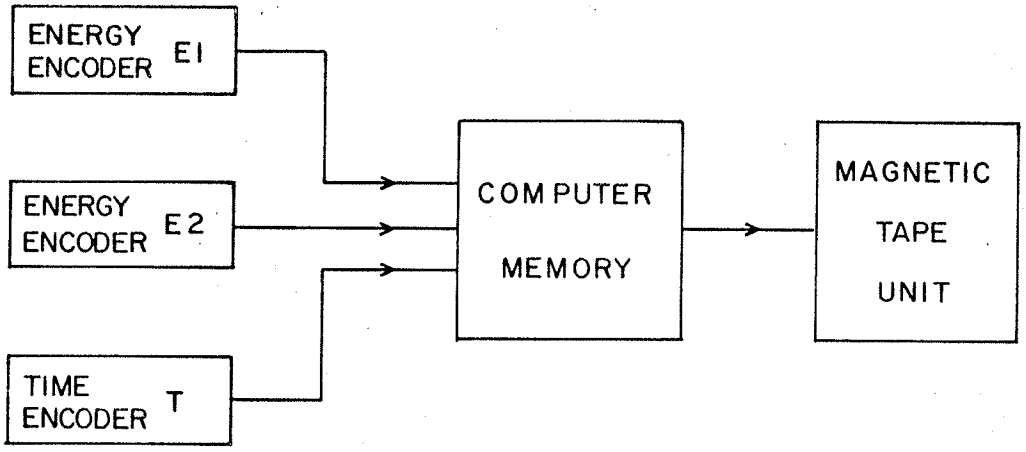

SECTION OF MAGNETIC TAPE

ADDRESS OF EVENT E1	ADDRESS OF EVENT E2	ADDRESS OF EVENT T	BLANK	ADDRESS OF EVENT E1	

80 GROUPS OF 4 ADDRESSES ARE RECORDED ON MAGNETIC TAPE AT ONE TIME

TIME SPECTRUM

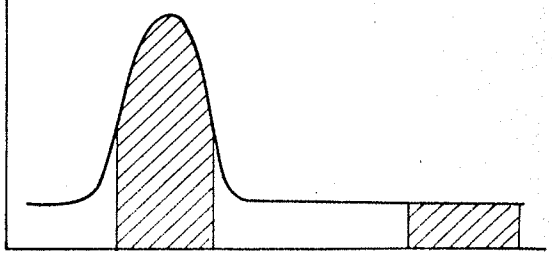

WINDOW FOR TRUE COINC.

WINDOW FOR RANDOM COINC.

Let us suppose that we wish to set a window on a gamma-ray whose full-energy peak occurs in channel 200 in encoder E1. The width of the window depends upon the gain of the amplifier system used but for the purpose of this description, let us suppose it is 5 channels wide. This means setting a window from channel 198 to 202 inclusive. In order to subtract off those events coincident with the Compton distribution, it is necessary to set another window just off the photopeak, e.g. from channel 204 to 208 inclusive, and then subtract this spectrum from the first. The large size of the PDP-1 memory allowed the setting of eleven such pairs simultaneously. The way the programme had been written, only one time window could be set at any one time. Thus the magnetic tapes had to be resorted to get the random coincidences using the same energy windows but a different time window as shown in Fig. 4-9. The time required for sorting the tapes was typically 15 minutes per tape. In one experiment, six tapes were used so that about 1½ to 2 hours of actual computer time was used per sort.

When the data were collected on the PDP-8 computer, only two energy encoders were used and the time relationship between the events was not recorded. The small memory of this computer restricted the number of windows which could be set at any one time to one. This meant that the tape had to be sorted with the window set on the photopeak, these data punched out on paper tape and then the magnetic tape resorted with a new window set just off the photopeak. This second sort was then punched out on paper tape and the two paper tapes were subtracted to give the coincidences with the photopeak. Each of these passes required

about 15 mins. so this was a timing consuming procedure.

A method of reducing the analysis time was found by reordering the magnetic tapes. As the tapes came from the PDP-8 computer, they were filled with pairs of related addresses, the first of which came from encoder E1 (see Fig. 4-10). These tapes were then taken to the G-20 computer and were reordered by a merge-sort programme (Hosken 1955). The result of this programme was 1024 blocks of spectra from encoder E2 which were sequentially in coincidence with channel 1 through 1024 of encoder E1. The time required for reordering 4×10^6 events was roughly 7 hours. The new tape was also considerably smaller than the original tapes, since only about 600 ft. of tape were used to write these 1024 blocks of spectra.

The new tape was then taken back to the PDP-8 for further analysis. If one wished to look at the spectrum in coincidence with channels 198 to 202, the PDP-8 then counted 197 blocks - a process which takes a few seconds from start to finish and then summed the next five blocks. In order to subtract off the coincident events with the Comptons, the computer then has only to subtract off the next five blocks of the tape. This whole procedure is extremely rapid and it allows the experimenter to change the position of the windows and see the results immediately as opposed to two fifteen minute searches per reel through the original tape.

Apart from the obvious convenience and speed of performing experiments by the related address technique, the need for an ultra-stable SCA is eliminated, since the digital windows set in the computer are absolutely stable. We are no longer troubled

Fig. 4-10

Schematic representation of the data re-ordering by the G-20 computer.

ORIGINAL DATA TAPE

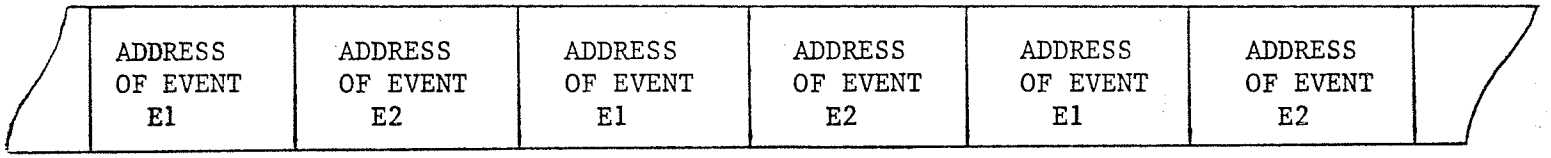

The original data tape has pairs of related addresses.

RE-ORDERED DATA TAPE

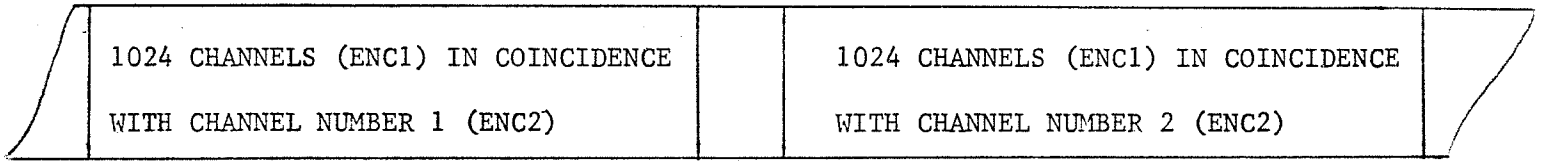

The re-ordered data tape has blocks of 1024 channel spectra in coincidence with successive channels in the other encoder.

with windows which drift up or down over a photopeak. Any drifts in the system broaden all of the photopeaks but do not have the effect of moving just one peak in or out of a window since no windows are set while the data are being collected.

4.6 Time Distribution

As explained in sec. 4.5, the time relationship between the coincident gamma-rays is recorded in the PDP-1 mode of operation. When it comes to setting the digital time windows, problems can arise as to the positioning of this window. The time distribution sketched in Fig. 4-9 is an idealized one which rarely occurs in actual practice. If one looks at all the events from encoder E1 in coincidence with all the events in encoder E2, by setting digital energy windows from channel 1 to 1024 in both encoders and then asking the computer to sort out the time distribution curve, a double peaked distribution may appear as indicated by the closed circles in Fig. 4-11. The explanation of this lies in the fact that the timing characteristics for the two detectors are not identical if the coincident gamma-rays have greatly differing energies.

In order to produce a timing pulse for the TAC, some sort of discriminator must be made to trigger. Let us suppose that we have a discriminator set to trigger after a certain amount of charge Q_1 is collected by the preamplifier. A high energy gamma ray produces more charge in the detector than a low energy one, so for a given field across the detector, it will take longer to collect an amount of charge Q_1 from the low energy gamma-ray than from the higher energy one. Let us, for the moment, suppose that there is no variation in this time, dependent upon

Fig. 4-11

Double peaked timing distribution obtained during the the ^{177}Yb experiments with two coaxial Ge(Li) detectors.

3374-D

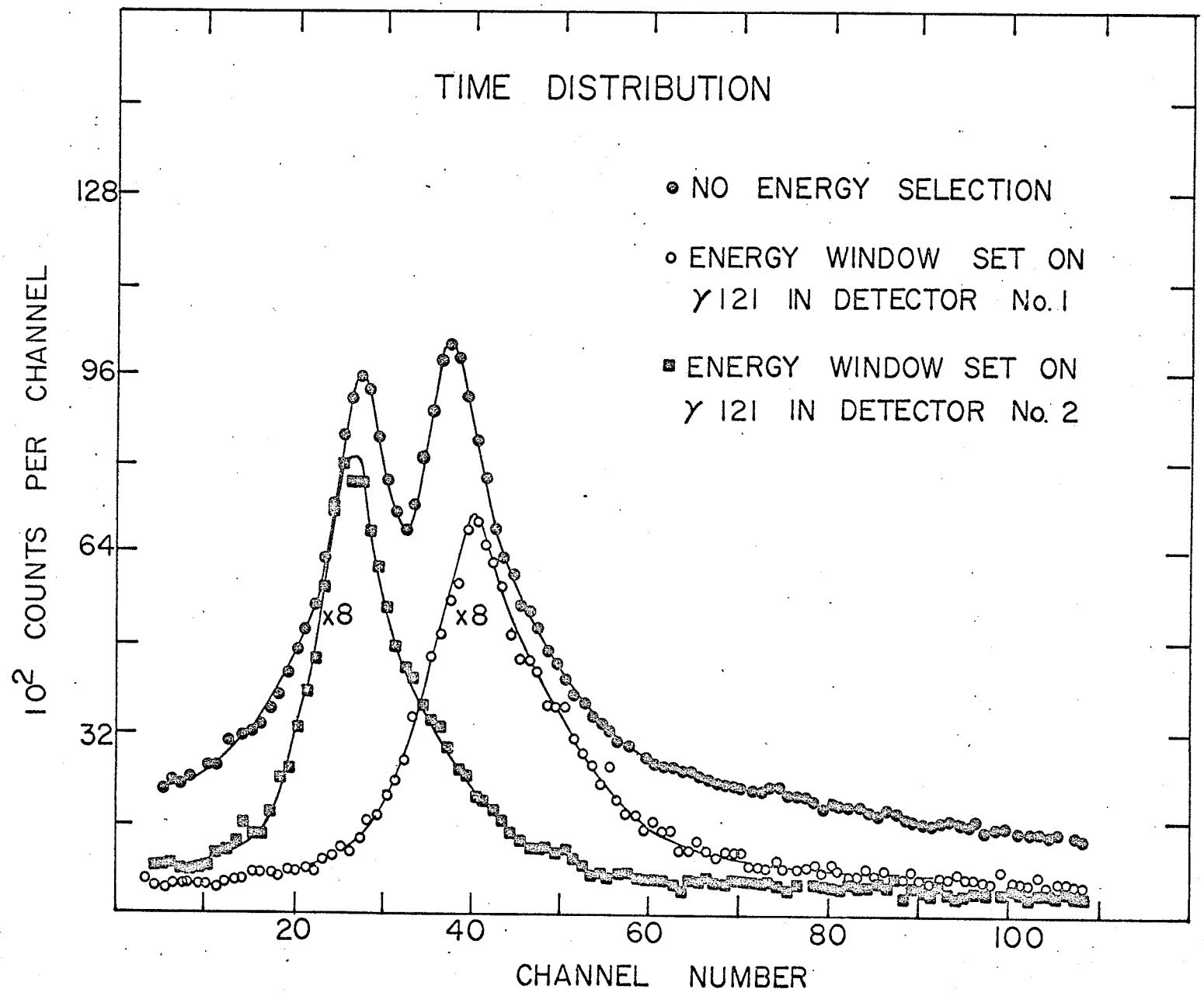
TIME DISTRIBUTION
NO ENERGY SELECTION
ENERGY WINDOW SET ON γ 121 IN DETECTOR No. 1
ENERGY WINDOW SET ON γ 121 IN DETECTOR No. 2
x8
x8
128
96
64
32
10^2 COUNTS PER CHANNEL
20
40
60
80
100
CHANNEL NUMBER

where in the detector the electron-hole pairs have been produced. The solid lines in Fig. 4-12 represent the variation in time required to fire the discriminator versus energy of incident gamma ray. As can be seen from the diagram this variation for detector 1 differs from that of detector 2. This can be caused by having unequal depletion depths or unequal collecting fields or a combination of both.

Let us suppose we have a high energy gamma-ray represented by γ_1 and a low energy event represented by γ_2. If γ_1 is detected in counter 1 and γ_2 is detected in counter 2 then the output signal from the T.A.C. will represent the time interval $t_2 - t_1'$. This will correspond to the position of the peak through the closed squares in Fig. 4-11. When γ_2 is detected in counter 1 and γ_1 in counter 2 then the peak position corresponds to $t_2' - t_1$. This corresponds to the curve drawn through the open circles in Fig. 4-11. As can be seen from Fig. 4-12, the only way $t_2 - t_1'$ can equal $t_2' - t_1$ is for the slopes to be identical.

In actual practice the situation is not as simple as that represented in the diagram. There should in fact be a series of slopes about the line shown, since the time required to collect the charge Q_1 is a function of where in the detector the electron-hole pairs are produced, the collecting field etc.

Since the peak position varies with the energies of the coincident events, it means that it is not always possible to set one time window and sort on eleven different energy windows as mentioned previously. The position of the peak from the time encoder must therefore be checked for each gamma-ray and this procedure was followed throughout the experiments on ^{177}Yb and ^{159}Gd.

Fig. 4-12

Graphical discussion of the double peaked timing distribution.

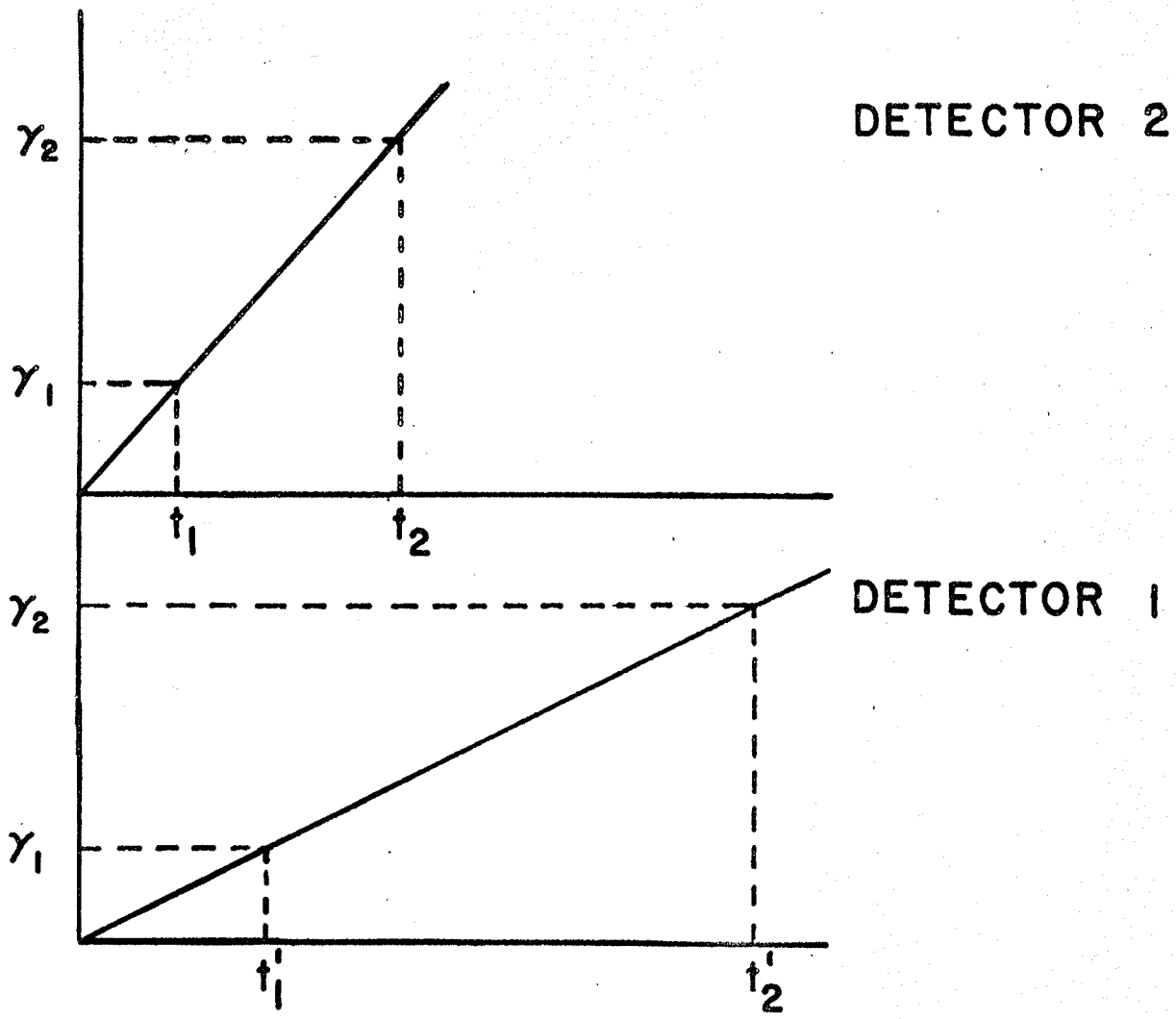

γ_1 IN DETECTOR 1, γ_2 IN DETECTOR 2,
PEAK POSITION CORRESPONDS TO $t_2 - t_1'$

γ_2 IN DETECTOR 1, γ_1 IN DETECTOR 2,
PEAK POSITION CORRESPONDS TO $t_2' - t_1$

$t_2 - t_1' = t_2' - t_1$ IF THE SLOPES ARE EQUAL

CHAPTER V

The Decay of 1.9 hr ^{177}Yb

5.1 Introduction

The decay of 1.9 hr ^{177}Yb has been studied by several groups in recent years. The work of Mize, Bunker and Starner (Mize 1956) indicated that there were four levels above the ground state and that the β-feed to the uppermost level at about 1240 keV had a very low log ft value. The gamma-ray data of Tavendale and Ewan (Tavendale 1963) showed that there were actually two levels, one at 1230 and the other at 1241 keV. In order to measure the log ft values of the β-feeds to these levels more accurately, Johansen et al (Johansen 1964) studied the continuous β-ray spectra and conversion lines with a 6 gap β-ray spectrometer. Their results showed that the log ft values indicated allowed unhindered transitions and on the basis of the Nilsson orbitals available in this region concluded that the levels at 1230 and 1241 keV were three-quasi-particle levels (see sec. 5.6). Further evidence for 3 particle levels in ^{177}Lu has been discussed by Kristensen et al (Kristensen 1964) and theoretical calculations have been made by Pyatov and Chernyshev (Pyatov 1964) and Soloviev (Soloviev 1966).

The electron conversion spectra of Johansen indicated new low energy transitions which were subsequently verified by Ewan (Ewan 1963a) using the Chalk River $\pi\sqrt{2}$ β-ray spectrometer. The high energy region of the gamma-ray spectrum was studied by Tavendale and Ewan (Tavendale 1963) using the $\pi\sqrt{2}$ β-ray spectrometer and a Ge(Li) detector. Energy sum considerations and elec-

tron-gamma coincidence studies were used to place most of the transitions into a level scheme with the exception of a prominent gamma-ray at 898.8 keV.

Levels in ^{177}Lu have been studied from the decay of the 155d isomer of ^{177}Lu (Kristensen 1964) and very well developed rotational bands have been observed. The thermal neutron capture reaction ^{176}Lu(n,γ)^{177}Lu has also been used to study the levels in this isotope (Balodis 1966, Maier 1965).

In order to position all of the transitions observed in the high resolution gamma-ray spectrum of ^{177}Yb into a level scheme, gamma-gamma coincidence experiments must be performed. However the short half-life of the isotope and complex nature of the gamma-ray spectrum prohibit the use of conventional NaI(Tl)-NaI(Tl) techniques. With the advent of large volume Ge(Li) detectors and event by event recording of coincidence data on magnetic tape using digital computers, it is now possible to perform Ge(Li)-Ge(Li) coincidence experiments on short lived isotopes.

The present work reports the results of a detailed analysis of the direct gamma-ray spectrum from ^{177}Yb. Several new transitions were observed. Gamma-gamma coincidence experiments have confirmed previously known features of the level scheme and have established the existence of at least two new levels.

5.2 Experimental Apparatus and Procedure

Sources of ^{177}Yb were prepared by irradiating Yb_2O_3 enriched to 98% ^{176}Yb in a flux of 2.5 x 10^{14} neutrons/sq cm/sec for periods of 2 minutes in the N.R.U. reactor. In order to

remove the radioactive lutetium decay products produced during irradiation, chemical separations were performed. The lutetium and ytterbium were separated by elution from an ion exchange column using α-hydroxy isobutyrate with a pH of 3.30 (Smith and Hoffmann 1956).

The direct gamma-ray spectrum was investigated with a 44cc coaxial Ge(Li) detector (No. G9C2) and a high resolution planar detector (GA6). These detectors had resolutions of 2.75 keV at 1 MeV and 1.0 keV at 100 keV respectively. The data were collected on either a Nuclear Data 3300 system or on a PDP-8 computer.

Three coincidence experiments were performed during the study of the decay of ^{177}Yb. The first of these was used to familiarize the author with the equipment. The second coincidence experiment was performed using two coaxial detectors G9C2 (44cm^3) and GLC6X (30 cm^3) placed side by side to give a large solid angle, and the data were collected on the PDP-8 computer. This experiment provided much useful information and indicated the existence of some previously unseen transitions. However as the time relationship between the events had not been recorded with the PDP-8, it was decided that the experiment should be repeated.

The third coincidence experiment was performed using the same coaxial detectors with the same geometry as above, but this time the PDP-1 computer was used to collect the data, enabling the time relationship as well to be recorded. Four sources were prepared for this experiment and each was counted for approximately two half lives. The method of analysing the magnetic tape was discussed in Chap. IV.

5.3 Direct Gamma-Ray Spectrum

Fig. 5-1 shows the direct gamma-ray spectrum of ^{177}Yb obtained with the 44 cm^3 coaxial detector. The low energy portion of the spectrum was taken with 0.045" Cd between the source and detector while the high energy region had 0.045" Cd plus 0.075" Pb to reduce the number of low energy gamma-rays detected. In order to cut down the background, due to ^{41}Ar from the reactors, the detector was surrounded by a lead shield during these measurements. The two unlabelled peaks in the upper portion of Fig. 5-1 are the Pb X-rays produced from this shield.

The decay of the source was followed through several half-lives in order to determine which gamma-rays belonged to the decay of 1.9 hr ^{177}Yb. Of the twenty-five gamma-rays seen in Fig. 5-1, twenty-one were established as belonging to this decay. The transitions with energies 113.8, 208.4, 282.6 and 396.1 keV all decayed with a half life which was longer than 1.9 hr. A subsequent coincidence experiment showed that the 208.4 and 282.6 keV gamma-rays were in coincidence with the 113.8 keV transition.

In order to determine the possible source of these gamma-rays, ^{174}Yb was irradiated to produce 101 hr ^{175}Yb since ^{174}Yb was present to the extent of 1.45% in the sample of enriched Yb_2O_3 originally irradiated. Six gamma-rays were seen in the decay of ^{175}Yb, as shown in Fig. 5-2, with energies of 113.8, 137.8, 144.8, 251.3, 282.6, and 396.1 keV. The most intense gamma-ray seen in this spectrum was the 396.1 with the 282.6 keV transition about one half as intense. Several runs were made to determine the decay rate and the results of these measure-

Fig. 5-1

The upper half of the figure shows the gamma-ray spectrum of ^{177}Yb up to about 700 keV. The data were taken with 0.045" Cd between the source and detector.
The lower portion shows the gamma-ray spectrum of ^{177}Yb above 600 keV with 0/045" Cd and 0.075" Pb between source and detector.

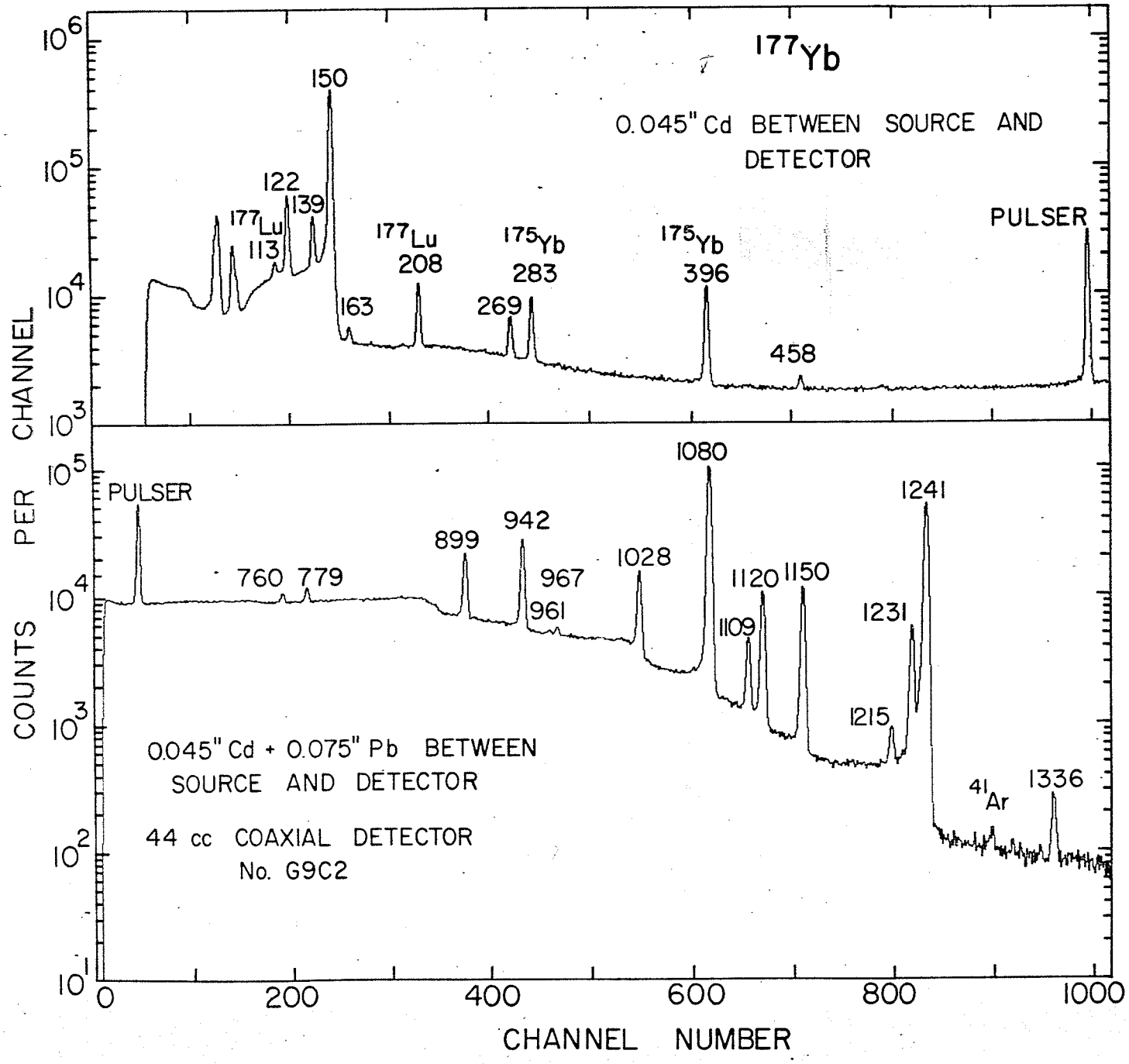
177Yb
0.045" Cd BETWEEN SOURCE AND DETECTOR
150
122
139
177Lu
113
177Lu
208
175Yb
283
175Yb
396
PULSER
163
269
458
PULSER
1080
1241
899
942
760 779
967
961
1028
1120
1150
1109
1231
1215
41Ar
1336
0.045" Cd + 0.075" Pb BETWEEN SOURCE AND DETECTOR
44 cc COAXIAL DETECTOR
No. G9C2
COUNTS PER CHANNEL
CHANNEL NUMBER
10^6
10^5
10^4
10^3
10^2
10^1
0
200
400
600
800
1000

ments indicated that the six gamma-rays previously mentioned all had the same half-life. The present intensity measurements of the ^{175}Yb gamma-rays differ from that obtained by Hatch et al (Hatch 1956) and a comparison of the intensities is given in Table 5-I.

Following the decay of ^{177}Yb to ^{177}Lu, the latter decays with a 6.7 day half-life to ^{177}Hf. The strongest transition in this decay has an energy of 208.36 keV I_γ = 171 (Table of Isotopes 1967) followed by a 112.97 keV gamma ray. I_γ = 100 (Table of Isotopes 1967). The presence of the 6.7d ^{177}Lu and the 101 hr ^{175}Yb would therefore explain the appearance of the 113.8, 208.4, 282.6 and 396.1 keV gamma-rays in the ^{177}Yb source. This is consistent with the coincidence experiment mentioned earlier since the energy window encompassed both the 113.8 and 112.97 keV transitions.

Previous studies by Ewan (Ewan 1963) of the low energy conversion electron spectrum using the Chalk River $\pi\sqrt{2}$ β-spectrometer indicated that there should be a transition at 147.05±0.15 keV with a K-conversion electron intensity 2% that of the 150.36 keV transition. Experiments by Johansen et al (Johansen et al 1964) confirmed the existence of this transition and they have assigned its multipolarity as 75% M1 + 25% E2. Their calculated intensity for this gamma-ray is 1.3% that of the 150.4 keV transition. The weakness of this transition and its proximity to the 150.4 keV gamma-ray make it unobservable with the 44 cc detector. Spectra obtained using the high resolution detector show a bump on the low energy tail of the 150.4 keV transition but only rough estimates of its intensity can be made. A more accurate measurement of the 147.05 keV intensity can be made from the coincidence spectrum with γ121.6 and the intensity

Fig. 5-2

Gamma-ray spectrum of ^{175}Yb observed with the high resolution Ge(Li) detector GA6.

3379-G

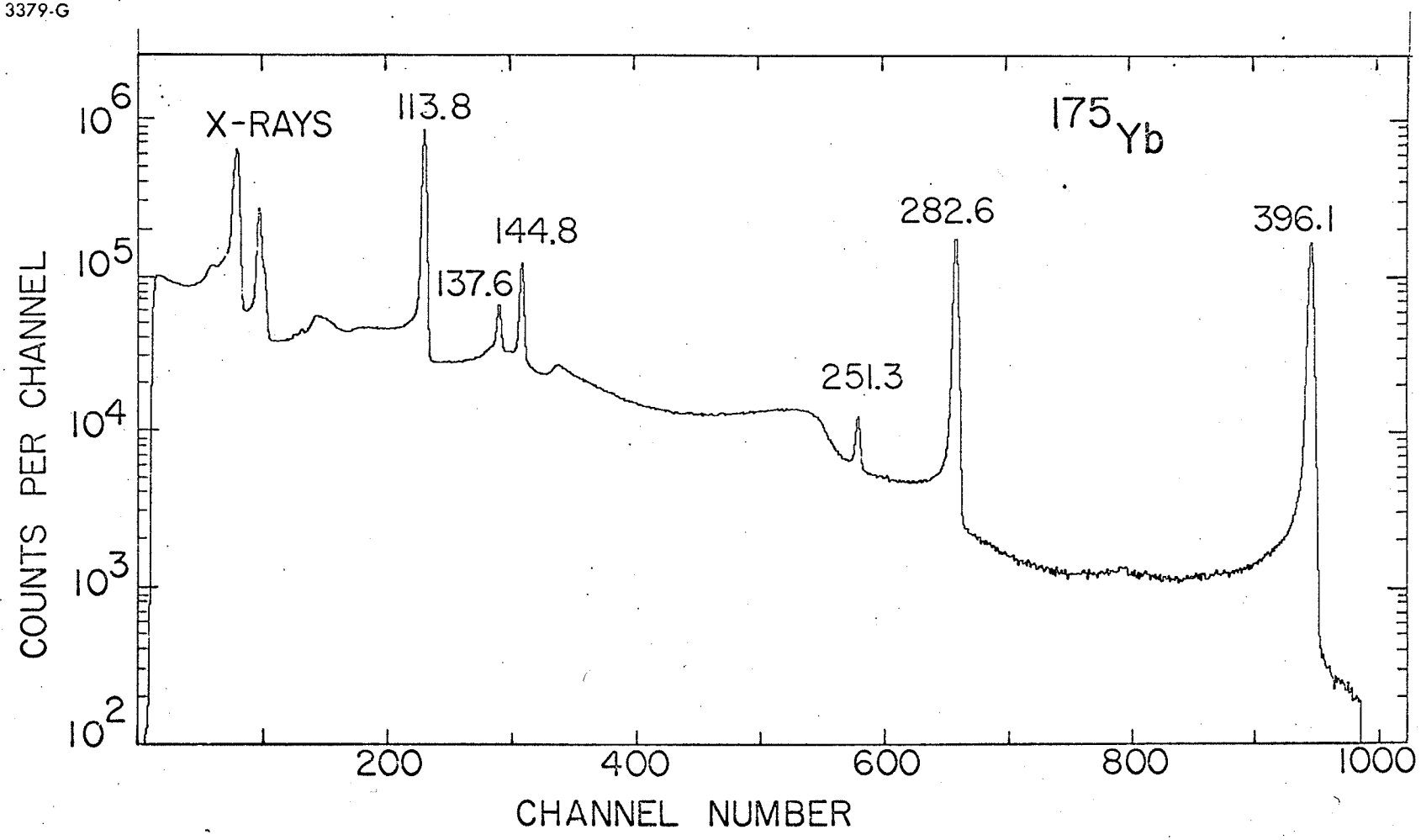
X-RAYS
113.8
144.8
137.6
251.3
282.6
396.1
175Yb
COUNTS PER CHANNEL
CHANNEL NUMBER
10^6
10^5
10^4
10^3
10^2
200
400
600
800
1000

TABLE 5-I

Gamma-Ray Spectrum of ^{175}Yb

Energy* (keV)	Relative Intensities	
	Present Work	Hatch
113.81±0.02	31 ±1.6	31
137.65±0.05	1,7±0.2	2.2
144.85±0.03	5.3±0.3	5.9
251.3 ±0.5	1.3±0.13	3.8
282.6 ±0.13	46 ±2.4	62
396.1 ±0.3	100 ±5	100

Ref. A.E.N. Hatch et al. Phys. Rev. 104, No. 3 (1956) 745.

*Energies taken from above reference.

TABLE 5-II

Gamma-Ray Energies ^{177}Yb

Present Work	Tavendale 1963
899.2±0.3	898.8±0.3
941.7±0.3	941.1±0.4
1028.0±0.3	1027.1±0.4
1080.1±0.3	1080.0±0.3
1109.0±0.3	———
1119.6±0.3	1119.5±0.4
1149.7±0.3	1148.3±0.4
1230.7±0.3	1230.3±0.4
1241.4±0.3	1240.9±0.3

shown in Table 5-III was arrived at in this way.

The weak transition at 458.8 ± 0.5 keV had not been previously reported. It decays with a half-life which indicates that it belongs to the β-decay of ^{177}Yb. The accuracy with which the energy has been determined rules out the possibility that it is the cross-over transition from the 451.6 keV level to the ground state. A gamma-ray with energy 457.90 ± 0.04 keV has been reported by Maier (Maier 1967) and by Balodis et al (Balodis 1966) from the thermal neutron capture reaction ^{176}Lu(n,γ)^{177}Lu. It is tempting to postulate that this is the same gamma-ray as seen in the present work, but this will be discussed later.

The accuracy with which the gamma-ray energies can be measured is largely determined by one's ability to correct for the non-linearity of the system being used. Since the non-linearity of the A.D.C.'s and amplifier system tends in some cases to be strongly dependent on counting rate, it is important that the standard sources used for energy calibration be run simultaneously with the source. This method was used in determining the gamma-ray energies in ^{177}Yb and we estimate that the energies are accurate to ± 0.3 keV with the exception of the extremely weak lines. More details of the method used to measure gamma-ray energies were given in Chap. II. The energies measured in the present work should be compared with those previously reported by Ewan using the Chalk River $\pi\sqrt{2}$ β-ray spectrometer. (Tavendale 1963). The new values are seen in Table 5-II and are consistently higher than the older ones. The short half life, low conversion intensity for the high energy gamma-rays and the large β-ray continuum upon which they sit, make it necessary to use

Table 5-III

PROPERTIES OF TRANSITIONS IN ^{177}Lu

Energy (keV)	Gamma-Ray Intensities: Present Work	Gamma-Ray Intensities: Ewan	Multipolarity	Transition Intensity % Per Disintegration (5)
121.620±0.003(1)	62±6		80%M1+20%E2(2)	9.0
138.606±0.005(1)	24.2±2.4		85%M1+15%E2(2)	2.7
147.165±0.005(1)	3.3±1.0		75%M1+25%E2(2)	0.33
150.392±0.003(1)	364±30		E1 (Anomalous)(4)	27.1
162.492±0.004(1)	1.1±0.25		Mainly M1(2)	0.10
268.801±0.014(1)	3.1±0.3			0.15
458.1 ±0.5	0.74±0.14			0.035
760.4 ±0.3	1.0±0.4			0.05
779.3 ±0.3	2.2±0.3			0.10
899.2 ±0.3	11.7±0.8	11.5±1.3	E2 (+M1)(3)	0.55
941.7 ±0.3	18.4±1.1	17.3±1.5	E1(3)	0.87
961.5 ±0.5	0.35±0.1			0.017
967.4 ±0.5	0.60±0.1			0.028
1028.0 ±0.3	11.5±0.8	8.5±1.2	E2 (+M1)(3)	0.54
1080.1 ±0.3	100±5	100±5	E1	4.72
1109.0 ±0.3	3.2±0.3	3,7±0.6		0.15
1119.6 ±0.3	9.9±0.7	9.8±1.0	M1 (+E2)(3)	0.47
1149.7 ±0.3	11.7±0.8	12.0±1.2	M1 (+E2)(3)	0.55
1214.8 ±0.3	0.50±0.07			0.024
1230.7 ±0.3	6.7±0.6	6.6±1.2	E2 (+M1)(3)	0.32
1241.4 ±0.3	61±4	63±4	E2 (+M1)(3)	2.88
1336.4 ±0.5	0.24±0.04			0.011

(1) Energy measurements from Maier (1965).
(2) Multipolarities taken from Johansen (1964).
(3) Multipolarities taken from Ewan (1964a).
(4) Multipolarity taken from Ewan (1963b).
(5) Transition intensities calculated using multipolarities given in column 4 and using the value of I_β = 60% to the ground state as measured in (2).

very strong sources in order to get reasonable statistics. As a result, the sources used for the β-ray spectrometer were quite thick and the loss of energy by electrons was probably not adequately accounted for, giving low values for the gamma-ray energies.

Table 5-III gives the values of the gamma-ray intensities determined in the present work. The calculations are based upon a relative efficiency curve obtained using the relative intensities of the ^{226}Ra lines (8) and a set of standard sources supplied by I.A.E.A. The estimated accuracy of the relative efficiency curve is ± 5% for the energy region covered in this work. For a more detailed account of the efficiency determination see Chapter II of this thesis.

A comparison of the intensities given by Ewan (Ewan 1964a) and those in the present work shows them to be in good agreement with the exception of the 1028 keV transition. This gamma-ray sits on the Compton edge of the 1241.4 keV transition and the better resolution and photopeak-to-Compton ratio of the detector used in the present work account for the difference.

5.4 Gamma-Gamma Coincidence Experiments

To establish the order of the gamma-rays in the level scheme, gamma-gamma coincidence experiments were performed using two large volume coaxial Ge(Li) detectors. Two layers of 0.015" Cd were placed between the source and each detector to reduce the number of x-rays detected. The detectors were placed side by side to give a large solid angle.

As mentioned in Chapter IV, the data were recorded on magnetic tape using the related address technique. Fig. 5-3

Fig. 5-3

"Coincidence singles" spectrum from ^{177}Yb experiment using two coaxial Ge(Li) detectors. The figure shows all the events in encoder B in coincidence with all of the events in encoder A.

3380-D

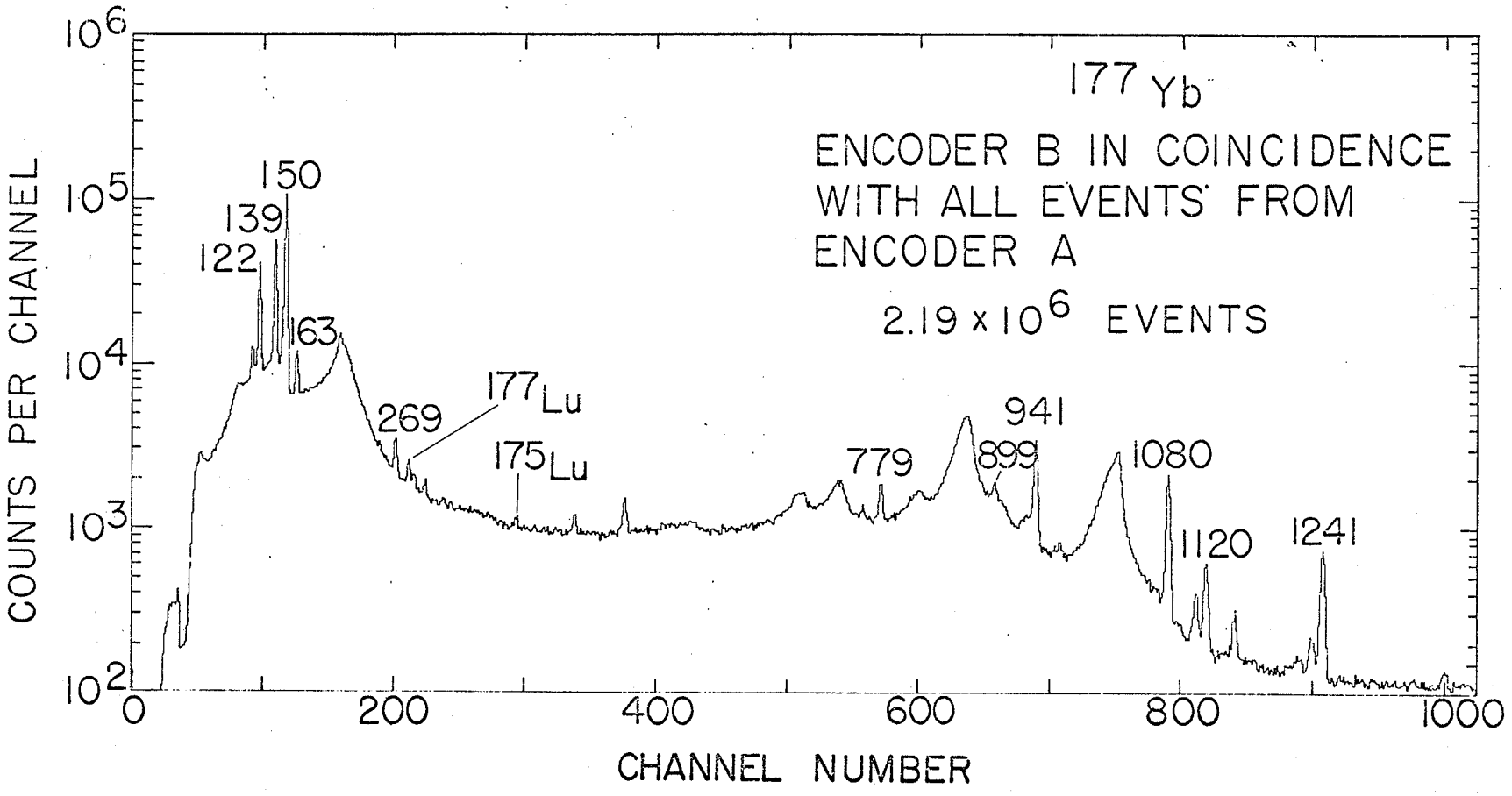
177 Yb
ENCODER B IN COINCIDENCE WITH ALL EVENTS FROM ENCODER A
2.19 x 10^6 EVENTS
COUNTS PER CHANNEL
CHANNEL NUMBER
10^6
10^5
10^4
10^3
10^2
0
200
400
600
800
1000
150
139
122
163
269
177Lu
175Lu
779
941
899
1080
1120
1241

Fig. 5-4

Subtraction of events coincident with the Compton distribution beneath a photopeak. The upper portion of the figure shows the spectrum obtained with a window set around -163. The lower portion shows the spectrum after the events in coincidence with the Compton distribution have been subtracted.

The baseline has been shifted by 50 counts per channel to facilitate the plotting of negative numbers.

3380-B

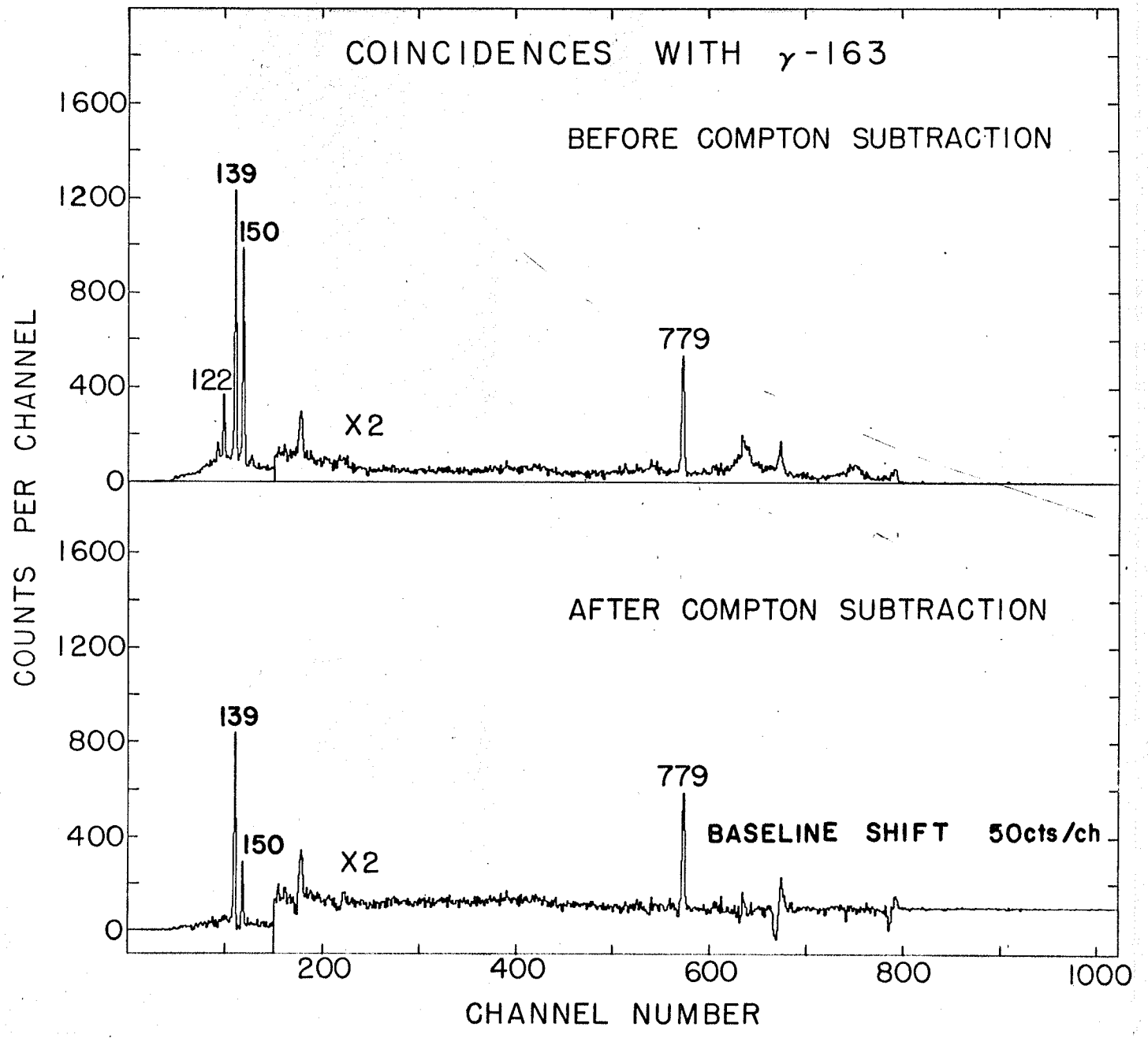
COINCIDENCES WITH γ-163
BEFORE COMPTON SUBTRACTION
AFTER COMPTON SUBTRACTION
139
150
122
779
X2
BASELINE SHIFT 50cts/ch
COUNTS PER CHANNEL
CHANNEL NUMBER
0
400
800
1200
1600
200
400
600
800
1000

shows an example of the "coincidence singles" obtained during the ^{177}Yb experiments. This figure was produced by instructing the computer to sort out all events from encoder B (ENCB) in coincidence with every event from encoder A. The gamma-ray peaks on which the windows were eventually set can be seen to be sitting on a continuum due to Compton scattered gamma-rays.

In order to get the net coincidence events with any gamma-ray, it is necessary to subtract off the events in coincidence with the Compton scattered gamma-rays.
Fig. 5-4 shows the coincidence spectrum with γ-163 before and after Compton subtraction. The peaks at 122 and 163 keV are completely removed and the number of counts in the 150 and 139 keV peaks are greatly reduced. The peaks at about channel 200, 680, and 800 due to backscattered gamma-rays have also been reduced. In the spectra shown in Figs. 5-5, 5-6, and 5-7 events coincident with the Compton scattered gamma-rays under the photopeaks have been subtracted.

The upper portion of Fig. 5-5 shows the spectrum in coincidence with γ-122 taken from the PDP-1 experiment. The random coincidence spectrum shown in the middle section removes the contribution from the 122 and 150 keV transitions leaving five gamma-rays in true coincidence with γ-122, namely the 147, 1027, 1109, and 1120 keV transitions and a very weak transition at 1215 keV which is shown on an expanded scale in the insert. Data obtained from the PDP-8 experiment was roughly a factor of 2 better in statistics and confirmed that the 1215 keV transition is in true coincidence with γ-122. An estimate of the intensity of γ-147 relative to the 1027 keV transition can be determined from this spectrum although correlation effects limit the accuracy with

Fig. 5-5

Upper portion: Coincidences with γ-122

Center portion: Random coincidences with γ-122

Lower portion: Net true coincidences with γ-122

79-A

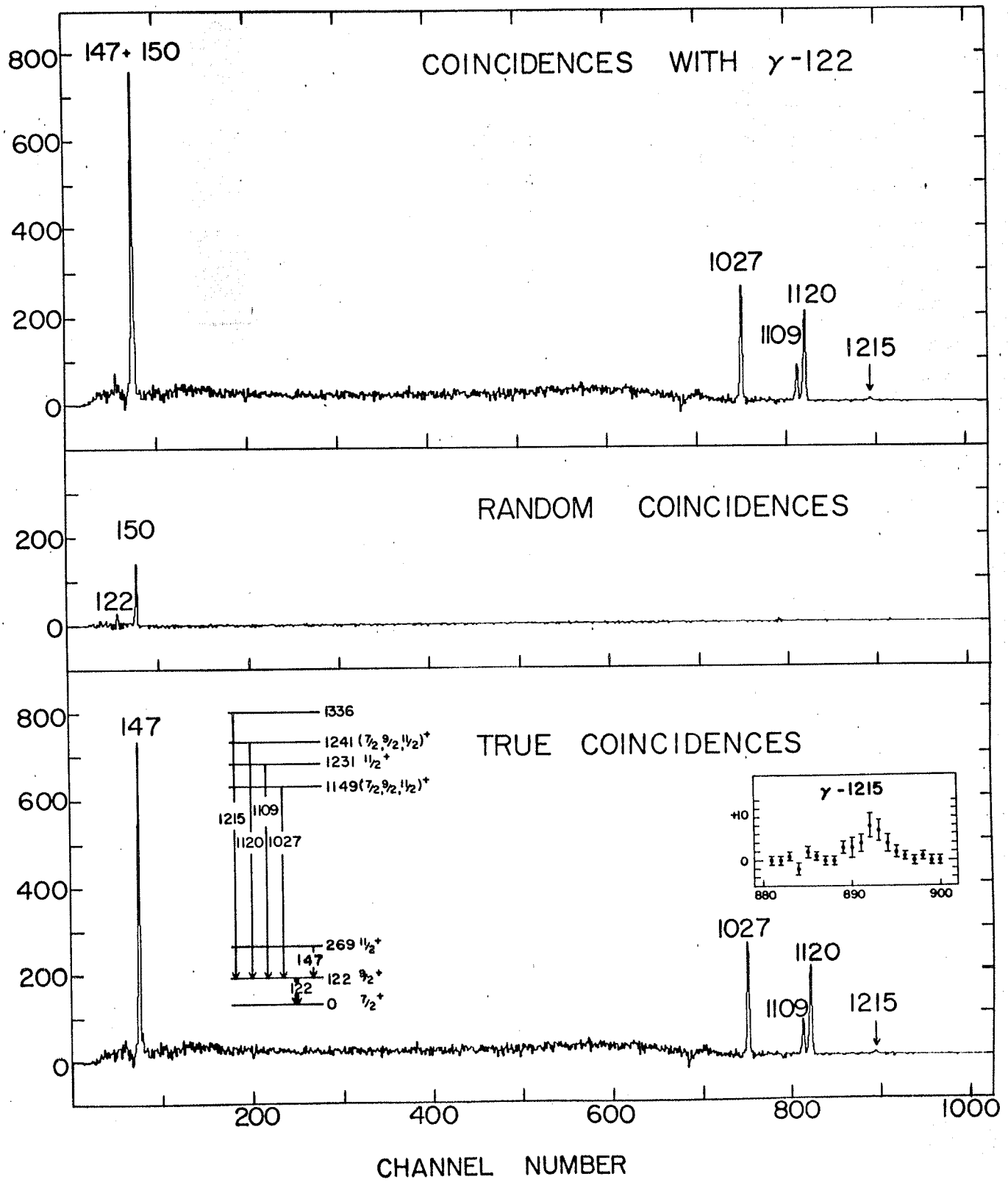
COINCIDENCES WITH γ-122
147+ 150
1027
1120
1109
1215
800
600
400
200
0
RANDOM COINCIDENCES
150
122
200
0
TRUE COINCIDENCES
147
1336
1241 (7/2, 9/2, 11/2)+
1231 11/2+
1149(7/2,9/2,11/2)+
1215
1109
1120
1027
269 11/2+
147
122 9/2+
122
0 7/2+
γ-1215
+10
0
880
890
900
1027
1120
1109
1215
800
600
400
200
0
200
400
600
800
1000
CHANNEL NUMBER

which it can be calculated. The value quoted in table 5-III was calculated from this spectrum. The relative intensities of the other transitions are in agreement with those from the direct spectrum and a partial level scheme is shown as an insert in the lower portion of Fig. 5-5.

Fig. 5-6 shows those transitions which are in coincidence with γ-150. Prominent peaks can be seen at 139, 163, 899, 942, and 1080 keV. A small contribution from γ-1080 can be seen in the random coincidences but this is due to the 1.2×10^{-7} sec half-life of the 150 keV level (de Waard 1955). With the time window for the random coincidences set well off the main peak (~300 nsec), it is still possible to get genuine coincidence events. The spectra in coincidence with γ-139 and γ-163 indicate that the 760 and 779 keV transitions are also in coincidence with γ-150. Their intensities are too low to show prominent peaks in the lower spectrum of Fig. 5-6 but their positions are indicated and some evidence for their existence can be seen.

Fig. 5-7 shows the spectra coincident with γ-139 and γ-163. These data were collected on the PDP-8 computer and as a result no time information was recorded. A time window of about 60 nsec was set on the T.A.C. output. The data shown in Fig. 5-7 have not been corrected for random coincidences. Typical true-to-random ratios for these experiments were approximately 8 to 1.

The fact that γ-760 is in coincidence with γ-139 and not with γ-163 indicates the presence of a new level at 1049 keV. This is further substantiated by the observed coincidences between γ-150 and γ-899 (see Fig. 5-6). The two partial level schemes at the side of the graphs indicate the positioning of these transi-

Fig. 5-6

Upper portion: Coincidences with γ-150

Center portion: Random coincidences with γ-150

Lower portion: Net true coincidences with γ-150

3379-B

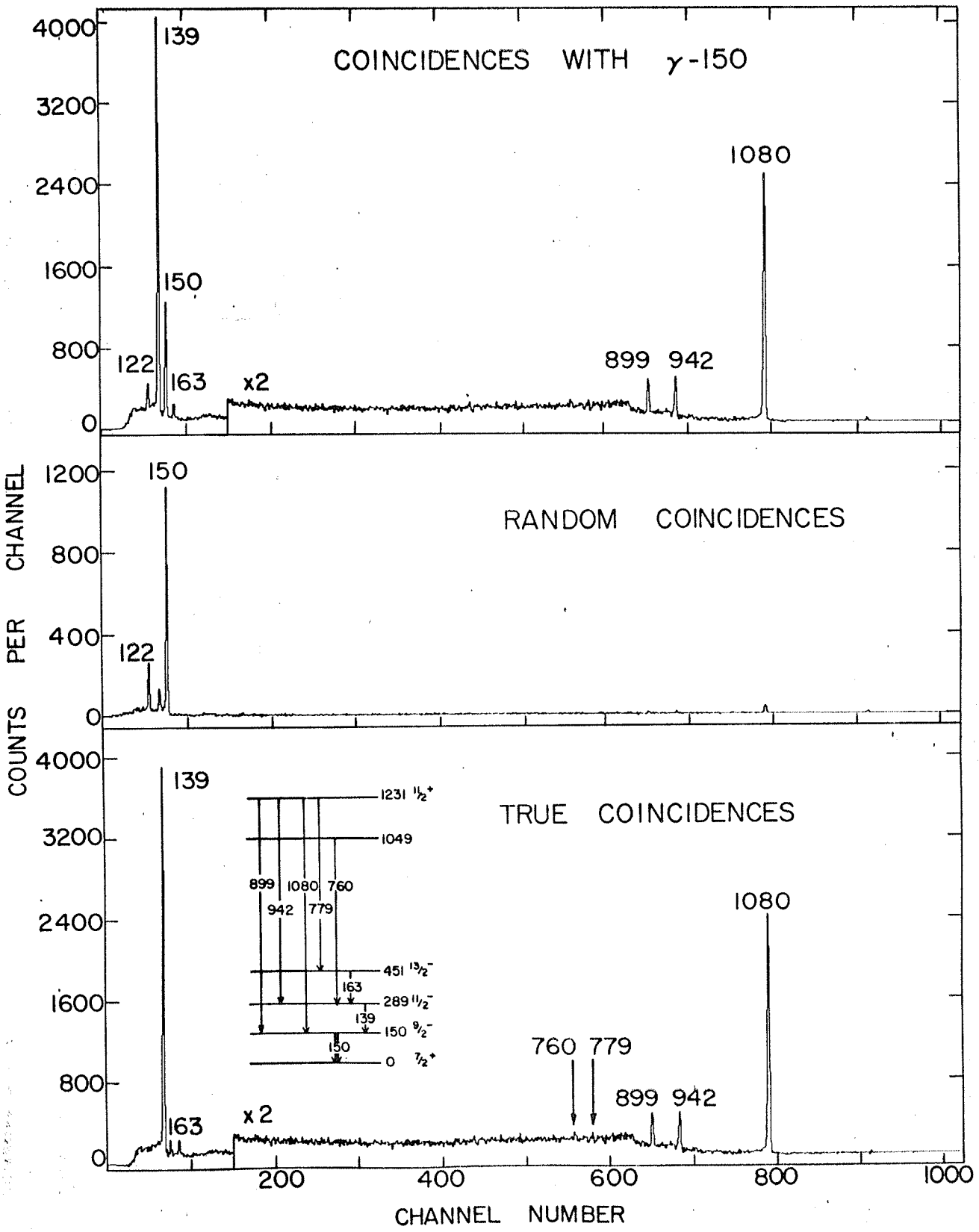
COINCIDENCES WITH γ-150
RANDOM COINCIDENCES
TRUE COINCIDENCES
COUNTS PER CHANNEL
CHANNEL NUMBER
139
150
122
163
x2
1080
899
942
760
779
1231 11/2+
1049
451 13/2−
289 11/2−
150 9/2−
0 7/2+
4000
3200
2400
1600
800
0
1200
400
200
600
1000

Fig. 5-7

Upper half: Coincidences with γ-163

Lower half: Coincidences with γ-139

Both spectra were taken with the PDP-8 system and therefore no random coincidences have been subtracted.

3379-K

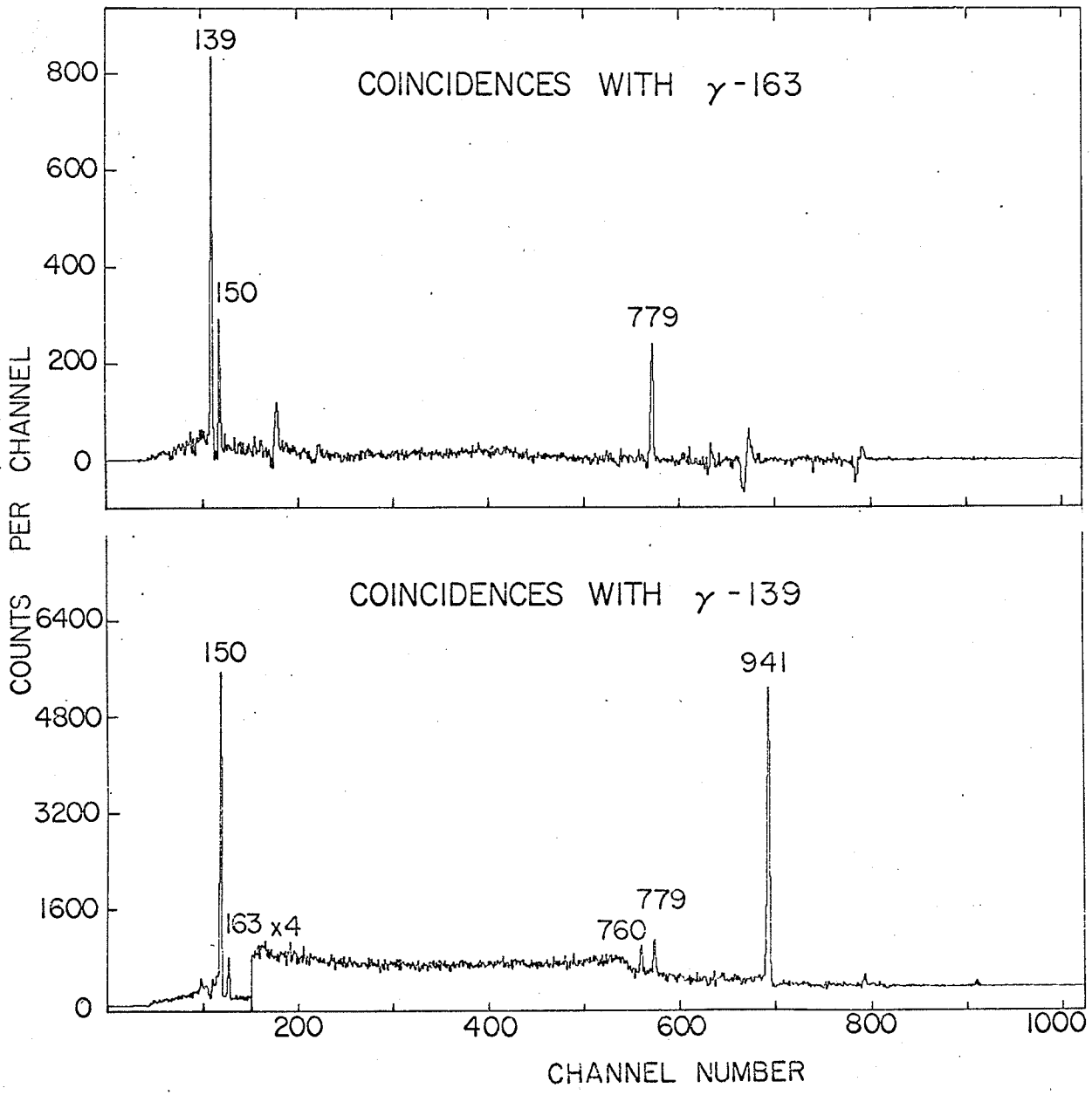
COINCIDENCES WITH γ-163
139
150
779
800
600
400
200
0
COINCIDENCES WITH γ-139
150
941
779
760
163 x4
6400
4800
3200
1600
0
200
400
600
800
1000
COUNTS PER CHANNEL
CHANNEL NUMBER

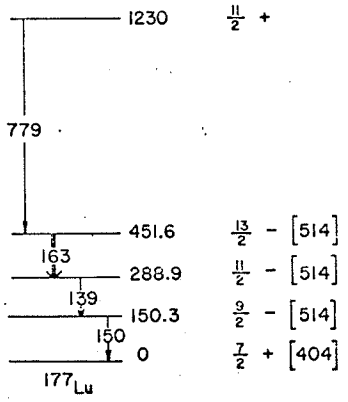
1230
11/2 +
779
451.6
13/2 − [514]
163
288.9
11/2 − [514]
139
150.3
9/2 − [514]
150
0
7/2 + [404]
177Lu

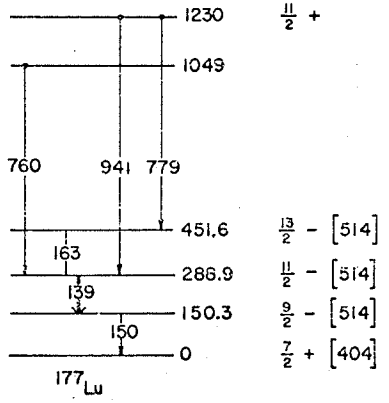
1230
11/2 +
1049
760
941
779
451.6
13/2 − [514]
163
286.9
11/2 − [514]
139
150.3
9/2 − [514]
150
0
7/2 + [404]
177Lu

tions in the level scheme. The small peaks to the right of the 942 keV peak in the lower part of Fig. 5-7 are present because the random coincidences have not been subtracted from this spectrum. A repetition of this experiment in which the random coincidences were measured confirmed this.

As can be seen from Fig. 5-3, γ-269 appears in the "coincidence singles" spectrum. From energy sum considerations the extremely weak 961 keV transition was thought to be in coincidence with γ-269. When the appropriate energy and Compton windows were set and the necessary subtraction performed, the net spectrum showed evidence of a backscattered peak occurring at the position of γ-961 which completely masked the effect being sought. This can be explained by again examining Fig. 5-3. A broad peak can be seen at about channel 750 due to backscattering of the 1241 keV gamma-ray from one detector into the other. For a 1241 keV gamma-ray, backscattering at about 120° deposits about 270 keV in one detector and about 970 in the other (Nelms 1953). For the geometry used in these experiments, this range of backscattering angles was permissible.

In order to overcome this problem, the data were analysed in a different manner. The magnetic tapes from the PDP-8 were taken to the G-20 computer and reordered as described in Chap. IV. A 1 channel wide window was then moved over the position of the 269 keV peak in ENCB. All of the counts in channels 0 to 1023 were then summed in ENCA for each of the 1 channel window positions and the results are shown in the upper left hand corner of Fig. 5-8. This confirmed the fact that there was something in coincidence with this transition.

Fig. 5-8

"Sliding window" analysis of coincidences with -269.

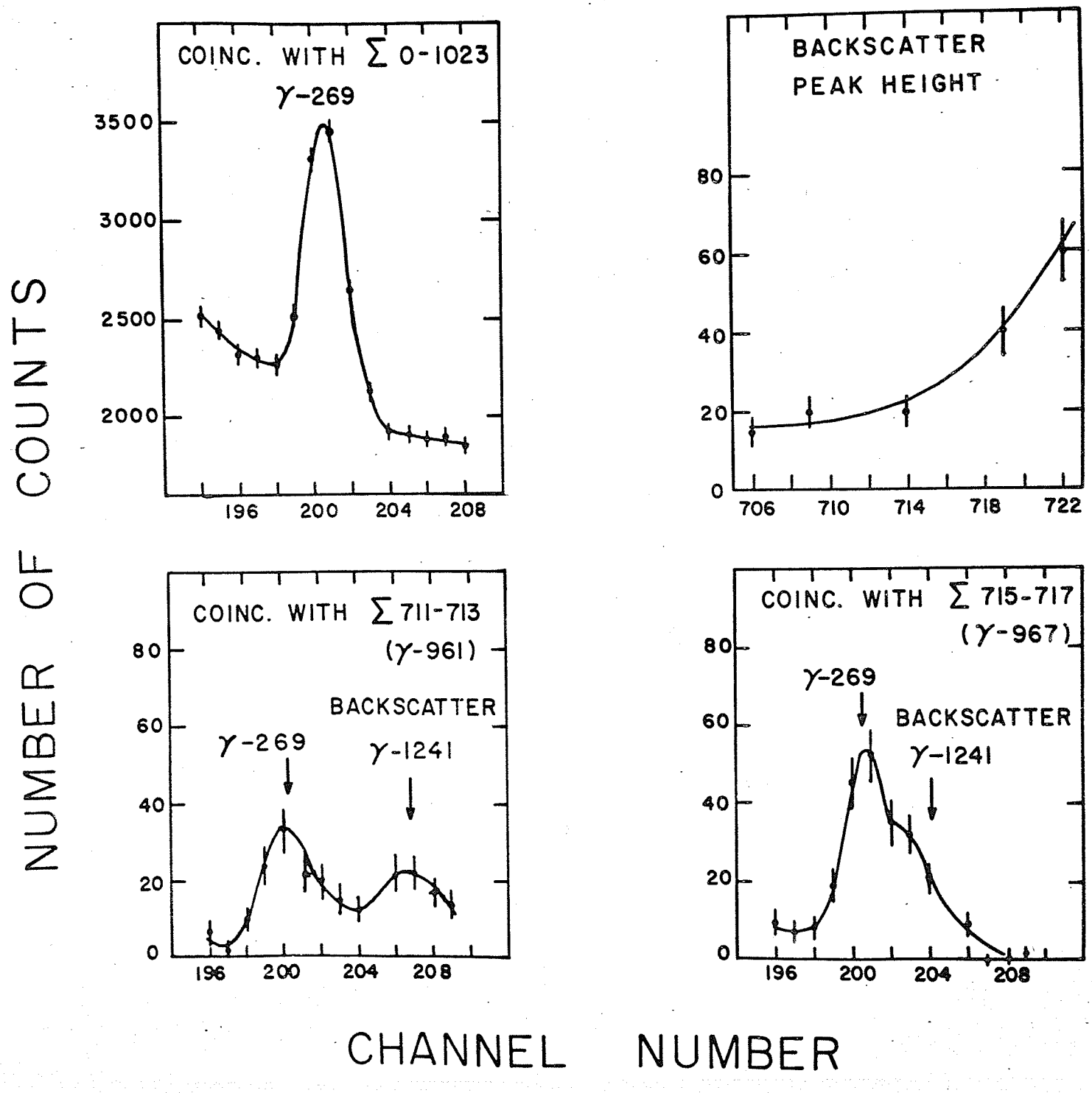
COINC. WITH Σ 0-1023
γ-269
3500
3000
2500
2000
196
200
204
208
BACKSCATTER
PEAK HEIGHT
80
60
40
20
0
706
710
714
718
722
COINC. WITH Σ 711-713
(γ-961)
BACKSCATTER
γ-269
γ-1241
80
60
40
20
0
196
200
204
208
COINC. WITH Σ 715-717
(γ-967)
γ-269
BACKSCATTER
γ-1241
80
60
40
20
0
196
200
204
208
NUMBER OF COUNTS
CHANNEL NUMBER

Since there was already some evidence suggesting that the 961 keV transition was in coincidence with γ-269, a three channel wide window was set from channels 711 to 713 in ENCA centered on γ-961. The counts in these channels were summed as the window in ENCB was moved over the position of the 269 keV transition. In effect, this is then a coincidence experiment using two S.C.A. One of these is fixed on γ-961 (CH 711-713) and the other window is moved over the position of γ-269. The total number of coincident events in the window set on γ-961 is then plotted as a function of the other window position. If the 269 keV gamma-ray is in coincidence with γ-961, then the number of counts in the 961 keV window should rise and fall as the other window moves over γ-269. The spectrum in the lower left hand corner of Fig. 5-8 shows that this does indeed happen.

As the one channel window is moved off the 269 keV peak, another peak appears due to the backscattering of γ-1241. In order to check that this is in fact from this backscattering and that the height of the peak is correct, the following experiment was performed. The three channel window was moved off the 961 keV peak and set at different positions (eg. 705 to 707, 708 to 710 etc.) as shown in the upper right hand diagram in Fig. 5-8. The one channel window was then moved across the region of the backscatter peak and the peak height was plotted as a function of the position of the three channel window. As can be seen from the upper right hand diagram, the backscatter peak height should be about 25 counts when the three channel window is set from channels 711-713 (γ-961). This is in agreement with the data shown in the lower left hand corner.

A new transition at 967 keV was observed in the direct spectrum. The same type of "sliding window" analysis was performed with this gamma-ray as with γ-961. The lower right hand diagram in Fig. 5-8 shows the result. The intensities of the 961 and 967 keV transitions calculated from the direct spectrum are 0.35 ± 0.1 and 0.60 ± 0.1 respectively. The data shown in Fig. 5-8 are not inconsistent with these numbers. On the basis of these results, it might be possible to postulate the existence of a level at 1236.2 ± 0.5 keV, but it must be remembered that this is the only piece of evidence for this level.

A very weak peak at 458.1 keV appears in the "coincidence singles" indicating that there is something in coincidence with this transition. The net coincidence spectrum obtained from the PDP-8 experiment exhibited evidence for a very weak transition at about 696.6 keV. Since the peak is so weak, the error associated with the energy measurement of this transition is estimated to be about ±1.5 keV. The summation of the energies involved yields 1149.7 ± 1.6 keV indicating that this transition could fit between the 1149.7 keV level and one at 458.1 keV although the agreement between the energy sum and the 1149.7 keV transition is probably accidentally good considering the large errors involved. This 691.6 keV transition was not seen in the direct gamma-ray spectrum however, and an upper limit to its gamma intensity can be set at <0.1 (I_γ 1080 ≈ 100 ± 5) giving a transition intensity of <0.005% per disintegration.

5.5 Level Scheme

The level scheme for ^{177}Lu following the β-decay of

Fig. 5-9

Level scheme of ^{177}Lu observed in the beta-decay of ^{177}Yb.

$^{177}_{70}Yb_{107}$

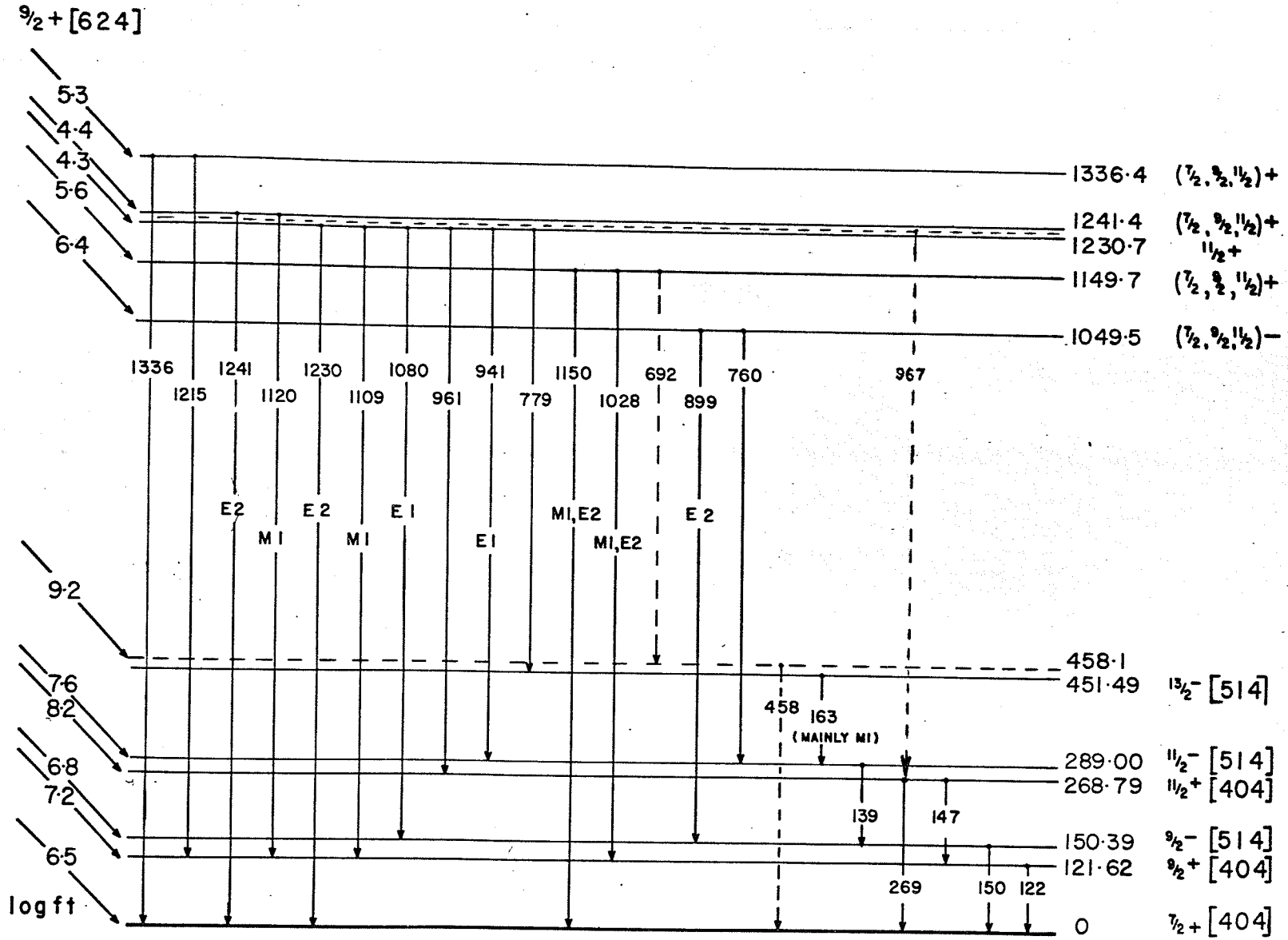

$^{177}_{71}Lu_{106}$

^{177}Yb is shown in Fig. 5-9. This decay scheme is based upon the gamma-ray measurements from the present work along with the β-ray and electron conversion studies of Johansen et al (Johansen 1964) and Ewan 1963a. The energy values shown are taken from several references and Table 5-III lists the most accurately known values. The log ft. values shown in Fig. 5-9 are obtained from the intensity balance of transitions feeding and de-exciting the levels based upon a 60% β-ray feed to the ground state as measured by Johansen.

The spin of the ground state has been measured by Peterson and Shugart (Peterson 1962) using atomic beam techniques and was found to be 7/2. Their values of the magnetic dipole and electric quadrupole moments were 2.236 ± 0.010 nm and 5.51 ± 0.06 barns respectively, which are very similar to the values for ^{175}Lu. The ground state has been identified as the [404] 7/2+ Nilsson proton state.

A study of the decay of the 155 day isomer in ^{177}Lu has revealed well developed rotational bands. Levels in the ground-state rotational band with spins up to 17/2 have been observed. From the energy spacing and the inertial parameters, the levels at 121.62 and 268.79 have been identified as the 9/2+ and 11/2+ members of the ground-state rotational band. The spin assignments of these levels are consistent with the experimentally determined multipolarities of the 122 and 147 keV transitions. From conversion coefficient and L subshell measurements, these have been reported as 80% M1 + 20% E2 and 75% M1 + 25% E2 respectively (Johansen 1965).

The L subshell ratios have been measured by Ewan and Herrlander (Ewan . 1963b) for the 150.35 keV transition. No possible

combinations of M1 + E2 or E1 + M2 can explain the experimentally observed ratios. This gamma-ray has been classified as an anomalous E1 transition making the spin of the 150.35 keV level either (5/2, 7/2, or 9/2)-. The log ft. value of 6.9 for the β-feed to this level tends to rule out the 5/2- value leaving only the 7/2- and 9/2- as possibilities. The only Nilsson orbital available in this region is the 9/2- [514] proton state and this level has therefore been classified as the 9/2- [514] state. Coincidence studies have confirmed that γ-163 and γ-139 are both in cascade with γ-150 as shown in Fig. 5-9. The energy spacing and multipolarity assignments are consistent with the interpretation that the levels at 288.92 and 451.6 keV are the 11/2- and 13/2- members of the K = 9/2 rotational band built upon the 9/2- [514] proton state at 150.35 keV.

From the foregoing discussion, it is clear that the first five excited states can be described as members of the 7/2 [404] and 9/2 [514] rotational bands. Recently studies of the thermal neutron capture reaction $^{176}Lu(n,\gamma)^{177}Lu$ have been made by Maier (Maier 1965) and by Balodis et al (Balodis 1966). Their interpretation of their data shows very well developed 7/2 [404] and 9/2 [514] bands and in addition they include a third 5/2 [402] band built upon a level at 457.9 keV which they interpreted as being the 5/2+ [402] single proton state. The energy of the transition from this level to the ground state is given as 457.90 ± 0.040 keV by Maier (Maier 1965).

The present investigation of the β-decay of ^{177}Yb has revealed a weak transition with an energy of 458.1 ± 0.5 keV which may possibly be in coincidence with an extremely weak 692

keV gamma-ray. If it is assumed for the moment that these gamma-rays are in coincidence and that I_T-692 ≈ 0.005% per disintegration, then there must be a β-feed to the 458.1 keV level with an intensity of about 0.030% per disintegration.

The log ft. value for such a transition is about 9.2. The most probable classification for such a transition is unique first forbidden (Wu 1966) with $\Delta I = \pm 2$ (yes). This would therefore mean that the 458.1 keV level has negative parity, since the ground state of ^{177}Yb is interpreted as the 9/2+ [624] Nilsson state, and spin of 5/2 or 11/2. Since there are no sharp boundaries in the classification of log ft. values, the next most probable classification is non unique first forbidden with $\Delta I = 0, \pm 1$ (yes). This again means that the 458.1 keV level would have negative parity and possible spin values of 7/2, 9/2, or 11/2. Of the 475 allowed transitions listed by Wu (Wu 1966) nine have log ft. values in the range 8.8 to 9.2 so the possibility of this transition to the 458.1 keV level being allowed cannot be overlooked. In this case the spin of the 458.1 keV level would be 7/2, 9/2 or 11/2 and the parity positive. Both the allowed or first forbidden classifications would therefore exclude the possibility of interpreting this level as the 5/2+ [402] Nilsson state.

The most probable type of transition which would allow this level to have a spin of 5/2 and positive parity is a second forbidden transition. However a log ft. value of 9.2 is too low for such a transition. On the basis of these arguments, it would appear that this possible level at 458.1 keV can not be interpreted as the 5/2+ [402] level at 457.9 keV reported by Maier

(Maier 1965) and Balodis et al (Balodis 1966). Since it has not been conclusively demonstrated that the 458.1 keV transition fits between a level at 458.1 keV and the ground state, the possible level is shown as a dashed line in the level scheme.

The level at 1049.5 keV is reported for the first time in the present work. The 899 keV gamma-ray had been reported earlier by Tavendale and Ewan (Tavendale 1963) but was not fitted into any level scheme. The present data (Figs. 5-6 and 5-7) show how γ-899 and γ-760 (not previously reported) were fitted into the level scheme. On the basis of the E2 (+M1) multipolarity assignment for γ-899 made by Ewan (Ewan 1964a) the parity of this level has been assigned as negative with the spin possibilities as 7/2, 9/2, or 11/2. The log ft. value for the β-feed to this level is consistent with this assignment.

The positive parity and possible spin values of 7/2, 9/2, or 11/2 for the 1149.7 keV level are arrived at from the M1, E2 multipolarity assignment for γ-1028 and γ-1150. These values are consistent with the log ft. values calculated from the present work.

The low log ft. values for the transitions to the levels at 1231 and 1241 keV indicate allowed unhindered transitions. The E1 multipolarity of the transitions de-exciting this 1231 keV level to members of the 9/2 [514] rotational band and the E2 nature of the transition to the ground state, indicate a positive parity for this level and a spin value of 11/2. The 779 and 961 keV transitions de-exciting this level are reported here for the first time. A positive parity assignment can be made to the level at 1241 keV and the spin value restricted to 7/2, 9/2 or 11/2 from the M1 and E2 assignments to γ-1120 and γ-1241. A

spin assignment of 7/2 would be consistent with the three-quasi-particle interpretation which will be discussed later.

The level at 1336.4 keV is introduced for the first time. It is seen to de-excite to members of the ground-state rotational band by means of 1215 and 1336 keV transitions. The log ft. value for the β-feed is 5.3 which indicates an allowed transition, and therefore positive parity, with possible spin values of 7/2, 9/2 or 11/2 for this level. The energy of the ground-state to ground-state β-feed is given as 1400 ± 20 keV by Johansen (Johansen 1964). Hence the energy of the feed to the 1336.4 keV level is 64 ± 20 keV. Since the ft. value for low energy transitions varies as $E^{7/2}$ (Wu 1966), where E is the β-energy in units of 511 keV, the limit of the accuracy on the energy of the above transition yields possible log ft. values from 4.8 to 5.6 for this transition. This however is still within the range of the allowed transitions and is consistent with the positive parity assignment to the 1336 keV level.

5.6 Three-Quasi-Particle Levels

The interactions between nucleons in a nucleus can be roughly separated into long range and short range parts. The former are responsible for the creation of the average nuclear field upon which the independent particle models are constructed, while the latter leads to the formulation of nuclear pairing correlations. Soloviev (Soloviev 1963) points out that strong correlations between nucleons occur only when the nucleons are in states with the same energy and quantum numbers except "m" (ie, between nucleons in state (j,m) and j,-m).

The nucleon states (j,m) constitute a set of non-interacting states of the self consistent potential, but they interact through the pairing force. In order to perform various calculations based upon models involving residual interaction, it is necessary to have a set of states which interact neither through the self consistent potentialnor the pairing force. This transformation is brought about with the introduction of the quasi-particle concept by Bogolyubov (Bogolyubov 1958). A quasi-particle in state (j,m) is a mixture of a nucleon in state (j,m) and a hole in state (j,-m). The particle wave function is present with amplitude U_j and the hole with amplitude V_j.

Soloviev (Soloviev 1961) also points out that there must also be three-quasi-particle levels as well as single quasi-particle ones among the excited states of a system consisting of an odd number of particles.

Three-quasi-particle states in deformed nuclei have been studied by Pyatov and Chernyshev (Pyatov 1964). They have shown that the three-quasi-particle state consists of a multiplet of four levels having the same parity. The splitting of the state is a consequence of the spin dependent part of the pairing interaction which they have treated in the first order of perturbation theory using Nilsson model wave functions (Nilsson 1955). Their results show that the highest energy state is that in which the asymptotic spins of the nucleons of the decoupled pair are parallel and the spin of the odd nucleon is anti-parallel to them ($\uparrow\uparrow\downarrow$); the other three configurations ($\uparrow\uparrow\uparrow$), ($\uparrow\downarrow\uparrow$) and ($\uparrow\downarrow\downarrow$) lie at a lower energy.

The three-quasi-particle states in ^{177}Lu are formed from the configurations

Fig. 5-10

Level spacing and variation with fraction of spin dependent forces for the three-quasi-particle multiplet formed from { n_1 7/2-(514)↓; n_2 9/2+(624)↑; p7/2+(514)↓ }

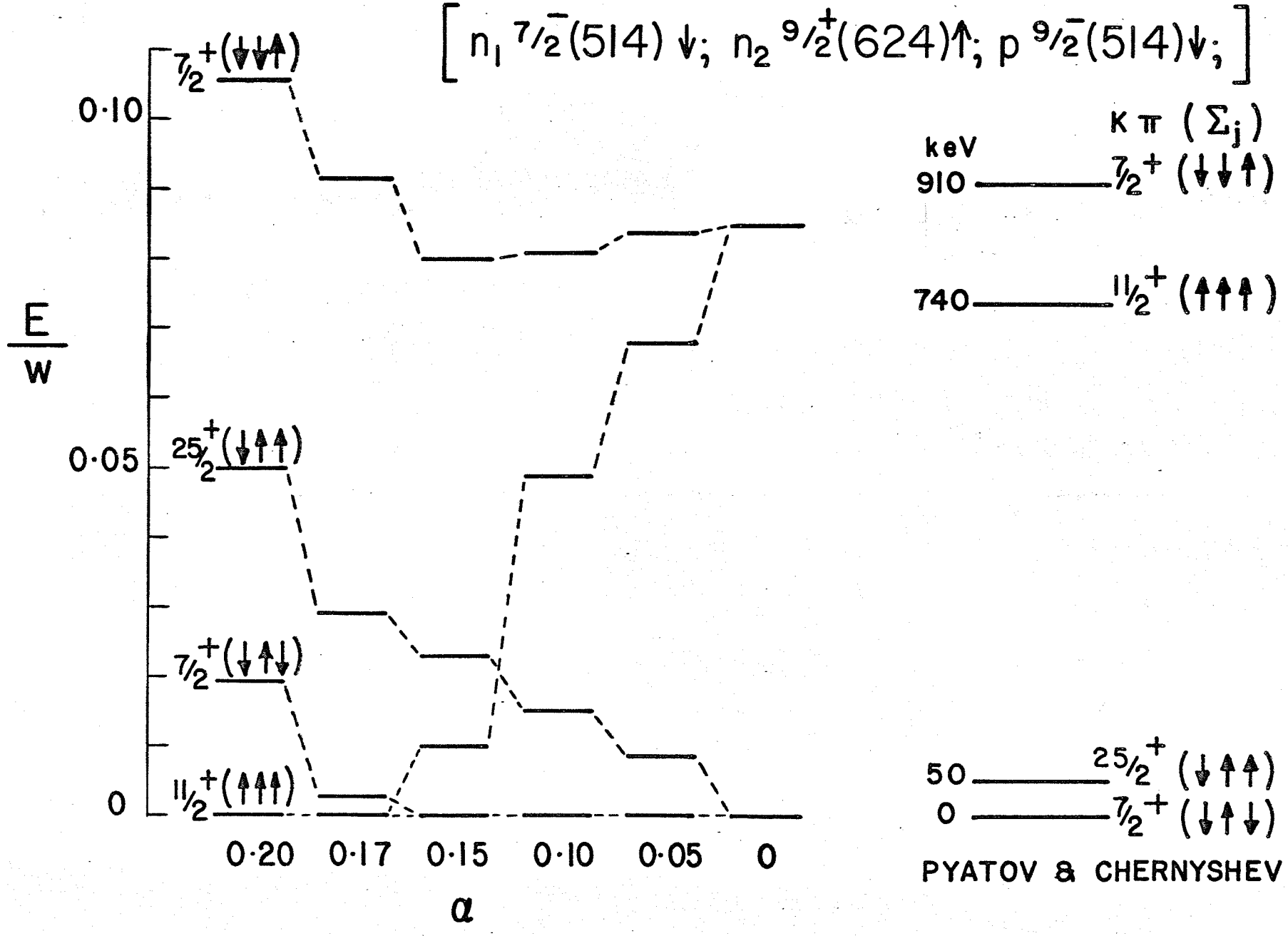
[n1 7/2⁻(514) ↓; n2 9/2⁺(624) ↑; p 9/2⁻(514) ↓;]
E/W
0·10
0·05
0
7/2⁺(↓↓↑)
25/2⁺(↓↑↑)
7/2⁺(↓↑↓)
11/2⁺(↑↑↑)
0·20
0·17
0·15
0·10
0·05
0
α
K π (Σj)
keV
910
7/2⁺ (↓↓↑)
740
11/2⁺ (↑↑↑)
50
25/2⁺ (↓↑↑)
0
7/2⁺ (↓↑↓)
PYATOV & CHERNYSHEV

Fig. 5-11

Level spacing and variation with fraction of spin dependent forces for the three-quasi-particle multiplet formed from
{ n_1 7/2-(514)↓; $n_2$9/2+(624)↑; p 7/2+(404)↓}

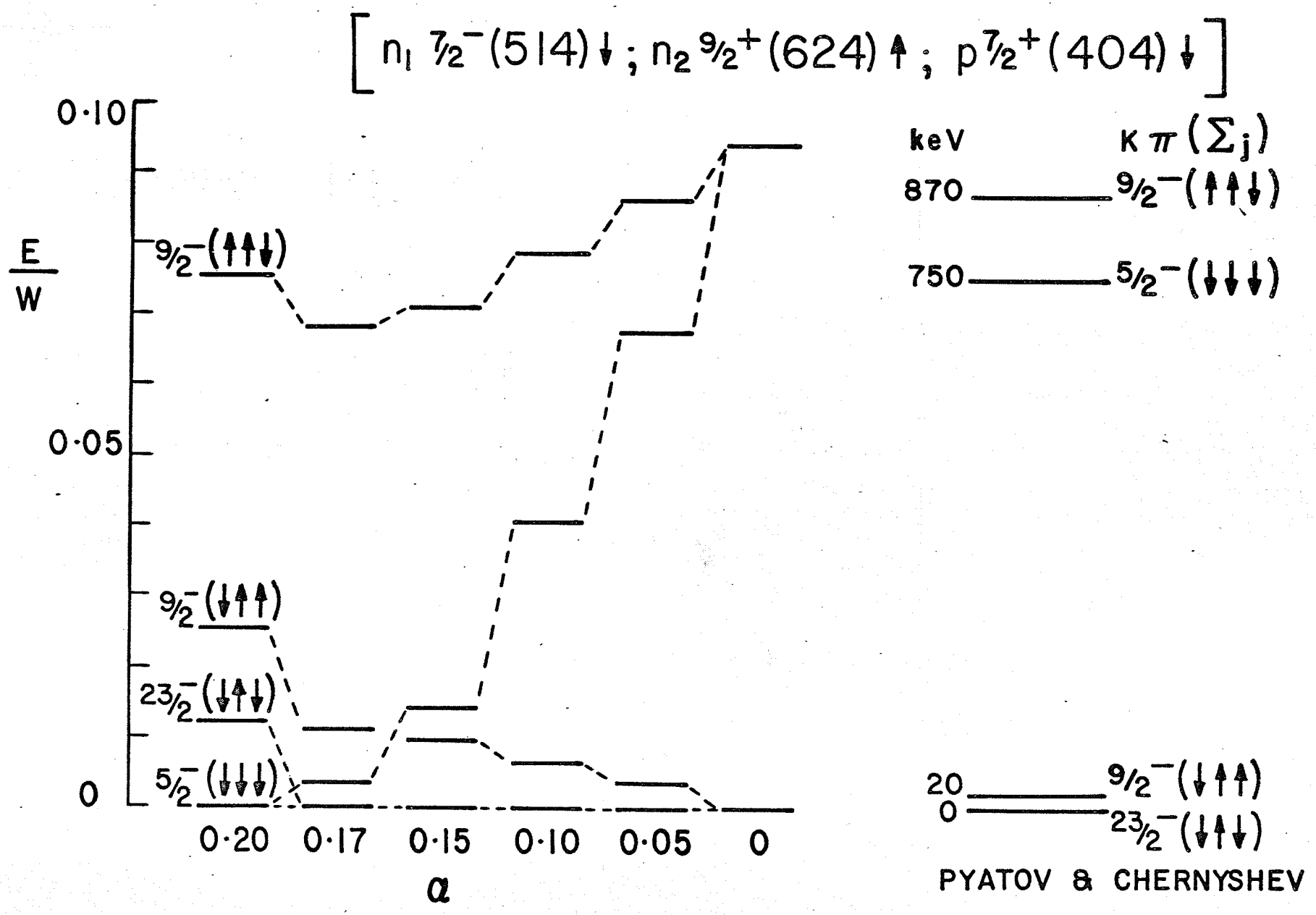
[n1 7/2⁻(514)↓ ; n2 9/2⁺(624)↑ ; p 7/2⁺(404)↓]
0·10
0·05
0
E/W
9/2⁻(↑↑↓)
9/2⁻(↓↑↑)
23/2⁻(↓↑↓)
5/2⁻(↓↓↓)
0·20
0·17
0·15
0·10
0·05
0
α
keV
K π (Σj)
870
9/2⁻(↑↑↓)
750
5/2⁻(↓↓↓)
20
9/2⁻(↓↑↑)
0
23/2⁻(↓↑↓)
PYATOV & CHERNYSHEV

$\{n_1\ 7/2 - (514)\downarrow;\ n_2\ 9/2 + (624)\uparrow;\ p\ 9/2 - (514)\uparrow\}$

and $\{n_1\ 7/2 - (514)\downarrow;\ n_2\ 9/2 + (624)\uparrow;\ p\ 7/2 + (404)\downarrow\}$

The notation uses the asymptotic quantum numbers $\Omega\Pi\ (Nn_z\Omega)\ \Sigma$ of Nilsson (Nilsson 1955) with $\Sigma = +\frac{1}{2}$ indicated by an upwardly directed arrow (↑). The positions of the three lowest levels of the multiplets depend strongly upon the ratio of the Wigner to the spin dependent forces and the level spacings predicted by Pyatov and Chernyshev are shown in Figs. 5-10 and 5-11.

The available Nilsson states in the region appropriate to 177^{Yb} are

Protons	Neutrons
73 9/2 - (514)	107 9/2 + (624)
71 7/2 + (404)	105 7/2 - (514)

The groundstate of ^{177}Yb is classified as $\left[7/2 - (514)\right]^2_n$ $\left[9/2 + (624)\right]_n$. The log ft. values for the β-feeds to the 1231 and 1241 keV levels indicate that these transitions should be classified as allowed unhindered (a.u.). However as can be seen from above, there is no available proton state into which the 9/2 + (624) neutron can decay by means of an a.u. transition. Thus the only possible way an a.u. transition can take place is by the transformation of a (514) neutron into a (514) proton, so the $\left[7/2 - (514)\right]$ neutron pair must be broken. This leads to states in ^{177}Lu formed by the coupling of a $\left[7/2 - (514)\downarrow\right]$ neutron, a $\left[9/2 + (624)\uparrow\right]$ neutron and a $\left[9/2 - (514)\uparrow\right]$ proton. These levels have therefore been classified as three-quasi-particle levels.

Fig. 5-12 summarizes the available information on known and postulated three-quasi-particle states in ^{177}Lu and ^{177}Hf. If the 1241 keV level in ^{177}Lu is interpreted as the low lying 7/2 + member of the multiplet, then the energy level positioning as postulated by Pyatov and Chernyshev, shown on the right hand side of Fig. 5-10, does not agree with the experimental data. The variation of the level position with α (the fraction of spin dependent forces) is also given in Fig. 5-10. Pyatov and Chernyshev chose the value of α and w by calculating the energy separation of two-quasi-particle states in even-mass nuclei and comparing the results with experiment. They used a value of about 0.03 but they point out however that the strong dependence of the positions of the lowest levels on the magnitude of the spin dependence forces makes it difficult to select these parameters properly. A value of α between 0.17 and 0.2 would make the lowest level 11/2 + ($\uparrow\uparrow\uparrow$) with the 7/2 + ($\downarrow\uparrow\downarrow$) and 25/2 + ($\downarrow\uparrow\uparrow$) levels, respectively, above it. This would give better agreement with the present experimental data.

The 23/2 - level at 969 keV is the 155d isomeric state reported by Jorgensen et al (Jorgensen 1962) and Kristensen et al (Kristensen 1964) and is interpeted as a member of the three-quasi-particle multiplet formed from the configuration

$$\{n_1\ 7/2 - (514)\downarrow;\ n_2\ 9/2 + (624)\uparrow;\ p\ 7/2 + (404)\downarrow\}$$

Pyatov and Chernyshev point out that the three-quasi-particle 9/2 - level of ^{177}Lu belonging to this multiplet might be

detected by means of a first forbidden (1u) β-transition to it from ^{177}Yb and they have calculated that the log ft. value for this transition should be 6.5. The results of the present experiments established the existence of a level at 1049.5 keV with spin (7/2, 9/2 or 11/2) and negative parity. The log ft. value calculated from intensity balance is 6.4 indicating that it is most probably a 1u β-transition. It seems reasonable, therefore, that this level might be interpreted as the lower of the 9/2 - levels belonging to this three-quasi-particle multiplet.

The variation of level position with α is shown in Fig. 5-11 along with the spacing predicted by Pyatov and Chernyshev. There is no experimental evidence to date for the existence of the 5/2 - level associated with this configuration, so one cannot say whether the 23/2 or the 5/2 level should be the lowest level of the multiplet. A value of α about 0.17 would be consistent with the choice for the other three-quasi-particle configuration and would give reasonable agreement with the experimental spacing of the 23/2 - and 9/2 - levels.

Fig. 5-12

Three-quasi-particle levels in ^{177}Lu and ^{177}Hf.

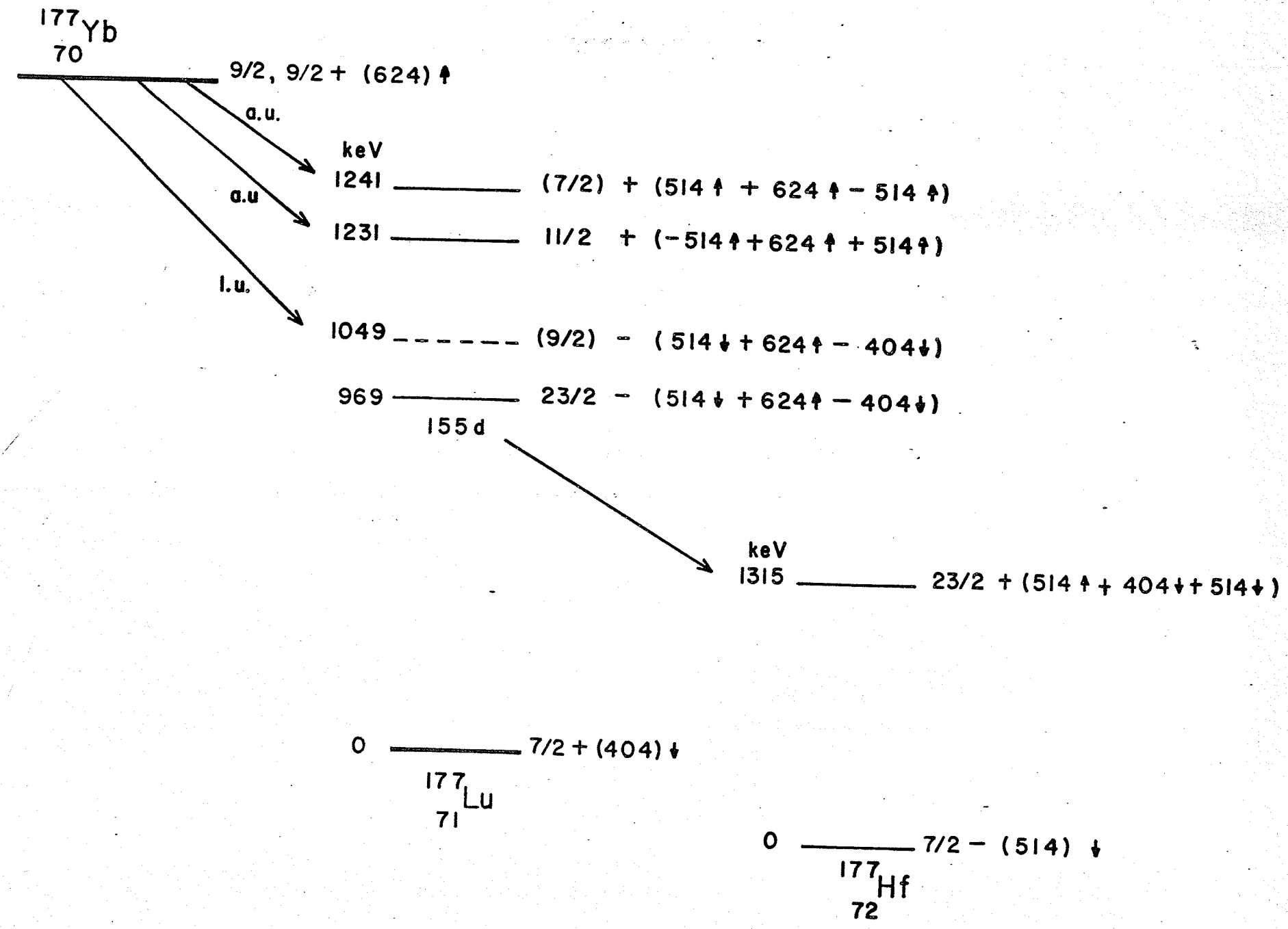
177 Yb
70
9/2, 9/2 + (624) ↑
a.u.
a.u
l.u.
keV
1241
(7/2) + (514 ↑ + 624 ↑ − 514 ↑)
1231
11/2 + (−514 ↑ + 624 ↑ + 514 ↑)
1049
(9/2) − (514 ↓ + 624 ↑ − 404 ↓)
969
23/2 − (514 ↓ + 624 ↑ − 404 ↓)
155 d
keV
1315
23/2 + (514 ↑ + 404 ↓ + 514 ↓)
0
7/2 + (404) ↓
177 Lu
71
0
7/2 − (514) ↓
177 Hf
72

CHAPTER VI

The Decay of 18 hr ^{159}Gd

6.1 Introduction:

Investigations prior to 1958 of the β-decay of 18 hour ^{159}Gd into ^{159}Tb had established that the gamma-ray branching ratios for the E1 transitions de-exciting the 363 keV level were in disagreement with the theoretical values predicted by the unified model (Alaga et al 1955). A more detailed investigation by Nielsen et al (Nielsen 1958) with two six gap β-ray spectrometers and β-γ coincidence experiments revealed three gamma transitions from a level at 364 keV to levels in the groundstate rotational band. The groundstate of ^{159}Tb has been classified as the 3/2 + [411] Nilsson orbital (Mottelson 1959) and levels at 57 and 136 keV were identified as the 5/2 + and 7/2 + members of the rotational band. Angular correlation experiments by Subba Rao (Subba Rao 1962) confirmed the spin assignment of these levels. The work of Nielsen confirmed the discrepancy between experimental and theoretical values of the branching ratios and they suggested that the deviation was connected with the E1 nature of the gamma rays and that these transitions were probably strongly retarded.

Further investigation of the levels in ^{159}Tb following the β-decay of ^{159}Gd were performed by Persson (Persson 1963) using a magnetic β-ray spectrometer and a gamma-ray spectrometer. In addition to confirming the results of Nielsen et al, four new levels were introduced at 348, 580, 616, and 674 keV. It was also pointed out by Persson that the 616 keV gamma-ray could be fitted

either between the level at 616 keV and the groundstate or between the 674 and 58 keV levels.

More recently Funke et al (Funke 1965) have performed two dimensional NaI(Tl) - NaI(Tl) coincidence experiments on this isotope and have discovered three new coincidence pairs necessitating the introduction of a new level at~860 keV. Their coincidence data also suggested that the 616 keV transition was complex with ~88% of it feeding the groundstate.

The levels in ^{159}Tb have also been studied by Diamond and Stephens (Diamond 1963) by means of Coulomb excitation experiments using 60 MeV ^{16}O ions. In addition to exciting members of the groundstate rotational band up to the 15/2 + level, they also established rotational bands at 348 and 580 keV and indicated the possible existence of rotational bands at 971 and 1280 keV.

The present work reports the results of an investigation of the gamma-ray transitions in ^{159}Tb following the β-decay of ^{159}Gd using Ge(Li) detectors. The direct gamma-ray spectrum was studied with a high resolution (1.0 keV at 100 keV) planar detectors, and a thin window planar and large volume coaxial detector were used to perform gamma-gamma coincidence experiments.

6.2 Source Preparation

Sources of ^{159}Gd were prepared by irradiating samples of Gd_2O_3 enriched to 97.6% ^{158}Gd in a flux of 2.5×10^{14} neutrons/sq. cm./sec in the N.R.U. reactor. When the direct gamma-ray spectrum of the first irradiated sample was examined, a contaminant with a half-life of~9 hours was observed. This was identified as ^{152}Eu. All subsequent irradiations were treated chemically before

use. The ^{152}Eu was separated from the galodinium isotopes by elution from an ion exchange column using α-hydroxy-isobutyrate with a pH of 3.75 (Smith and Hoffman 1956). The separated Gd fraction was deposited in a small plastic tube and this form of liquid source was then used for both the direct and coincidence studies.

6.3 Experimental Procedure

The direct gamma-ray spectra were obtained using a planar Ge(Li) detector 5.0 sq. cm. in area with a depletion depth of 5mm. The resolution of this detector is 1.0 keV at an energy of 100 keV. The coincidence spectra were taken with a 44cc coaxial detector (G9C2), a 30cc coaxial detector (GLC6X) and a thin window planar detector (G1P7) with a depletion depth of 10 mm.

The data from the direct gamma-ray spectra were recorded on a Nuclear Data 3300 system and the coincidence data were recorded on either a PDP-8 or PDP-1 computer using the techniques described in Chapter IV of this thesis.

Three coincidence experiments were performed during the present work on ^{159}Gd. For the first of these experiments, two large volume coaxial Ge(Li) detectors were used and the data were recorded by means of the related address technique using a PDP-8 computer. In this experiment, the time relationship between coincident events was not recorded, so the experiment was repeated using the PDP-1 computer and the time information was recorded as a third parameter. When the data from this second run were analysed, it was found extremely difficult to set windows on γ-58 and γ-80 and get meaningful results. This was caused by the fact that

the timing distribution for large volume coaxial detectors is very poor when low energy transitions are involved.

To improve the timing characteristics, it was decided that one of the coaxial detectors (GLC6X) should be replaced with a thin window (~60μ) planar detector (G1P7), and the experiment repeated. By this time a third encoder had been installed with the PDP-8 computer and this system was used for the third coincidence experiment.

The capacitance of the planar detector was ~10 pf, so this side of the coincidence arrangement could now be triggered at a lower level. It was set to trigger at ~15 keV while the coaxial detector was set to trigger at ~30 keV. The amplifier gains were adjusted so that the planar detector covered the energy range from ~30 to ~380 keV while the coaxial detector spanned from ~75 to ~950 keV. The resulting time distribution for events coincident with γ-58 was narrower than in the previous experiment and time windows ~100 nsec were set.

In the initial coincidence experiments the counters were placed close together (~½" apart) in 180° geometry. In this configuration a large number of the coincidence events recorded were produced by gamma-rays backscattering from one detector into the other. An example of this can be seen in Fig. 6-1 which shows the "coincidence singles" from the second coincidence experiment. As can be seen from Fig. 6-1, most of the events recorded came from backscattering and were consequently of no interest.

To reduce the number of backscattered events recorded in the third experiment, a lead shield was placed between the detectors as shown in Fig. 6-2. Two sheets of Cd (~0.030") covered the side

Fig. 6-1

"Coincidence singles" spectrum for ^{159}Gd obtained during the gamma-gamma coincidence experiments with two coaxial detectors.

3380-E

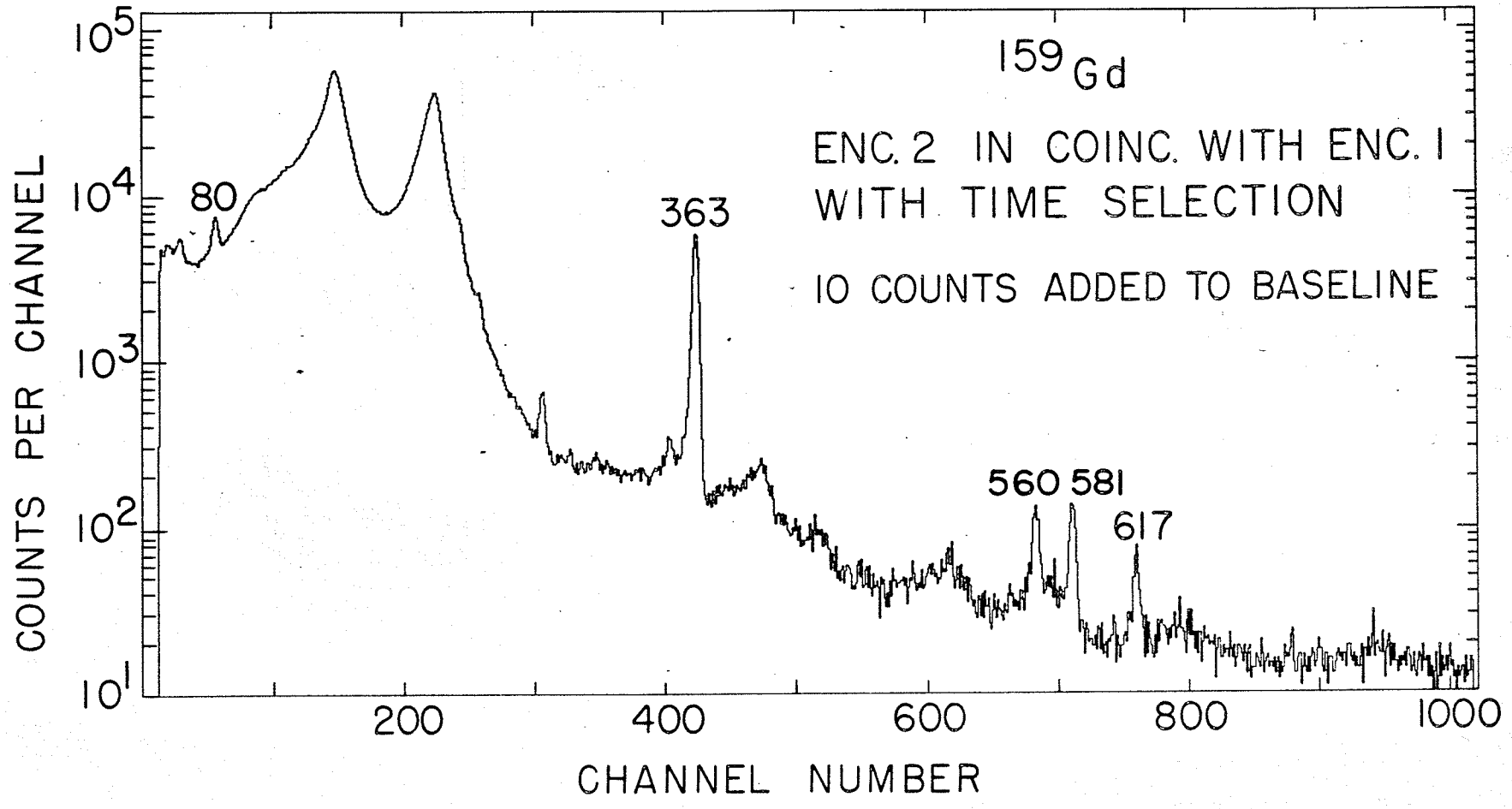
159 Gd
ENC. 2 IN COINC. WITH ENC. 1
WITH TIME SELECTION
10 COUNTS ADDED TO BASELINE
80
363
560 581
617
COUNTS PER CHANNEL
CHANNEL NUMBER
10^5
10^4
10^3
10^2
10^1
200
400
600
800
1000

Fig. 6-2

Schematic diagram of the detector geometry used in the ^{159}Gd coaxial-planar experiment.

3378-G

GEOMETRY FOR ^{159}Gd COINCIDENCE EXPERIMENT

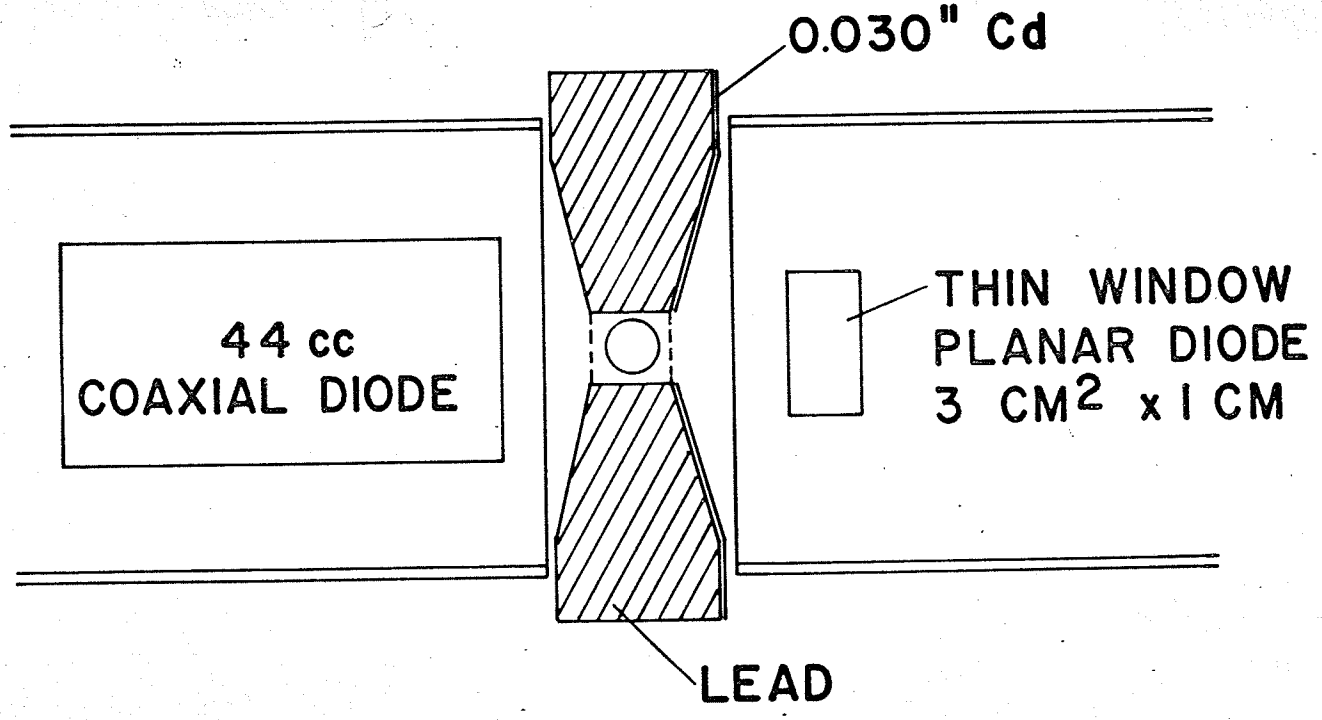

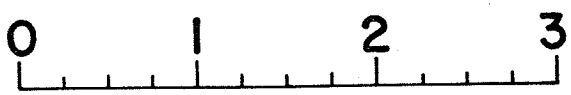

SCALE IN INCHES

facing the planar detector in order to reduce the number of lead x-rays observed by this diode. Fig. 6-3 shows the "coincidence singles" obtained with this type of geometry.

The most intense gamma-ray in ^{159}Tb is the 363.3 keV transition. Since this transition is about 50 times stronger than any of the others, random coincidences with this gamma-ray become a significant problem. For this reason weak sources were used for the third coincidence experiment and as a result, the coincidence counting rate was low (15-20 coincidences/sec). Several sources, each with strength increasing by a factor of two, were prepared from a 16 hour irradiation of 2 mg. of ^{158}Gd in a flux of 2.5×10^{14} neutrons/sq./cm./sec. These sources were each counted for one half-life and the data were collected over a period of ~72 hours.

The small memory in the PDP-8 (4096 channels) made it impractical to do the three parameter sorting on this machine so the magnetic tapes were taken to the G-20 where several windows could be sorted at one time. The position of the time window for each gamma-ray was determined by examining a few records on the PDP-8. In order to remove the contribution from the Compton distribution a window, one half the width of the window set on the full-energy peak, was set on either side of the full-energy peak. The events coincident with these windows were then added together and subtracted from those events coincident with the full-energy peak.

Fig. 6-3

Comparison of the "coincidence singles" spectra showing the reduction in peaks due to back-scattering.

Upper half: coaxial-planar experiment

Lower half: coaxial-coaxial experiment.

3380-E

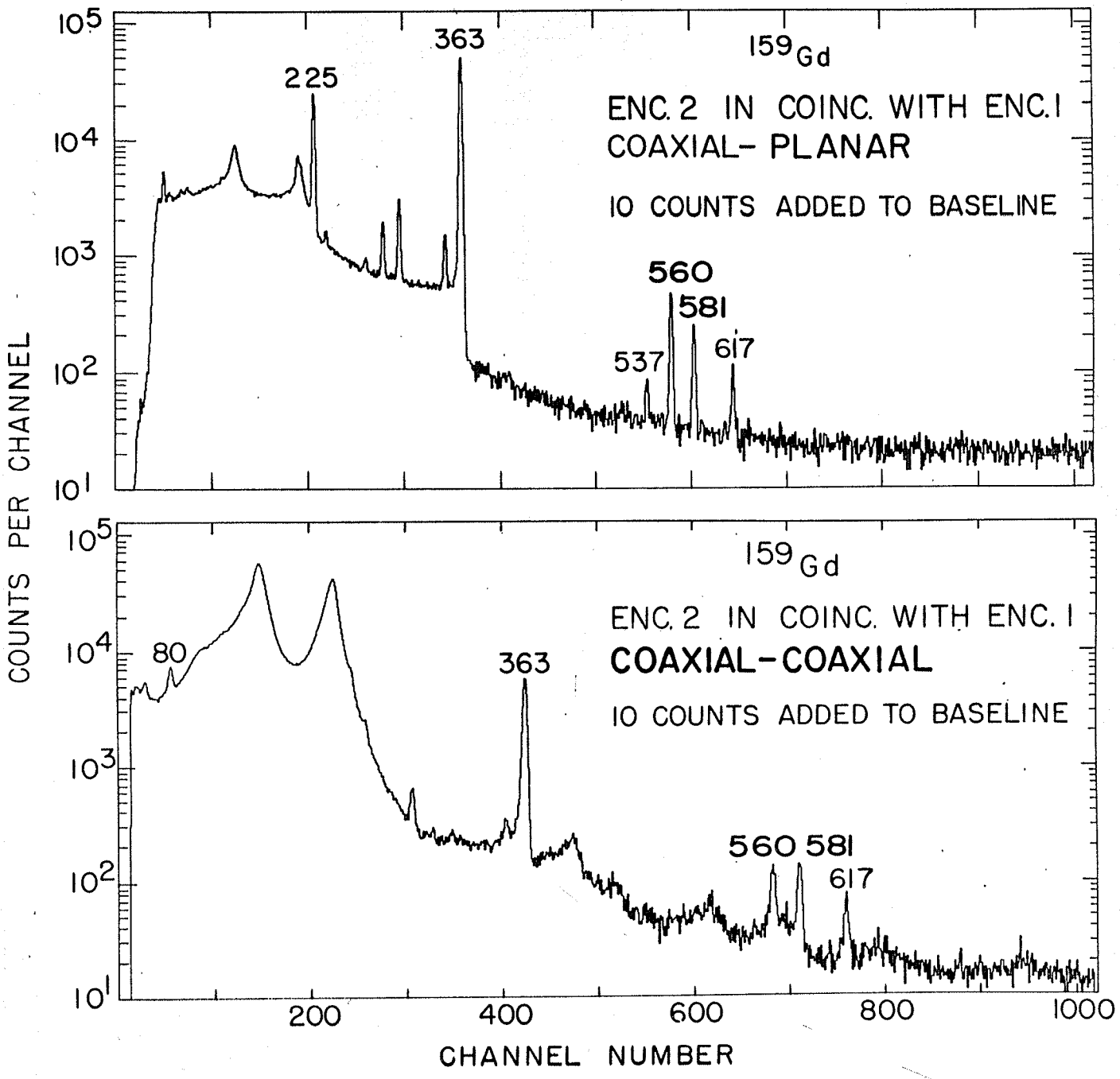
159Gd
ENC. 2 IN COINC. WITH ENC. 1
COAXIAL- PLANAR
10 COUNTS ADDED TO BASELINE
225
363
537
560
581
617
159Gd
ENC. 2 IN COINC. WITH ENC. 1
COAXIAL-COAXIAL
10 COUNTS ADDED TO BASELINE
80
363
560 581
617
COUNTS PER CHANNEL
CHANNEL NUMBER
200
400
600
800
1000

Results

6.4 Direct Gamma-Ray Spectrum

The direct gamma-ray spectrum of ^{159}Gd obtained with the 5.0 mm deep planar detector is shown in Fig. 6-4. This spectrum was taken with 0.015" Cd between the source and detector. The decay of the source was followed through several half lives in order to identify those transitions in ^{159}Tb following the decay of 18 hour ^{159}Gd. Eighteen transitions were identified as belonging to this decay and these are listed in Table 6-I. It can be seen from this table that this is the first time all of these transitions have been observed in the direct spectrum.

The three small unlabelled peaks around the 80 keV line can be attributed to Pb X-rays. The next two peaks are the doublet at 97.43 and 103.18 keV in ^{153}Gd (Table of Isotopes 6th edition) which was produced from the ^{152}Gd present in the enriched Gd_2O_3. The peak in the bottom section of the diagram marked contaminant can be attributed to a ^{137}Cs source in the room background. The energy region up to ~1200 keV was scanned and the only other peak found above the 854 keV transition was identified as belonging to ^{60}Co present in the background.

Coulomb excitation experiments on ^{157}Tb have been performed by Diamond and Stephens (Diamond 1963). Their results indicate a level at 674 keV which de-excites by the emission of gamma-rays with energies 536, 617 and 674 keV. They give the relative gamma intensities of the 536 and 674 keV transitions as 41 and 11 respectively. Since this level is populated in the β-decay of ^{159}Gd, the 674 keV transition should also appear in the present study. In order to search for this gamma-ray,

Fig. 6-4

The direct gamma-ray spectrum of ^{159}Gd observed using the high resolution planar detector GA6 with 0.015" Cd absorber between the source and the detector.

3379-H

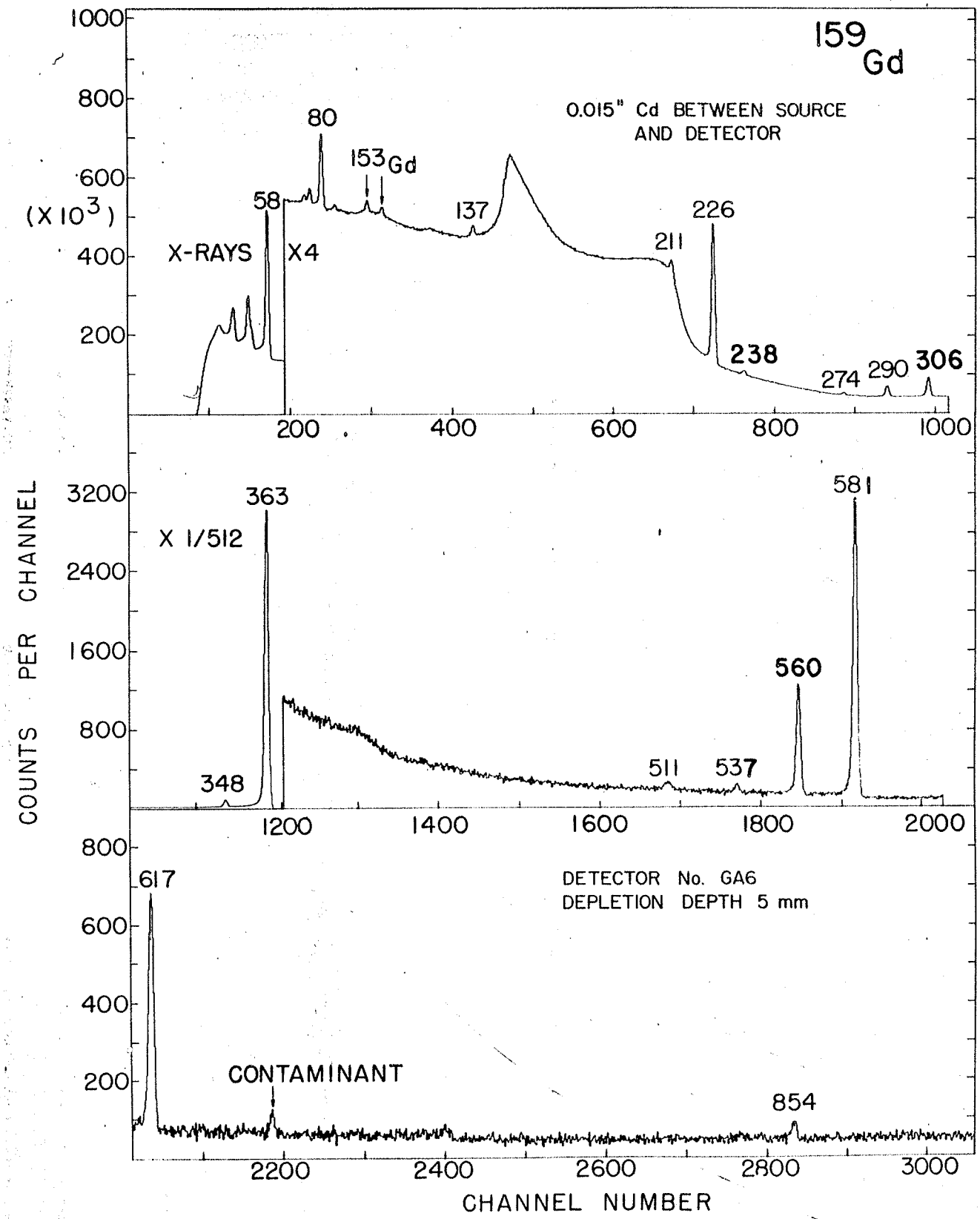
159 Gd
0.015" Cd BETWEEN SOURCE AND DETECTOR
80
153 Gd
58
137
226
211
X-RAYS
X4
238
274
290
306
(X 10^3)
X 1/512
363
581
560
348
511
537
DETECTOR No. GA6
DEPLETION DEPTH 5 mm
617
CONTAMINANT
854
COUNTS PER CHANNEL
CHANNEL NUMBER

GAMMA-RAY SPECTRUM OF ^{159}Gd

ENERGY (keV)	RELATIVE INTENSITIES					
	BROWN	EWAN	FUNKE	PERSSON	SUBBA RAO	NIELSEN
58.00±0.05	21±2	19±3			42±8	23.6
79.52±0.10	0.38±0.04	0.43±0.05	0.44±0.08		0.35±0.10	0.43
137.4±0.2	0.06±0.01		0.10±0.03			
210.9±0.5	0.165±0.025	)				
		)	2.1±0.4			
226.2±0.2	1.96±0.10	1.9±0.02)			1.9±0.2	2.8
237.5±0.2	0.072±0.011		0.09±0.03			
274.2±0.2	0.054±0.013		0.065±0.03			
290.3±0.2	0.28±0.03	0.35±0.06)			)	
		)	1		)	1.08
305.5±0.2	0.55±0.04	0.75±0.08)			0.85±0.15)	
348.1±0.2	2.0±0.15	2.4±0.3)		2.0±0.3		
		)	100±30			
363.3±0.2	100±5	100±5)		100±5	100	100
536.8±0.2	0.010±0.003		≤0.02	0.07±0.04		
559.57±0.15	0.20±0.02	0.21±0.03	0.23±0.04	0.25±0.10		
580.84±0.15	0.57±0.04	0.64±0.07	0.5±0.2	0.70±0.15		
616.5±0.3	0.02±0.005)		0.02±0.01)			
	)	0.15±0.03	)	0.20±0.08		
617.7±0.2	0.13±0.02)		0.15±0.05)			
674.3±0.5	0.0034±0.001					
854.9±0.2	0.021±0.003		0.015±0.007			

several sources of increasing strength were prepared and the data were gathered over several half lives. The intense 363 keV transition gave severe "pile-up" problems from accidental coincidences and in order to reduce this 0.280" Pb plus 0.075" Cd were placed between the source and the detector (30cc coaxial detector no. GLC6X). The results of this investigation can be seen in Fig. 6-5 where the gamma-ray can be clearly seen and its energy was measured to be 674.2 ± 0.5 keV. After corrections had been made for detector efficiency and absorption in the Pb and Cd, the intensities of γ-536 and γ-674.2 were calculated to be 0.010 ± 0.003 and 0.0034 ± 0.001 (γ-363 = 100 ± 5) respectively. This gives a branching ratio

$$\frac{I_\gamma\ (536)}{I_\gamma\ (674)} = 2.9 \pm 1.2$$

in agreement with the Diamond and Stephens value.

The gamma-ray energies listed in column 1 of Table 6-I are the values measured in the present work. The method used for these measurements has already been described in this thesis. Unless otherwise stated the values are accurate to ±0.2 keV. The energy of γ-58 was measured relative to the 59.543 ± 0.015 keV (Yamazaki 1966) transition in ^{241}Am using the thin window planar detector G1P7. Fig. 6-6 shows the separation of the two lines. A precision pulse generator was used to determine the deviation from linearity of the system. After correcting for the system non-linearity and using the ^{159}Tb K β$_1$ x-ray line, ^{241}Am and ^{153}Gd sources to determine the keV/CH, the calculated value for the energy of γ-58 is 58.00 ± 0.05 keV.

A comparison of the relative intensities in column 2 and column 3 (Ewan 1964a) of Table 6-I shows them to be in reasonably

Fig 6-5

High energy region of the ^{159}Gd spectrum between 500 keV and 870 keV obtained using the coaxial detector GLC6X with 0.280" Pb and 0.075" Cd between the source and detector.

3392-F

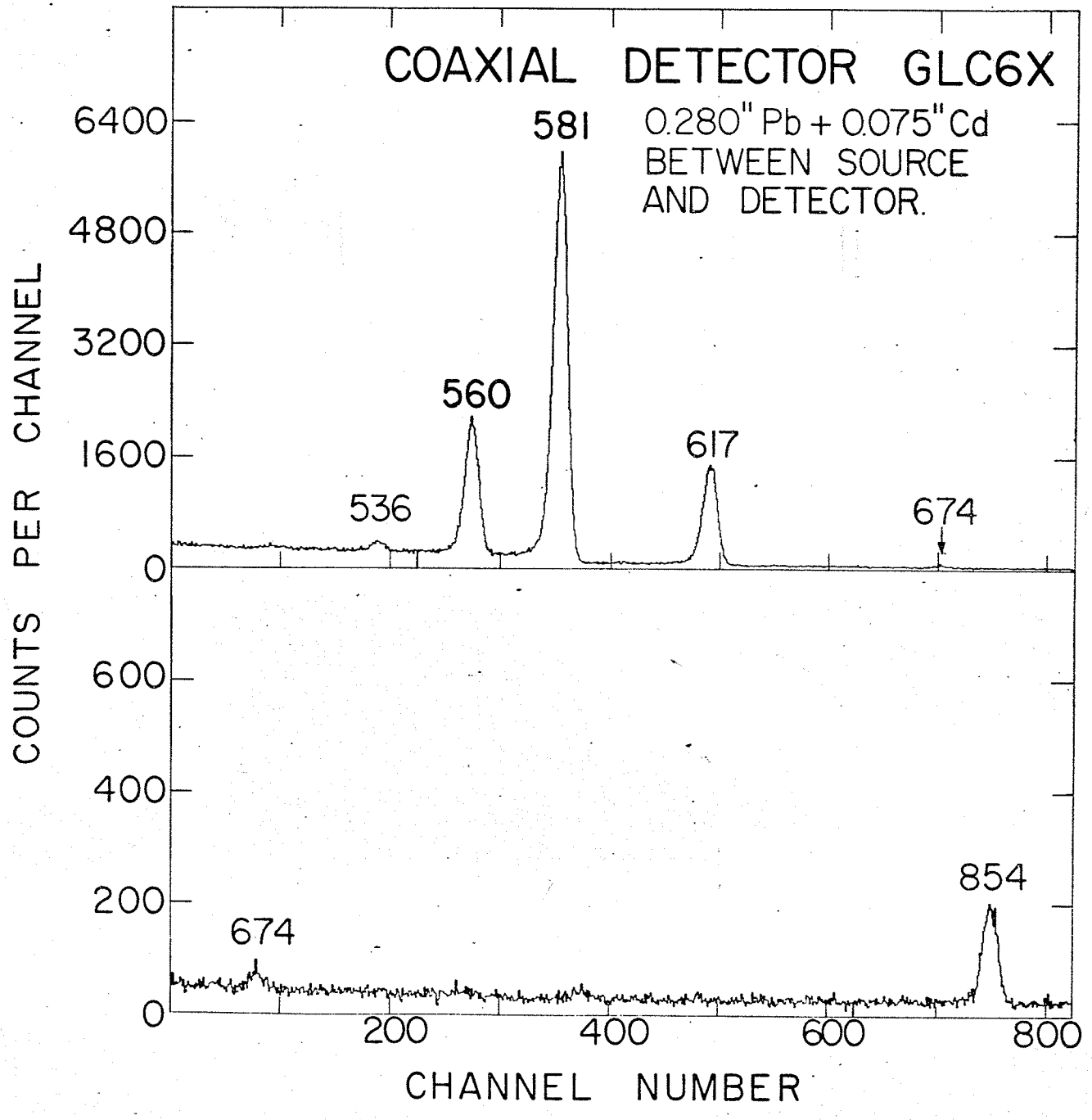
COAXIAL DETECTOR GLC6X
0.280" Pb + 0.075" Cd
BETWEEN SOURCE
AND DETECTOR.
581
560
617
536
674
854
674
6400
4800
3200
1600
0
600
400
200
0
200
400
600
800
COUNTS PER CHANNEL
CHANNEL NUMBER

Fig. 6-6

Measurement of the energy of γ-58 relative to the 59.543 keV line in ^{241}Am using the thin-window planar detector GIP7.

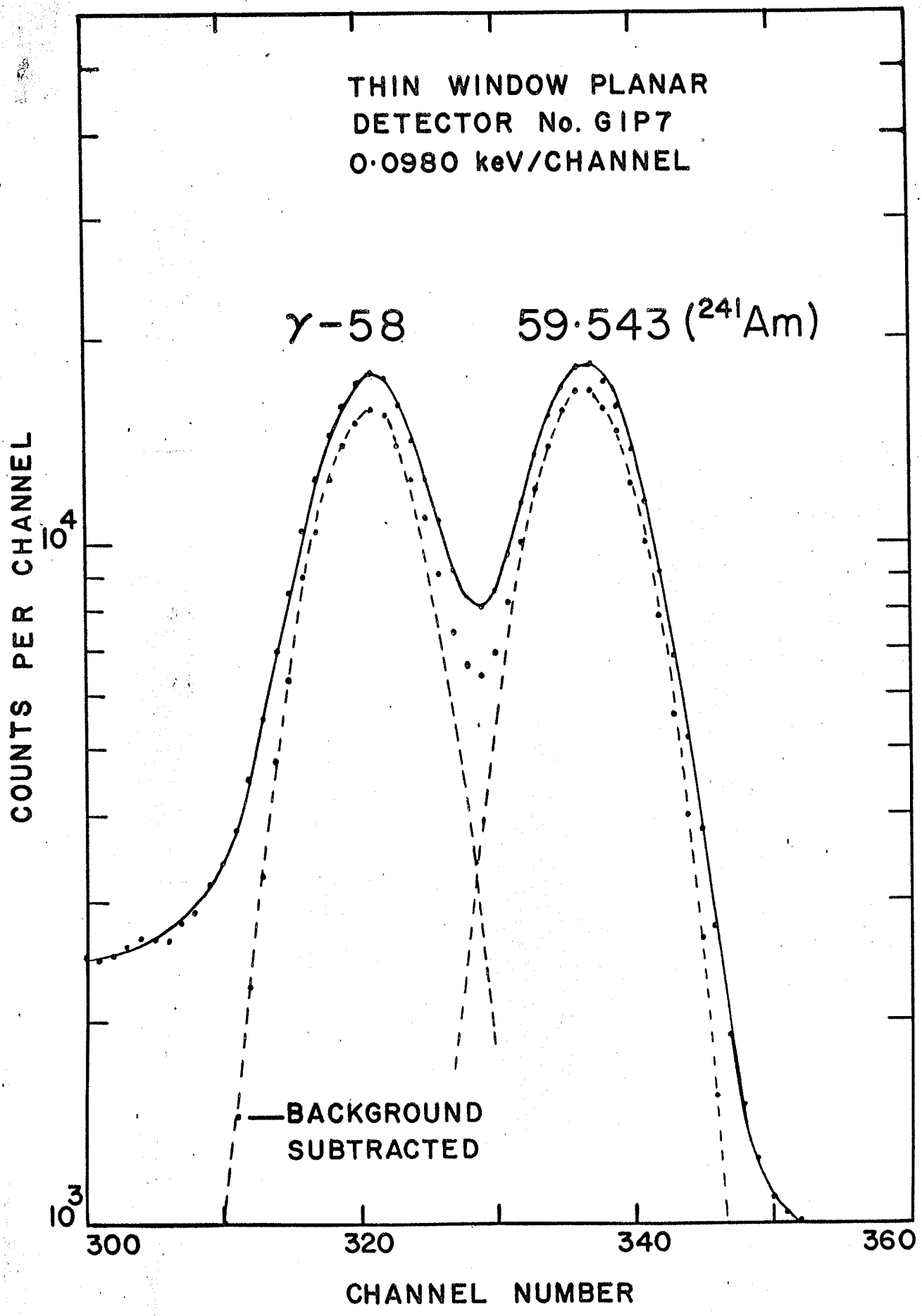
THIN WINDOW PLANAR
DETECTOR No. GIP7
0·0980 keV/CHANNEL
γ-58 59·543 (241Am)
COUNTS PER CHANNEL
10⁴
10³
BACKGROUND
SUBTRACTED
300
320
340
360
CHANNEL NUMBER

good agreement. In that reference the authors reported a gamma-ray with energy 334 keV with a relative intensity of 0.42 ± 0.06 (I_{γ}-363 = 100 ± 5). A detailed scan of this energy region in the present work showed no trace of this transition and an upper limit of<0.004 (γ-363 = 100 ± 5) can be assigned. It is concluded that this 334 keV transition must have been an impurity present in the source used in that work.

The results obtained by Funke et al (Funke 1965) are in good agreement with those of the present work. The weak transitions measured by Funke as 245 ± 5, 280 ± 5, and 860 ± 10 keV from his two parameter NaI(Tl) - NaI(Tl) coincidence experiment are identified as the 237.5, 274.2 and 854.9 keV transitions in the present work. Funke also reports that the 617 keV transition is complex and that it feeds the groundstate and 58.0 keV level with intensities 0.15 ± 0.05 and 0.02 ± 0.01 (I_{γ}-363 = 100 ± 5) respectively.

Attempts to fit γ-617 between the 58 keV and the 674 keV levels however did not give a good energy balance. The summation of γ-58.0, γ-79.5 and γ-536.8 energies gave 674.3 keV in agreement with the groundstate transition measured at 674.3 ± 0.5 keV. However summation of γ-58.0 and γ-617.5 energies gave 675.5 ± 0.16 keV. No evidence of doublet structure had been seen with the coaxial detector (GLC6X), so this region was re-examined with the thin window planar detector (GlP7). The result of this investigation is shown in Fig. 6-7 which clearly shows that the 617 keV line is double. The line shape used to determine the peak positions is that of the 661.6 keV line in ^{137}Cs which was recorded simultaneously with the ^{159}Gd spectrum. The

Fig. 6-7

The doublet at 617 keV resolved with the high resolution thin-window detector GIP7

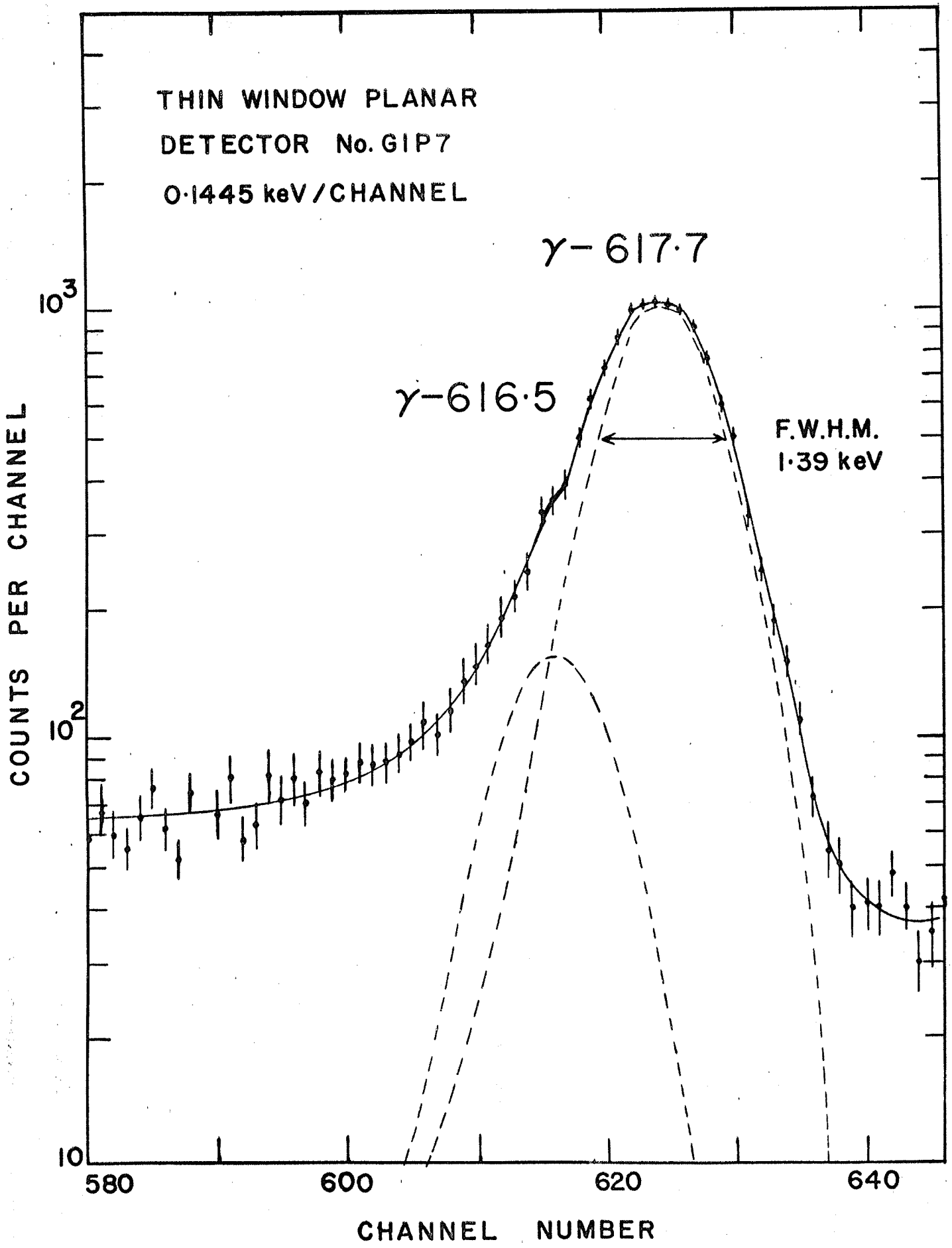
THIN WINDOW PLANAR
DETECTOR No. GIP7
0·1445 keV/CHANNEL
γ-617·7
γ-616·5
F.W.H.M.
1·39 keV
10³
10²
10
COUNTS PER CHANNEL
580
600
620
640
CHANNEL NUMBER

peak separation as measured from Fig. 6-7 is 1.21 ± 0.07 keV. This gives the energies of the two lines as 616.5 ± 0.3 and 617.7 ± 0.2 keV and the relative intensities are calculated to be 0.02 ± 0.005 and 0.13 ± 0.02 respectively (I_γ-363 = 100 ± 5).

6.5 Coincidence Spectra

The nature of the 58.0 keV transition has been studied by Novakov and Hollander (Novakov 1964). From a measurement of the L subshell ratios they have established that it is 98.6% M1 plus 1.4% E2. Nielsen et al (Nielsen 1958) were unable to resolve the K X-rays and 58 keV gamma-ray peak in their gamma-ray spectrum, but from the asymmetry of the peak shape they estimated that $\alpha_K \simeq 6$ which is in agreement with the predominantly M1 nature of the transition. The high internal conversion of this transition was utilized to give good statistics in the coincidence experiment with γ-58. The energy window around γ-58 was set so that the K X-rays as well as γ-58 were encompassed by it. Fig. 6-8 shows the net coincidence spectrum obtained with the above energy window set in the planar detector. The events coincident with the Compton distribution and the random coincidence events have been removed.

This spectrum shows eight gamma-rays in coincidence with γ-58. The energy range covered by the coaxial detector was such that the 80 keV transition was not recorded. From other spectra to be presented later in this section, it can be shown that γ-80 is also in coincidence with γ-58 giving a total of nine such coincident transitions.

Fig. 6-8

Net coincidence spectrum with γ-58+ X-rays. Spectrum shown was recorded by coaxial detector in coincidence with window set in planar detector encompassing γ-58 + X-rays.

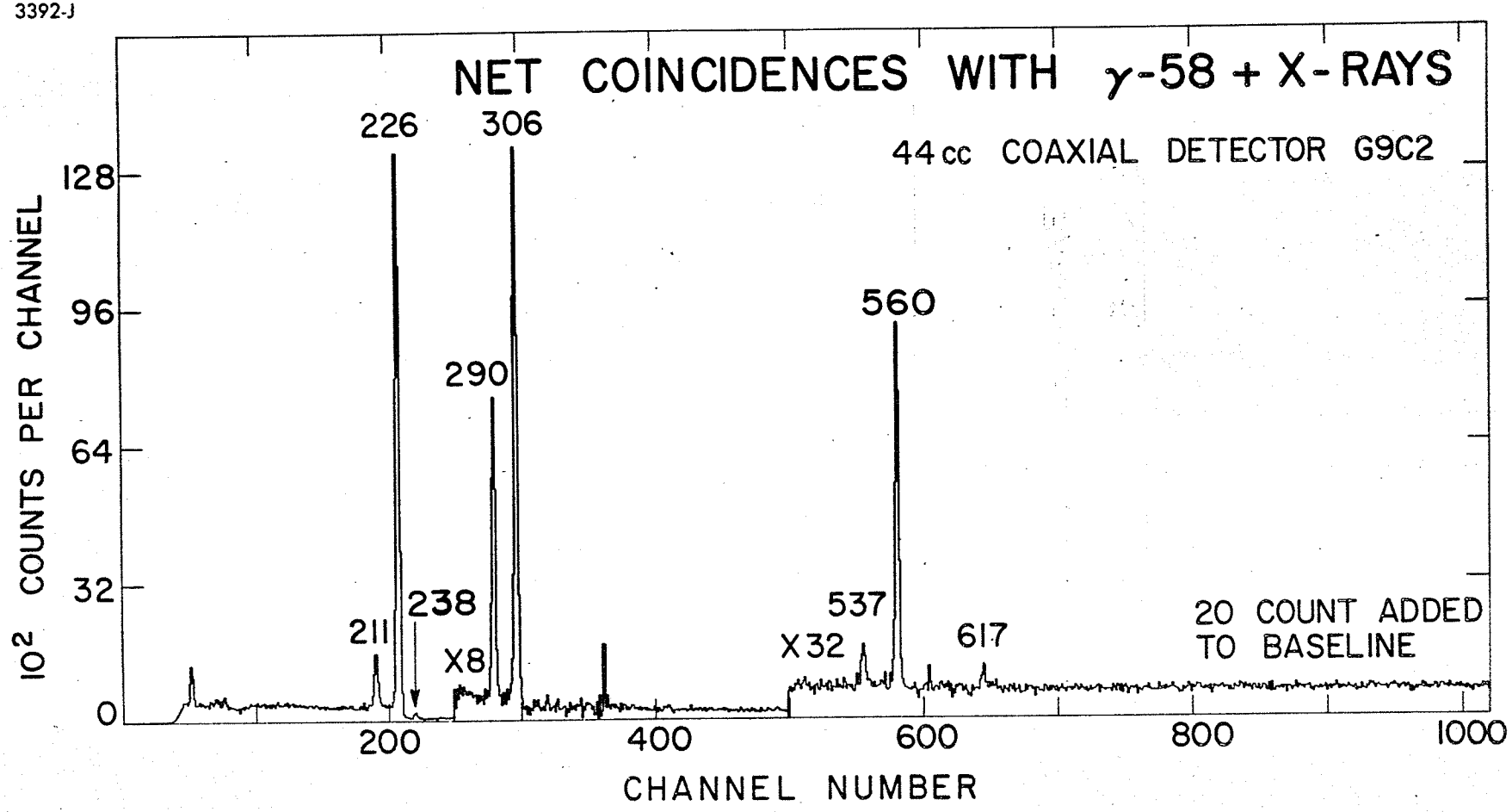
3392-J
NET COINCIDENCES WITH γ-58 + X-RAYS
44 cc COAXIAL DETECTOR G9C2
226
306
560
290
211
238
537
617
X8
X32
20 COUNT ADDED TO BASELINE
128
96
64
32
0
10² COUNTS PER CHANNEL
200
400
600
800
1000
CHANNEL NUMBER

When allowance has been made for the x-ray contribution from the 79.5 keV transition, a measurement of the intensity of γ-618 relative to γ-559 and γ-537 gives a value of 0.016 ± 0.005 (I_γ-363 = 100 ± 5). This is in good agreement with the value from the direct spectrum and is also in agreement with the measurement of Funke et al.

Three gamma-rays with energies 211, 226 and 537 keV can be seen in Fig. 6-9 which is the net coincidence spectrum with γ-80. As in the above case, the energy range covered by the coaxial detector was not sufficient to include γ-58. The number of counts in the 537 keV peak is very small but intensity measurements from this spectrum for γ-211, γ-226 and γ-537 yield the values 0.17 ± 0.04, 1.96 ± 0.4 and 0.015 ± 0.005 which are in good agreement with the values 0.165 ± 0.025, 1.96 ± 0.10 and 0.010 ± 0.003 obtained from the direct spectrum.

The net coincidence spectrum with γ-226 is shown in Fig. 6-10. This spectrum was obtained by setting an energy window in the coaxial detector and the data shown are from the thin window planar detector. Fig. 6-10 shows that the 58 and 80 keV gamma-rays are in coincidence with γ-226. The x-rays in this spectrum arise from the high conversion coefficients of both γ-58 and γ-80. A measurement of the relative intensities of these two transitions from this spectrum yields the ratio of the total conversion coefficients from the relationship

$$\frac{I_\gamma\text{-}80}{I_\gamma\text{-}58} = \frac{1 + \alpha_T(58)}{1 + \alpha_T(80)}$$

Fig. 6-9

Net coincidence spectrum with γ-80. Spectrum shown was recorded by coaxial detector in coincidence with γ-80 in the planar detector.

3392-K

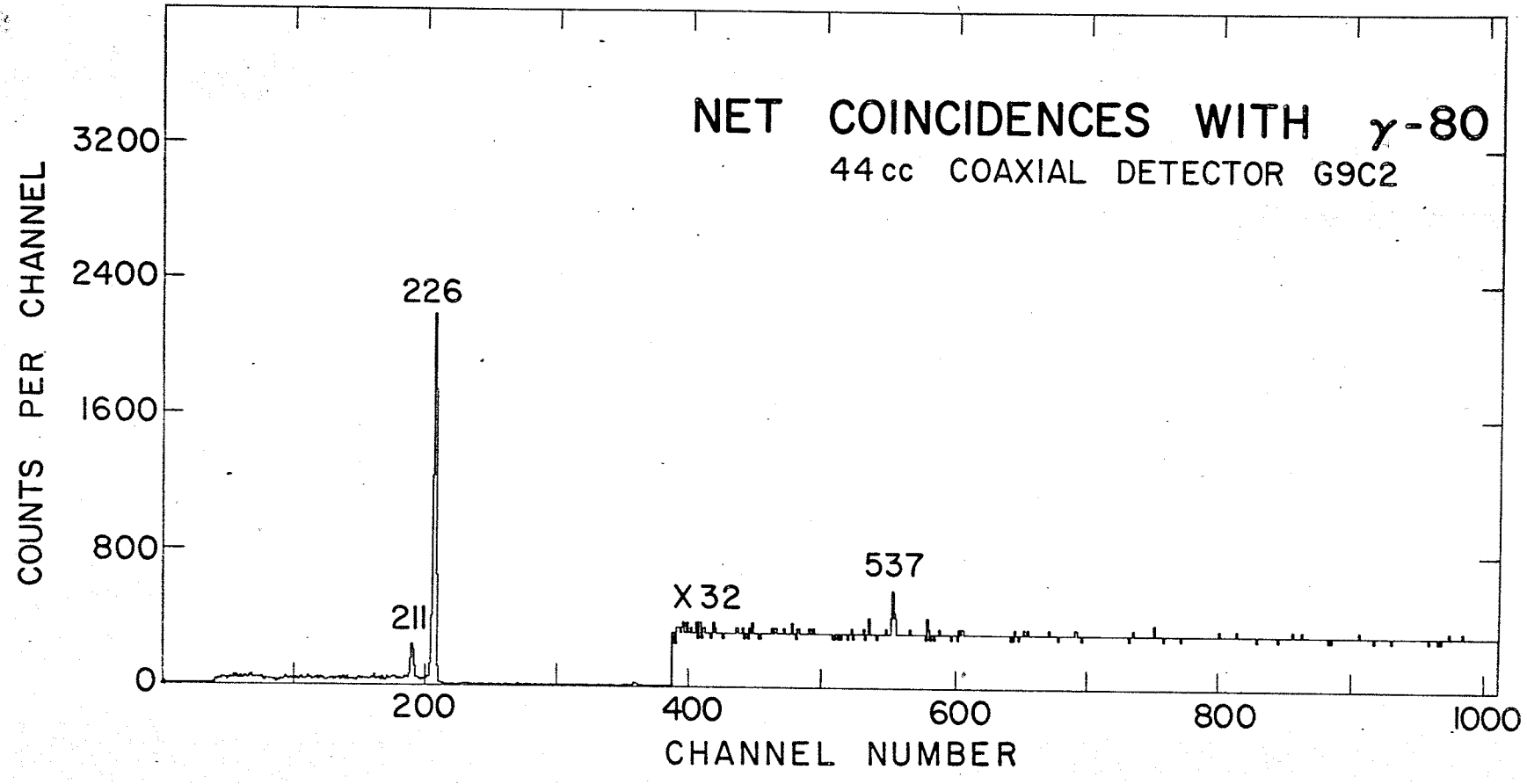
NET COINCIDENCES WITH γ-80
44 cc COAXIAL DETECTOR G9C2
COUNTS PER CHANNEL
3200
2400
1600
800
0
226
211
X32
537
200
400
600
800
1000
CHANNEL NUMBER

Fig. 6-10

Net coincidence spectrum with γ-226. Spectrum shown was recorded by planar detector in coincidence with γ-226 in coaxial detector.

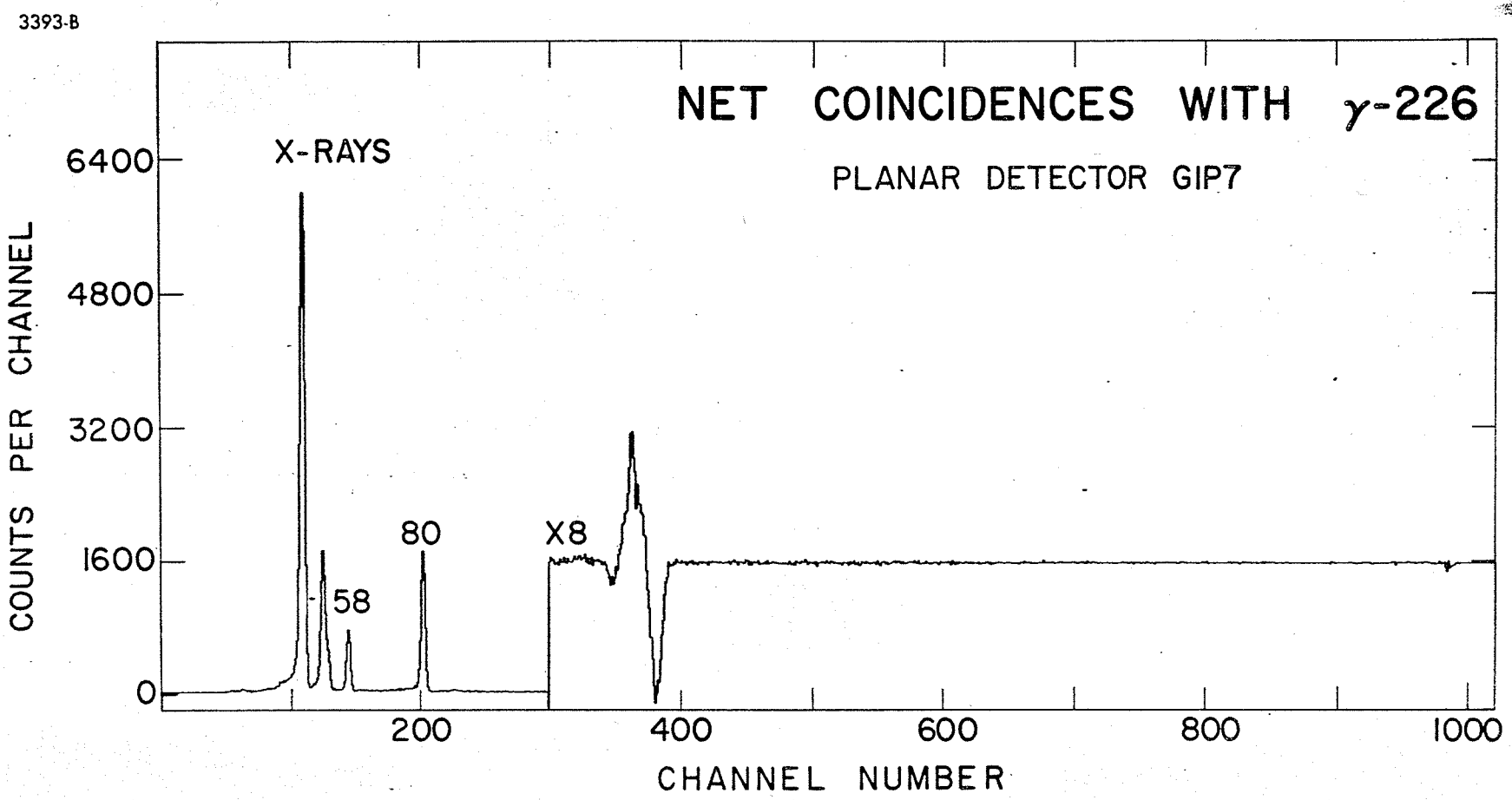
3393-B
NET COINCIDENCES WITH γ-226
PLANAR DETECTOR GIP7
X-RAYS
58
80
X8
6400
4800
3200
1600
0
COUNTS PER CHANNEL
200
400
600
800
1000
CHANNEL NUMBER

If the values of the appropriate $^{\alpha}T$'s, on the basis of the previously assigned multipolarities, are substituted into this expression, the theoretical value of $\frac{I_\gamma - 80}{I_\gamma - 58} = 2.11$. The experimental value obtained from Fig. 6-10 is 2.5 ± 0.5 which is consistent with the theoretical value.

Transitions coincident with γ-238 are shown in Fig. 6-11. These data were taken from the first coincidence experiment performed on the PDP-8 computer using two large volume coaxial detectors (G9C2 and GLC6X). This experiment did not use a third encoder to record the time relationship between coincident events, so no random coincidences have been subtracted in this spectrum. Fig. 6-11 clearly shows that there are two transitions in coincidence with γ-238 viz. γ-560 and γ-618. The intensity of γ-618 was measured relative to γ-560 from these data. The intensity was found to be 0.12 ± 0.025 with I_γ-363 set equal to 100 ± 5. This is in good agreement with the value of 0.13 ± 0.02 obtained from the direct spectrum.

The statistics obtained in the above experiment were better than those obtained in the planar-coaxial experiment. This was due to the fact that although the same amount of magnetic tape was used in both experiments, coincidences with γ-58 were not recorded in the former experiment whereas they were in the latter and these events occupied most of the tape. The spectrum in coincidence with γ-238 obtained from the planar-coaxial experiment is shown in the lower portion of Fig. 6-12. The intensity of γ-618 calculated from these data is in agreement with the values already quoted. It is shown here for comparison with the upper portion of Fig. 6-12 which shows the spectrum in coincidence

Fig. 6-11

Net coincidence spectrum with γ- 238.
Data shown were recorded by coaxial detector
in the PDP-8 coaxial-coaxial experiment.
Random coincidences have not been subtracted.

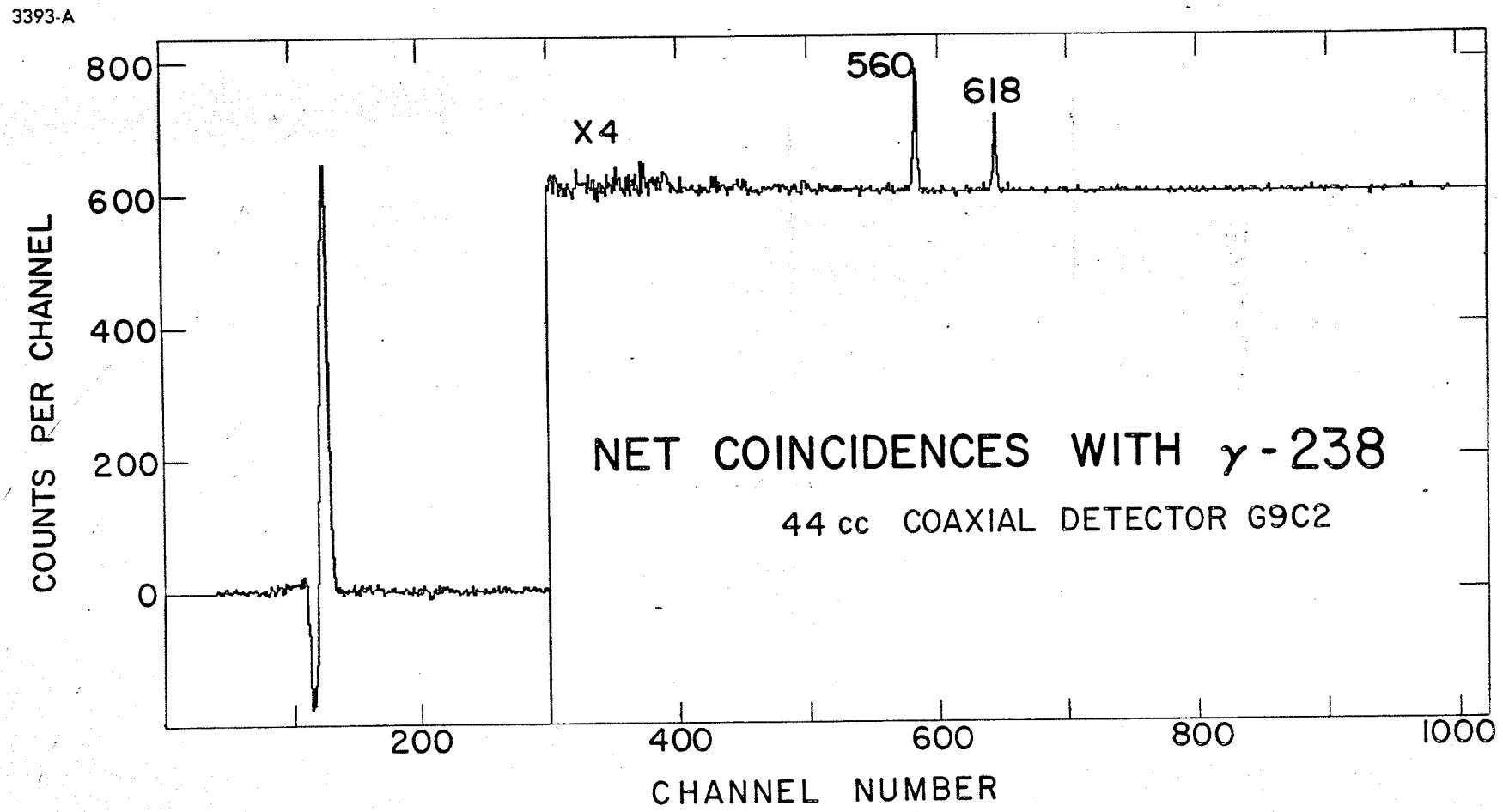
3393-A
800
600
400
200
0
COUNTS PER CHANNEL
560
618
X4
NET COINCIDENCES WITH γ-238
44 cc COAXIAL DETECTOR G9C2
200
400
600
800
1000
CHANNEL NUMBER

Fig. 6-12

Upper portion: Net coincidence spectrum recorded by planar detector in coincidence with γ-560 in the coaxial detector.

Lower portion: Net coincidence spectrum recorded by the coaxial detector in coincidence with γ-238 in the planar detector.

3392-H

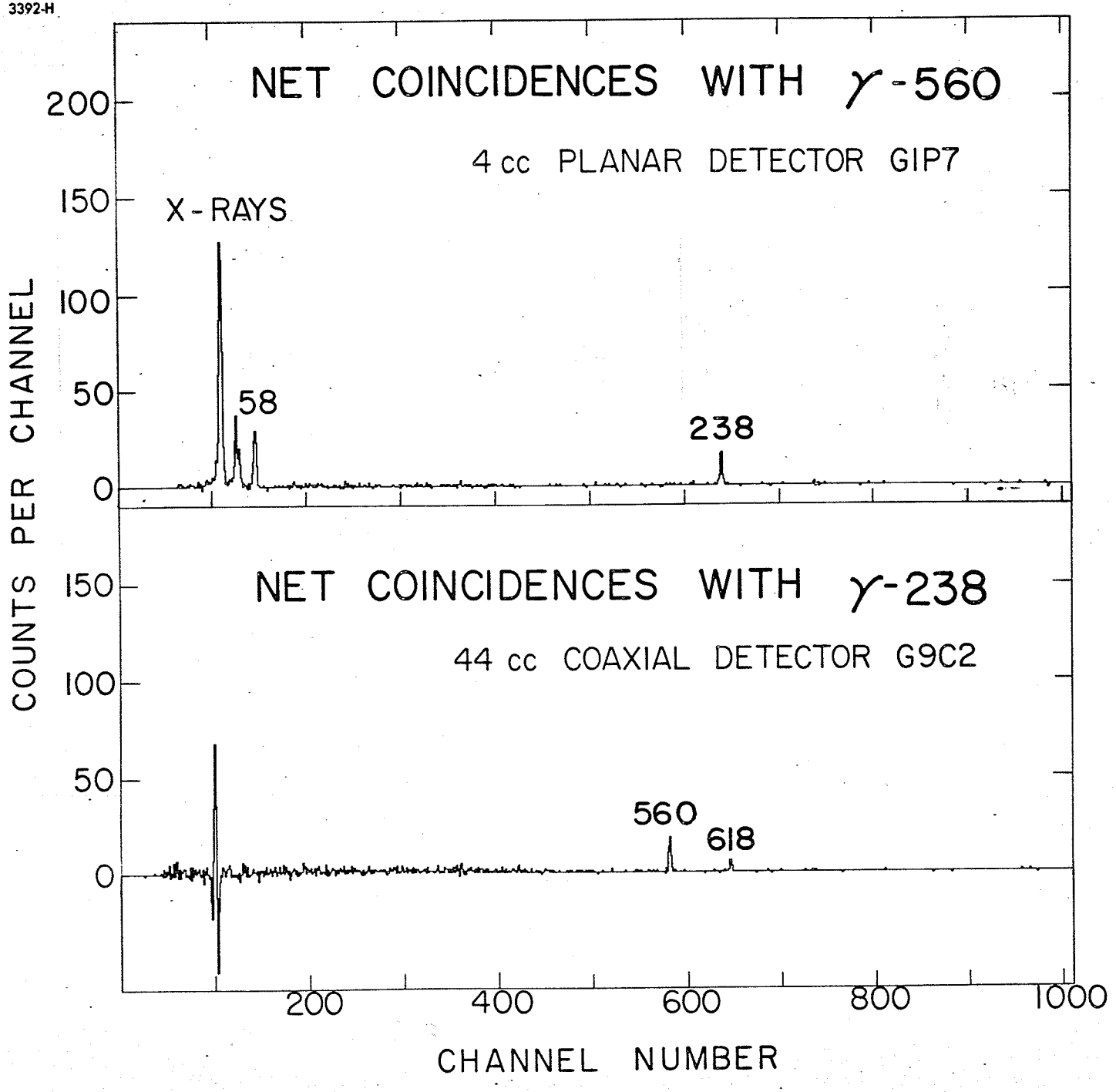
NET COINCIDENCES WITH γ-560
4 cc PLANAR DETECTOR GIP7
X-RAYS
58
238
NET COINCIDENCES WITH γ-238
44 cc COAXIAL DETECTOR G9C2
560
618
COUNTS PER CHANNEL
CHANNEL NUMBER
0
50
100
150
200
400
600
800
1000

Fig. 6-13

Coincidence spectra with γ-274 and γ-581. The data shown were recorded with the PDP-8 system during the coaxial-coaxial experiment and no random coincidences have been subtracted.

3394-K

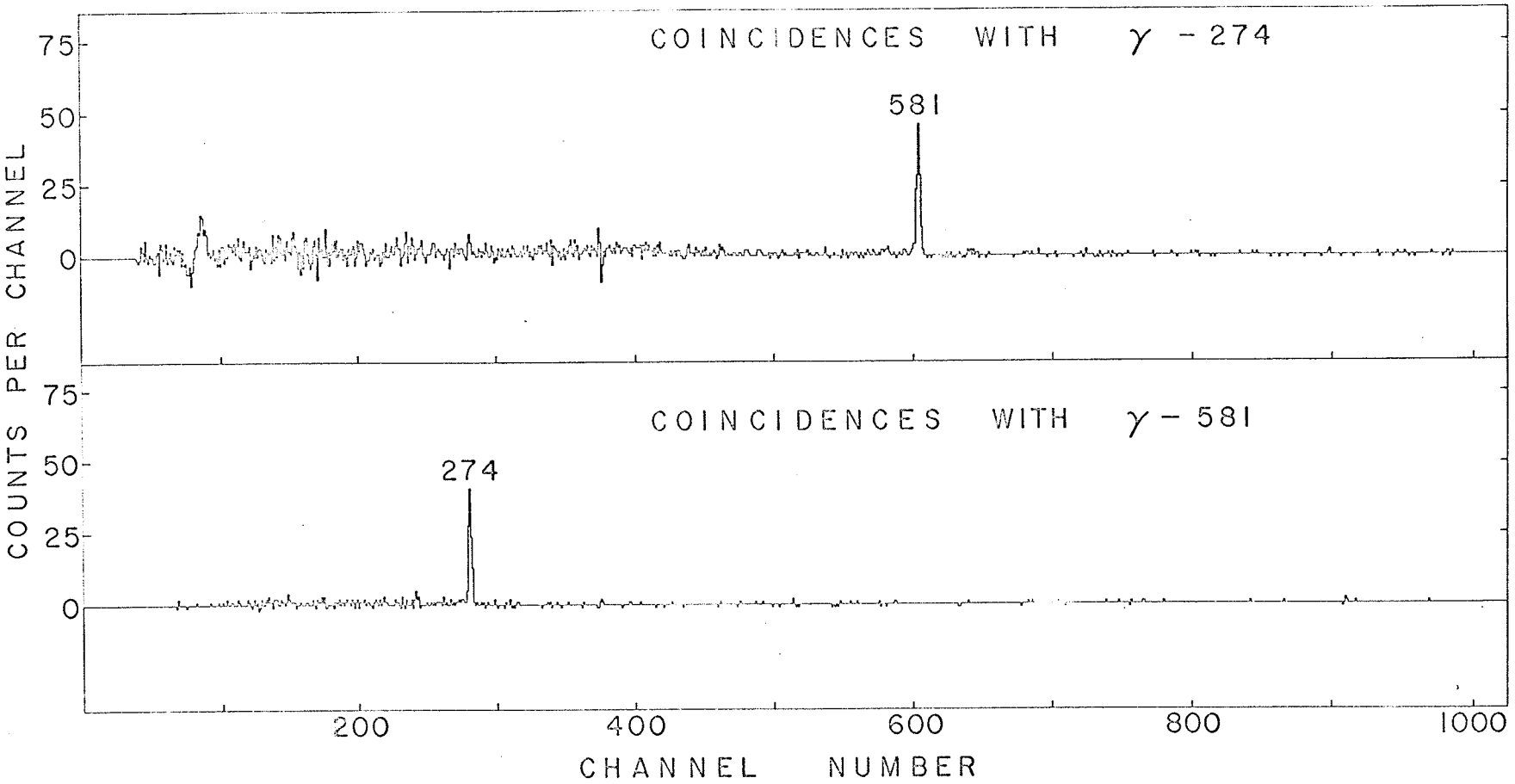
COINCIDENCES WITH γ - 274
581
COINCIDENCES WITH γ - 581
274
75
50
25
0
COUNTS PER CHANNEL
200
400
600
800
1000
CHANNEL NUMBER

with γ-560 This spectrum shows only γ-238 in coincidence with γ-560, but it should be remembered that γ-58 is not observed in the coaxial detector. The 560 keV transition is observed in the coincidence spectrum with γ-58 thus the 560 keV gamma-ray is fitted between the levels at 58.0 and 617.7 keV. The coincident pair (γ-238 and γ-560) therefore substantiates the existence of the level at 854.9 keV.

Further evidence for a level at 854.9 keV can be seen in Fig. 6-13. The upper portion of Fig. 6-13 shows the spectrum in coincidence with γ-274 while the lower portion shows the coincidence spectrum with γ-581. The spectrum in coincidence with γ-58 shows no evidence of either γ-274 or γ-581 so it is concluded that they form a coincidence pair which depopulates the 854.9 keV level to the groundstate via a level at 580.8 keV.

6.6 Level Scheme of ^{159}Tb

The energy levels in ^{159}Tb following the β-decay of ^{159}Gd are shown in Fig. 6-14. The intensity of the β-feed to the groundstate (63% per disintegration) was taken from the paper by Nielsen et al (Nielsen 1958) and the intensities of the other β-feeds were obtained from intensity balance of transitions feeding and de-exciting the levels. The log ft. values were calculated using the nomograph of Ver all et al (Verrall 1966). Table 6-II lists the properties of the gamma-ray transitions in ^{159}Tb. The multipolarities are taken from the references indicated in column 3 of this table.

The study of ^{159}Gd by Nielsen et al (Nielsen 1958) yielded a value of α_k (58) ≈ 6 which suggested a predominantly M1 character

Table 6-II

PROPERTIES OF GAMMA TRANSITIONS IN ^{159}Tb

Energy (keV)	Relative Gamma-Ray Intensity	Multipolarity	Ref.	Transition Intensity[1] % Per Disintegration
58.0	21±2	98.6%M1+1.4%E2	a	25.3
79.52	0.38±0.04	M1	b	0.22
137.4	0.06±0.01	E2		0.0125
210.9	0.165±0.025	M1-E2	c	0.023
226.2	1.96±0.10	E1	b	0.23
237.5	0.072±0.011	(M1)		0.010
274.2	0.054±0.013	(M1)		0.007
290.3	0.28 ±0.03	M1-E2	c	0.035
305.5	0.55 ±0.04	E1	d	0.064
348.1	2.0 ±0.15	M1-E2	d	0.24
363.3	100 ±5	E1	b,e	11.5
536.8	0.010±0.003	M1	c	0.0011
559.57	0.20±0.02	M1	c	0.0024
580.84	0.57±0.04	M1	c	0.066
616.5	0.02±0.005	(M1)[2]	c	0.0023
617.7	0.13±0.02	M1[2]		0.0150
674.2	0.0034±0.001	M1	c	0.0004
854.9	0.021±0.003			0.0024

References for multipolarity assignments:

a) Novakov 1964
b) Nielsen 1958
c) Diamond 1963
d) Persson 1964
e) Metzger 1959

1) Based upon 63% β-feed to ground state (ref. b).
2) Both members of the doublet are assumed to be M1.

Fig. 6-14

Level scheme of ^{159}Tb observed in the β-decay of ^{159}Gd.

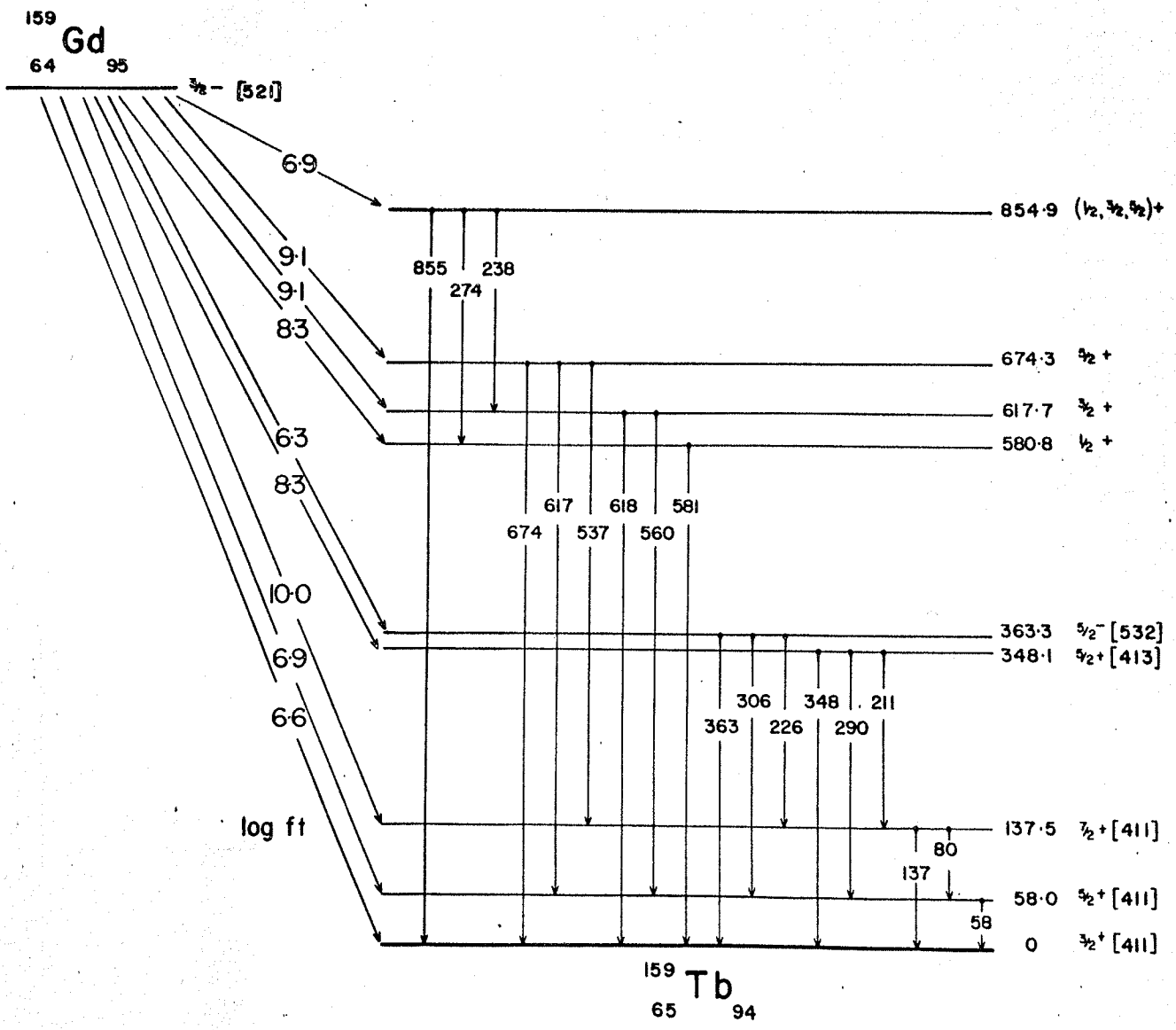
159 Gd 64 95
3/2− [521]
6·9
9·1
9·1
8·3
6·3
8·3
10·0
6·9
6·6
log ft
855
274
238
674
617
537
618
560
581
306
363
226
348
290
211
80
137
58
854·9 (1/2, 3/2, 5/2)+
674·3 5/2 +
617·7 3/2 +
580·8 1/2 +
363·3 5/2− [532]
348·1 5/2+ [413]
137·5 7/2+ [411]
58·0 5/2+ [411]
0 3/2+ [411]
159 Tb 65 94

for this transition. More recently Novakov and Hollander (Novakov 1964) have determined it to be 98.6% M1 + 1.4% E2 from a study of the L subshell ratios. This is in accord with the value of 99% M1 + 1% E2 reported by Ewan et al (Ewan 1963a).

The K/L ratio for γ-80, measured to be 6 ± 1 by Nielsen et al, is in agreement with the theoretical value of 7 for an M1 transition given by Sliv and Band (Sliv 1956). The groundstate of ^{159}Tb is known to have a spin of 3/2 (Baker 1955) and according to the Mottelson and Nilsson classification (Mottelson 1959) is interpreted as the 3/2 + [411] orbital. Angular correlation experiments by Subba Rao (Subba Rao 1962) have substantiated the spin sequence 3/2+, 5/2+, 7/2+ for the groundstate, 58.0 and 137.5 keV levels suggested by the predominantly M1 character of γ-58 and γ-80. Energy spacings indicate that the 58.0 and 137.5 keV levels are the 5/2+ and 7/2+ members of the ground-state rotational band. The Coulomb excitation experiments of Diamond and Stephens (Diamond 1963) revealed members of this band up to the 15/2+ level.

The conversion coefficient for the 348.1 keV transition has been measured by Persson (Persson 1964) to be 6.2 ± 1.2 x 10^{-2}. The theoretical values (Sliv 1956) for M1 and E2 are 5.9 x 10^{-2} and 3.1 x 10^{-2} respectively, which suggests that the 348 keV transition is predominantly M1, although an E2 admixture is possible. This transition was assumed by Persson to de-excite a level at 348.1 keV. This level has also been seen in the electron capture decay of 144d ^{159}Dy by Ryde et al (Ryde 1963). Their results indicated that the level feeds members of the ground-state rotational band through three transitions; γ-348, γ-290 and γ-211

all of which have an M1, E2 assignment with unknown mixing ratios. These three transitions are also seen in the present work and a comparison of the relative intensities with those of Ryde is given in Table 6-III.

Table 6-III

Gamma-Ray Energy	Relative Intensities	
	$^{159}Dy \rightarrow ^{159}Tb$	$^{159}Gd \rightarrow ^{159}Tb$
348.1	1,0 ± 0.1	1.0 ± 0.075
290.3	0.13± 0.04	0.14± 0.015
210.9	0.04± 0.02	0.082± 0.012

The possible spin values for the 348.1 keV level are 3/2, 5/2 or 7/2 with a positive parity assignment. This level has been classified by Ryde as the $5/2 + [413]$ Nilsson orbital since there are no single particle states with spin 3/2 or 7/2 in this energy region.

The 363.3 keV level is seen to de-excite to members of the groundstate rotational band with the emission of 363.3, 305.5 and 226.2 keV gamma-rays. The K-conversion coefficient of the 363.3 keV gamma-ray has been measured by Nielsen et al (Nielsen 1958) and the multipolarity has been assigned as E1. Nielsen's measurements also put an upper limit on the intensity of the conversion lines for γ-226 which corresponds to an E1 assignment for this transition. In a similar manner Persson (Persson 1964) put an upper limit on the conversion intensity of γ-305 and an E1 character is suggested for this transition. Since this

level de-excites to states with spin 3/2+ and 7/2+ by E1 transitions, its spin and parity are therefore 5/2- and it has been classified as the 5/2- [532] Nilsson orbital.

The levels at 580.8, 617.7 and 674.3 keV are seen to feed the ground-state rotational band. Persson (Persson 1964) and Funke (Funke 1965) both reported the existence of these levels and gave their energies as 580, 616 and 674 keV. Persson was unable to say whether the transition they saw at 616 keV should be fitted between the 616 keV level and the ground state, or between the 674 keV and 58 keV levels. Funke's coincidence data indicated that the 616 keV transition was complex with a branching ratio of about 7 or 8 to 1, the stronger transition feeding the ground state. The present investigation shows that the line in question is in fact a doublet with energies 616.5 and 617.7 keV, the latter being the more intense feed to the ground state. The ground-state transition from 674.3 keV level, following the β-decay of ^{159}Gd is reported here for the first time.

These three levels have also been seen in the Coulomb excitation experiments on ^{159}Tb reported by Diamond and Stephens (Diamond 1963). They reported that the lines at 536, 560 and 580 keV exhibited symmetrical Doppler broadening. This indicates lifetimes of about 5×10^{-13} secs which suggests M1 transitions. Their measurement of the average K-conversion coefficients for these transitions also indicated that the group was mainly M1. For these reasons a positive parity assignment has been made for the levels at 580.8, 617.7 and 674.3 keV. The log ft. values for the β-transitions feeding these levels, calculated from the present results, are consistent with this assignment.

The level at 854.9 keV was first introduced by Funke et al (Funke 1965) as a level at 860 keV. The present coincidence data with γ-238 and γ-274 confirm the existence of this level. The log ft. value of 6.9 for the β-feed to this level indicates that it is most probably a first forbidden transition. This limits the spin values for the 854.9 keV level to 1/2, 3/2 or 5/2 with positive parity.

6.7 E1 Transition Intensities

The intensity ratios for electromagnetic transitions between levels of two rotational bands in axially deformed nuclei should follow the relationship proposed by Alaga (Alaga 1954) namely

$$\frac{B(L,\ I_i \rightarrow I_f)}{B(L,\ I_i \rightarrow I_f')} = \frac{\langle I_i\ L\ K_i\ K_f\text{-}K_i \mid I_i\ L\ I_f\ K_f\rangle^2}{\langle I_i\ L\ K_i\ K_f'\text{-}K_i \mid I_i\ L\ I_f'\ K_f\rangle^2}$$

where $B(L,\ I_i \rightarrow I_f)$ is the reduced transition probability for the transition $I_i \rightarrow I_f$ and $\langle I_i\ L\ K_i\ K_f\text{-}K_i \mid I_i\ L\ I_f\ K_f\rangle$ is the Clebsch-Gordan coefficient for the addition of angular moments I_i and L to form I_f. This relationship is observed to be true in a large number of cases, but for transitions which violate the asymptotic selection rules (Mottleson 1959), deviations of up to two or three orders of magnitude occur. For the case of dipole transitions with $\Delta K = \pm 1$, these deviations are very large, whereas for transitions with $\Delta K = 0$, the deviations are about 10 to 20%.

Of particular interest in the decay of ^{159}Gd are the intensities of the E1 transitions which de-excite the 5/2- [532] level to members of the rotational band built upon the 3/2+[411] ground state. The experimental intensities for γ-363:γ-306:γ-274

are in the ratio 100:0.55:2.0 whereas the theoretical ratios based upon the Alaga formula are 100:26:1.7. The asymptotic selection rules for E1 transitions (Mottleson 1959) are given in Table 6-IV. These clearly show that the selection rule for Δn_z is violated for the transitions in ^{159}Gd.

Table 6-IV

Transition Multipolarity	ΔK	ΔN	Δn_z	$\Delta\Lambda$	$\Delta\Sigma$
E1	± 1	$+1,-1$	0	± 1	0
	0	$+1$	± 1	0	0

It has been proposed by Grin and Pavlichenkov (hereafter abbreviated to GP) (Grin 1965) that the reason for the large deviations from Alaga's intensity ratios for $\Delta K = \pm 1$ may be associated with the action of Coriolis forces. This interaction is small in strongly deformed nuclei and does not alter significantly the probability for allowed transitions, but it may be substantial in the case of "forbidden" transitions.

The Coriolis forces produce a coupling between the rotational and intrinsic motion. The interaction Hamiltonian has the form

$$H' = -\frac{\hbar^2}{2J}\,(I_+ j_- + I_- j_+)$$

where $I_+ = I_1 \pm iI_2$ and $j_\pm = j_1 \pm ij_2$, $\vec{I}$ being the total angular momentum and $\vec{j}$ the angular momentum of the odd nucleon. This coupling is small when the collective frequency is very much

larger than the single particle frequency, and is neglected in first approximation. Only the diagonal terms of this operator are taken into account when the energy of the system is calculated, and these occur only for the case of $\Omega = \frac{1}{2}$.

When the operator is considered as a perturbation, the off diagonal matrix elements are given by (Prior 1958)

$$\langle I'K'\Omega' \mid I_+j_- + I_-j_+ \mid IK\Omega\rangle = \sqrt{(I+K)\ (I-K+1)}\ \ \delta_{I'I}\delta_{K'K-1}\langle f|j_-|i\rangle$$

$$\langle I''K''\Omega'' \mid I_+j_- + I_-j_+ \mid IK\Omega\rangle = \sqrt{(I-K)\ (I+K+1)}\ \ \delta_{I''I}\delta_{K''K+1}\langle f|j_+|i\rangle$$

where f and i are the final and initial particle states. These expressions show that the Coriolis forces may couple states which have the same value of I but values of K differing by ±1.

GP have investigated the conditions under which E1 transition intensities may differ radically from Alaga's rules. They point out that the transition must be forbidden by the asymptotic selection rules but the matrix elements of j± and the electromagnetic transition operator in the admixture must be allowed. Using the wave functions given by Nilsson (Nilsson 1955), Prior (Prior 1958) has examined the selection rules for the operator j± connecting the intrinsic wave function of the groundstate with the admixture wave functions. On the basis of these selection rules, GP show that for the transitions of interest in the present work ($\Delta K = \pm 1$, $\Delta N = \pm 1$, $\Delta n_z = \pm 2$, $\Delta\Lambda = \pm 1$, $\Delta\Sigma = 0$), the admixture transitions always contain transitions allowed by the asymptotic quantum numbers. They therefore point out that these transitions should show large deviations from Alaga's rule. It should be pointed out that these deviations exist only for the one type of transition considered. It is possible to have twice forbidden E1 transitions with different changes in asymptotic quantum numbers for which $\Delta K = \pm 1$ transitions show no deviation from Alaga's predictions.

GP have derived theoretical expressions for the transition probabilities for electromagnetic transitions. For the case where $\Delta K = \pm 1$, the ratios of the reduced transition probabilities for electromagnetic dipole radiations are given by

$$\eta_1 (I,K,\Delta K) = \frac{B(1,Ikn \rightarrow Ik'n')}{B(1,Ikn \rightarrow I-1,k'n')} \quad \eta_2 (I,K,\Delta K) = \frac{B(1,Ikn \rightarrow I+1k'n')}{B(1,Ikn \rightarrow Ik'n')}$$

For $\Delta K = \pm 1$ these ratios depend upon one parameter and are given by

$$\eta_1 (I,K,\pm 1) = \eta_1^o (I,K,\pm 1) \left[1 - IZ_{\pm}(K)\right]^{-2}$$

$$\eta_2 (I,K,\pm 1) = \eta_2^o (I,K,\pm 1) \left[1 - IZ_{\pm}(K)\right]^{2}$$

where $\eta_1^o (I,K,\Delta K) = \frac{\langle I1;K\ \Delta K | IK' \rangle^2}{\langle I1;K\ \Delta K | I-1K' \rangle^2}$ $\eta_2^o (I,K,\Delta K) = \frac{\langle I1,K\ \Delta K | I+1K' \rangle^2}{\langle I1,K\ \Delta K | IK' \rangle^2}$

and $Z_{\pm}(K)$ is a function involving matrix elements with the electromagnetic transition operator.

The value of Z can be determined from one of the experimental ratios and this value used to predict the other ratio. Since the reduced transition probabilities depend quadratically on the parameter Z, two values of Z are obtained. The calculated value of η_1 for both these values of Z are shown in Table 6-V. The value of Z quoted by GP, calculated from the experimental data of Subba Rao (Subba Rao 1962), was chosen so that it best explained the experimental results. Using this criterion and a value of Z calculated from the present data, the agreement between the calculated and experimental value of η_1 can be seen to be excellent. Either value of Z gives theoretical results for this ratio which are closer to the experimental value than that predicted by Alaga.

Grin and Pavlichenkov have compared their results with the experimental data from several isotopes and have found good agreement. This tends to suggest that the observed deviations from Alaga's rules in ^{159}Tb are connected with the Coriolis coupling of rotational and

Table 6-V

RATIOS OF REDUCED E1 TRANSITION PROBABILITIES IN ^{159}Tb

Single Particle Transition	η_1 ($\times 10^{-3}$)			η_2			Z
	Experimental	Alaga	Grin	Experimental	Alaga	Grin	
	$14^{(1)}$	430	13	$5.7^{(1)}$	0.17	--	-1.95
			72				+1.38
5/2 532 → 3/2 411							
	$9.2\pm0.9^{(2)}$	430	9.1	$8.78\pm0.8^{(2)}$	0.17	--	-2.35
			36.0				+1.78

(1) B.N. Subba Rao Nucl. Phys. 36 (1962) 342

(2) Present work

intrinsic motion.

6.7 High Energy Levels in ^{159}Tb

Diamond and Stephens (Diamond 1963) have interpreted the levels at 580.8, 617.7 and 674.3 keV as members of a K = ½ rotational band. Only by such an interpretation can a reasonable value be obtained for the rotational constant and they give the value of the decoupling constant as a = +0.054±0.012. As mentioned previously the transitions from these levels are predominantly M1 in character. A comparison of the experimental branching ratios, derived from the present work, with the theoretical predictions (Alaga 1955) for M1 transitions is given in Table 6-VI, which shows them to be in fairly good agreement.

Table 6-VI

Branching Ratios for Transitions From K= ½ Band

	Theoretical	Experimental
$\frac{B(M1;\ 5/2 \rightarrow 5/2)}{B(M1;\ 5/2 \rightarrow 7/2)}$	0.96	1.32 ± 0.42
$\frac{B(M1;\ 5/2 \rightarrow 3/2)}{B(M1;\ 5/2 \rightarrow 7/2)}$	0.14	0.17 ± 0.06
$\frac{B(M1;\ 3/2 \rightarrow 3/2)}{B(M1;\ 3/2 \rightarrow 5/2}$	0.67	0.48 ± 0.11

The K= ½ band could be interpreted as a rotational band built upon the ½+[411] single particle state, which is expected in this region, or the K_o-2 γ-vibrational level of the groundstate. For several reasons the latter assignment is the one preferred by Diamond and Stephens. They point out that the experimental B(E2) values for Coulomb exciting the members of this band are larger

than would be expected if the 581 keV level were a single particle state. They also give the ratios B(E2; 3/2 → 1/2):B(E2; 3/2 → 3/2): B(E2; 3/2 → 5/2) as 1.0: 0.50±0.21: 0.66±0.21. The large errors were due to the uncertainty in the branching of γ-617. Using the information obtained in the present work about the 617 keV doublet, the above B(E2) ratios are 1.0: 0.66±0.2: 0.50±0.15. This should be compared to the theoretical values of 1.0: 0.91: 0.40 given by Lütken and Winther (Lütken 1963). Diamond and Stephens attribute this discrepancy to Coriolis coupling with the groundstate band which is possible since $\Delta|K| = 1$. They also point out that the band cannot be of pure vibrational character since M1 transitions from it would be forbidden.

The small value for the decoupling constant might also be explained on this basis, since the theoretical prediction for a pure vibrational band is zero. The $\frac{1}{2}+$ [411] band has been seen in ^{169}Tm and ^{171}Tm and the decoupling constant in these cases was found to be -0.76 and -0.86 respectively (Mottelson 1959). This evidence therefore tends to support the contention that the 581 keV level is a γ-vibrational level.

As mentioned in sec. 6-5, the spin of the 854.9 keV level is limited to 1/2, 3/2 or 5/2 and the parity assignment is positive. Nothing is known about the multipole character of the transitions de-exciting this level and either an M1 or E2 assignment would be consistent with their positioning in the level scheme. However the fact that the 854.9 keV state de-excites to levels with spins of 3/2+ and $\frac{1}{2}+$ but not to 5/2+ or 7/2+ levels suggests that the $\frac{1}{2}+$ assignment might be preferred for this level, the dominant mode of de-excitation then being M1.

If the ½+ assignment to this level is for the moment accepted, then an interesting point arises regarding the nature of this level. As previously stated, the ½+ [411] single particle level is expected in this region (Nilsson 1955). However the Coulomb excitation experiments of Diamond and Stephens (Diamond 1963) revealed gamma-rays with energies of 920, 949, 965 and 978 keV which they interpreted as originating from the 3/2+, 5/2+ and 7/2+ members of a K= ½ rotational band built upon a level at 971 keV. They did not observe a 971 keV transition but point out that it would have been obscured by the transitions at 965 and 978 keV. They obtained values of 12.0 keV for the rotational constant ($\hbar^2/2J$) and -0.81 for the decoupling constant which do not seem unreasonable when compared with the values for ^{169}Tm and ^{171}Tm (12.3 keV, a = -0.76; 12.0 keV, a = -0.86, Mottelson 1959). If this interpretation is correct, then it is difficult to find an explanation for the nature of the 854.9 keV level.

Another interpretation however might be possible and more insight into this may be gained by comparing the level schemes of ^{157}Tb and ^{159}Tb as shown in Fig. 6-15. The ^{157}Tb level scheme is taken from the work of Persson et al (Persson 1963). The similarity between the isotopes is readily apparent. The 992 keV transition was seen by Persson to have a high internal K-conversion coefficient which he attributed to a mixture of E0 and E2 multipoles. This mixture of multipolarities is expected in transitions which de-excite β-vibrational levels and Persson therefore suggests that this level may be the groundstate β-vibrational level with K= 3/2.

Since two gamma-rays are seen by Diamond and Stephens to de-excite their proposed level at 979 keV, it can be taken that this

Fig. 6-15

Comparison of the energy levels in ^{157}Tb and ^{159}Tb.

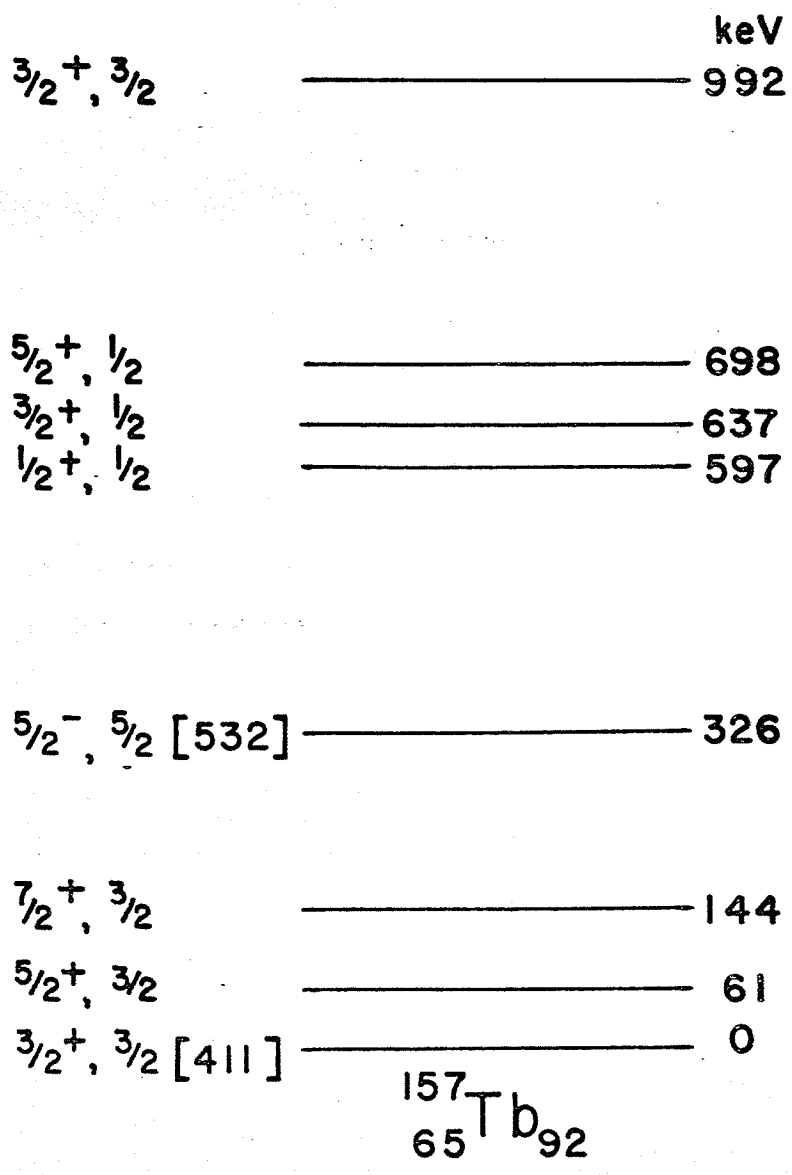
keV
3/2+, 3/2
992
5/2+, 1/2
698
3/2+, 1/2
637
1/2+, 1/2
597
5/2−, 5/2 [532]
326
7/2+, 3/2
144
5/2+, 3/2
61
3/2+, 3/2 [411]
0
157 65Tb92

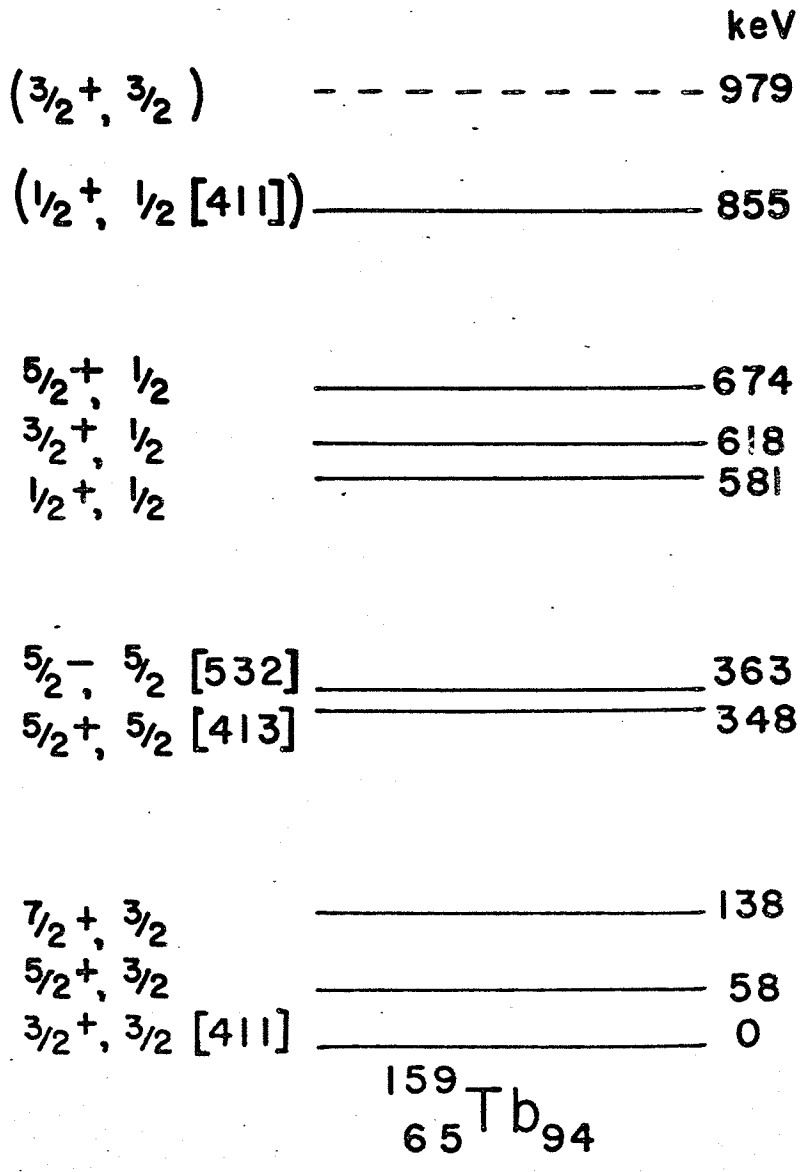
keV
(3/2+, 3/2)
979
(1/2+, 1/2 [411])
855
5/2+, 1/2
674
3/2+, 1/2
618
1/2+, 1/2
581
5/2−, 5/2 [532]
363
5/2+, 5/2 [413]
348
7/2+, 3/2
138
5/2+, 3/2
58
3/2+, 3/2 [411]
0
159 65Tb94

level is fairly well established. Furthermore, since these gamma-rays exhibited symmetrical doppler broadening and hence lifetimes which suggest that they are predominantly M1 transitions, it is possible for this level to have a spin and parity assignment of 3/2+. In analogy to the case of ^{157}Tb, it might therefore be postulated that this level is the corresponding ground - state β-vibrational level. This would then permit the level at 854.9 keV to be interpreted as the $\frac{1}{2}$+ [411] Nilsson state.

However it should be re-iterated that this is only one possible hypothesis and should by no means be taken as having been established. The difficulties with this interpretation are the predominantly M1 mode of de-excitation, (since M1 transitions are forbidden for pure vibrational bands), the reasonable values obtained for the rotational and decoupling parameters and the fitting of the observed transitions at 945 and 965 keV into the level scheme. From the experimental data available at this time, it is not possible to give an unequivocal assignment to the nature of the 854.9 keV level.

REFERENCES

Abdul-Malek A. and Naumann R.A. 1968 Nucl. Phys. A106 225

Alaga G., Alder K., Bohr A. and Mottelson B.R. 1955 Dan. Mat. Fys. Medd. 29 No. 9

Baker J.M. and Bleaney B. 1955 Proc. Phys. Soc. 68 257

Balodis M.K., Kramer N.D., Prokof'ev P.T. and Fainer U.M. 1966 Soviet Journal Nucl. Phys. 3 No. 2 141

Bashandy E. and El-Haliem A. Abd. 1966 Atomkem 11 316

Bogolyubov N.N. 1958 J.E.T.P. 34 58

Blankenship J.L. and Nowlin C.H. 1966 I.E.E.E. Trans. Nucl. Sci. NS-13 No. 3, 495

Bromley D.A. 1961 Proc. Asheville Conf. NAS-NRC Publication 871 P.61

Bromley D.A. 1962 I.R.E. Trans. Nucl. Sci. NS-9 No. 3,135

Castro-Faria N.V. de and Lévesque R.J. 1966 I.E.E.E. Trans. Nucl. Sci. NS-13 No. 3,363

Chasman C. and Ristenen R.A. 1965 Nucl. Inst. and Methods 34 250

Clarkson J.E., Diamond R.M., Stephens F.S. and Perlman I 1967 Nucl. Phys. A93 272

Comite G., Ricci R.A. and Speranza R. 1965 quoted by Ricci et al Nuovo Cim. 37 1752

Das Gupta S. and Gunye M.R. 1964 Can. J. Phys. 42 762

Davydov A.S. and Fillipov G.F. 1958 Nucl. Phys. 8 237

Davydov A.S. 1961 Nucl. Phys. 24 682

Dearnaley G. and Northrop D.C. 1963 "Semiconductor Counters for Nuclear Radiations" published by E. and F.N. Spon Ltd., London

Dearnaley G. and Northrop D.C. 1966 2nd edition of above book

Dearnaley G. 1967 Contemp. Phys. 8 No. 6, 607

Diamond R.M., Elbek B. and Stephens F.S. 1963 Nucl. Phys. 43 560

Ewan G.T. 1963a A.E.C.L. Progress Report PR-P-58 Sec. 3.3.2

Ewan G.T. and Herrlander C.J. 1963b A.E.C.L. Progress Report PR-P-57 Sec. 3.3.1

Ewan G.T. and Tavendale A.J. 1964a Can. J. Phys. 42 2286

Ewan G.T. and Tavendale A.J. 1964b Nucl. Inst. and Methods 26 183

Ewan G.T. 1964c Bull. Am. Phys. Soc. 9 Ser. 2, 47.Chalk River Report A.E.C.L. - 1960

Ewan G.T., Graham R.L. and McKenzie I.K. 1966a I.E.E.E. Trans. Nucl. Sci. NS-13 No. 3, 297

Ewan G.T., Malm H.L. and Fowler I.L. 1966b Lithium-Drifted Germanium Detectors (I.A.E.A. Vienna) P.102

Ewan G.T. 1968 Private Communication. To be published in "Progress in Nuclear Techniques and Instrumentation".

Fowler I.L. and Toone R.J. 1966 Chalk River Report A.E.C.L. - 2569

Freck D.V. and Wakefield J. 1962 Nature 93 669

Funke L., Graber H., Kaun K.H., Sodan H. and Werner L. 1965 Nucl. Phys. 43 560

Gerschel G., Pautrat M., Ricci R.A. Teillac J. and Van Horenbeeck J. 1964 Congrès International de Physique Nucléaire, Paris

Gerschel G., Pautrat M., Ricci R.A., Teillac J. and Van Horenbeeck J. 1965 Nuovo. Cim. 37 No. 4, 4472

Gibson W.M., Miller G.L. and Donovan P.F. 1965 in Alpha-Beta and Gamma-Ray Spectroscopy edited by K. Seigbahn (North Holland Publ. Co., Amsterdam) 1,345

Goulding F.S. 1965 U.C.R.L. 16231. Lectures given at Herceg-Novi, Yugoslavia, August 1965

Goulding F.S. 1966 Nucl. Inst. and Methods 43, 1

Goulding F.S., Landis D.A. and Pehl R.H. 1967 U.C.R.L. 17560 paper presented at Gatlinburg Conference on Semiconductor Detectors and Associated Circuits May 1967

Graham R.L., Ewan G.T. and Geiger J.S. 1960 Nucl. Inst. and Methods 9, 245

Graham R.L., McKenzie I.L. and Ewan G.T. 1966 I.E.E.E. Trans. Nucl. Sci. NS-13 No. 1, 72.Chalk River Report A.E.C.L. 2505

Grin Y.T. and Pavlichenkov I.M. 1965 Nucl. Phys. 65 686

Hamilton J.H. 1966 "Internal Conversion Processes" publ. by Academic Press, New York

Hankla A.M., Hamilton J.H. and Stockendal R.V. 1963 Ark. f. Fys. 24 429

Hansen O. and Nathan O. 1963 Nucl. Phys. 42 197

Hatch E.N., Boehm F., Marmier P. and DuMond J.W.M. 1955 Phys. Rev. 104 745

Haverfield A.J. 1966 Thesis University of California Berkeley UCRL-16969

Heath R.L., Black W.W. and Cline J.E. 1966 I.E.E.E. Trans Nucl. Sci. NS-13, No. 3, 445

Hollander J.M. 1966 Nucl. Inst. and Methods 43 65

Hoskin, J.C. 1955 Proc. of the Eastern Joint Computer Conf. Nov. 7-9, Boston, p 39

Hsu H.H. and Emery G.T. 1968 Bull. Am. Phys. Soc. Ser. II 13 69

Johansen H.S., Jorgensen M., Nielsen O.B. and Sidenius G. 1964 Physics Letters 8 No. 1 61

Jorgensen M., Nielsen O.B. and Sidenius G. 1962 Physics Letters 1 No. 8 321

Jungclassen H. 1965 Kernergie 8 514

Julian G.M. and Jha S. 1964 Bull. Am. Phys. Soc. 9 No. 6 663

Julian G.M. and Jha S. 1967 Nucl. Phys. A.100 392

Julian G.M. 1968 Private Communication

Kerman A.K. 1956 Dan. Mat. Fys. Medd. 30 No. 15

Kristenson L., Jorgensen M., Nielsen O.B. and Sidenius G. 1964 Physics Letters 8 No. 1 57

Lutken H. and Winther A. 1963 reported by Diamond et al Nucl. Phys. 43 560

Maier B.P.K. 1965 Z.Physik 184

Malm H.L. and Fowler I.L. 1965 I.E.E.E. Trans. Nucl. Sci. NS-13 No. 1, 62.Chalk River Report A.E.C.L. - 2504

Malm H.L. 1966 I.E.E.E. Trans. Nucl. Sci. NS-13 No. 3, 285. Chalk River Report A.E.C.L. - 2550

Mann H.M., Haslett J.W. and Janarek F.J. 1962 Proc. Third Annual Nucl. Eng. Education Conf. Argonne National Lab.

Mann H.M., Bilger H.R. and Sherman I.S. 1966 I.E.E.E. Trans. Nucl. Sci. NS-13 No. 3,252

Marion G. 1968 To be published.

Marshalek E., Persson L.W.U. and Sheline R.K. 1963 Rev. Mod. Phys. 35 108

McKenzie I.L. and Ewan G.T. 1961 I.R.E. Trans. Nucl. Sci. NS-8 No. 1, 50

Merritt J.S. and Taylor J.G.V. 1965 Analytical Chem 37 351

Metzger F.R. and Todd W.B. 1959 Nucl. Phys. 13 177

Mize J.P., Bunker M.E. and Starner J.W. 1956 Phys. Rev. 103 182

Mottelson B.R. and Nilsson S.G. 1959 Mat. Fys. Skr. Dan. Vid. Selsk. 1 No. 8

Moszkowski S.A. 1966 in "Alpha-Beta and Gamma-Ray Spectroscopy" edited by K. Seigbahn (North Holland Publ. Co., Amsterdam)

Nilsson S.G. 1955 Dan. Mat. Fys. Medd. 29 No. 16

Nielsen K.O., Nielsen O.B. and Skilbreid O. 1958 Nucl. Phys. 7 561

Novakov T. and Hollander J.M. 1964 Nucl. Phys. 60 593

Nuclear Data Sheets compiled by K. Way et al (National Academy of Sciences - National Research Council, Washington, D.C.)

Patwardhan P.K. 1964 Nucl. Inst. and Methods 31 169

Pehl R.H., Landis D.A. and Goulding F.S. 1966 I.E.E.E. Trans. Nucl. Sci. NS-13 No. 3,274

Pehl R.H., Goulding F.S., Landis D.A. and Lenzlinger M. 1967 U.C.R.L. - 17770

Pell E.M. 1960 J. Appl. Phys. 31 291

Persson L., Ryde H. and Oelsner - Ryde K. 1963 Ark. f. Fys. 24 No. 34,451

Persson L. 1964 Ark. f. Fys. 25 No. 21,307

Peterson F.R. and Shugart H.A. 1962 Phys. Rev. 126 252

Pigneret J., Samueli J.J. and Sarazin A. 1966 I.E.E.E. Trans. Nucl. Sci. NS-13 No. 3, 306

Preston M.A. 1962 "Physics of the Nucleus" Publ. by Addison-Wesley Publ. Co.

Prior A.C. 1960 J. Phys. Chem. Solids 12, 175

Prior O. 1958 Ark. f. Fys. 14 No. 28,451

Pyatov N.I. and Chernyshev A.S. 1964 Dubna Report JINR-P-1338. Also Akad Nauk. SSSR Ser. Fiz. 28 1173 (English translation 28 1073)

Raeside D.E., Reidy J.J. and Wiedenbeck M.L. 1967 Nucl. Phys. A98 54

Reising R. and Pate B.D. 1965 Nucl. Phys. 65 609

Ricci R.A., Comite G. and Speranza R. 1965 Nuovo Cim. 37 No. 4, 4468

Rose M.E., Goertzel H., Spinard B.J., HarrJ. and Strong P. 1951 Phys. Rev. 83, 79

Rose M.E. 1958 Internal Conversion Coefficients (North Holland Publ. Co., Amsterdam)

Rose M.E. 1965 "Theory of Internal Conversion" in Alpha-Beta and Gamma-Ray Spectroscopy edited by K. Seigbahn (North Holland Publ. Co., Amsterdam)

Ryde H., Persson L. and Oelsner - Ryde K. 1963 Ark. f. Fys. 23 No. 20,195

Schriber S.O. and Hogg B.G. 1963 Nucl. Phys. 48 647

Sheline R.K., Sikkeland T. and Chanda R.N. 1961 Phys. Rev. Letters 7 No. 12 446

Sliv L.A. and Band I.M. 1956 Tables of Internal Conversion Coefficients (Academy of Sciences U.S.S.R. Press., Moscow)

Sliv L.A. and Band I.M. 1965 "Tables of Internal Conversion Coefficients" in Alpha-Beta and Gamma-Ray Spectroscopy edited by K. Seigbahn (North Holland Publ. Co.)

Smith H.L. and Hoffman D.C. 1956 J. Inorg. and Nuclear Chem. 3 243

Smith K.F. and Cline J.E. 1966 I.E.E.E. Trans. Nucl. Sci. NS-13 No. 3, 468

Soloviev V.G. 1961 Mat. Fys. Skr. Dan. Vid. Selsk. 1 No. 11

Soloviev V.G. 1963 "Selected Topics in Nuclear Theory" Publ. by I.A.E.A. Vienna

Soloviev V.G., Vogel P. and Jungklassen G. 1966 JINR-E4-3051

Strauss M.G., Larsen R.N. and Sifter L.L. 1966 I.E.E.E. Trans. Nucl. Sci. NS-13, No. 3

Storm E., Gilbert E. and Israel H. 1958 Los Alamos Report L.A. 2237

Subba Rao B.N. 1962 Nucl. Phys. 36 342

Table of Isotopes 6th Edition 1967. Edited by Lederer C.M., Hollander J.M. and Perlman I. Publ. by J. Wiley and Sons.

Tavendale A.J. and Ewan G.T. 1963 Nucl. Instr. and Methods 25 183

Tavendale A.J. 1964a Electronique Nucléaire (E.N.E.A., Paris) 235

Tavendale A.J. 1964b I.E.E.E. Trans. Nucl. Sci. NS-11 No. 3,191

Tavendale A.J. 1965a Nucl. Instr. and Methods 36 325

Tavendale A.J. 1965b I.E.E.E. Trans. Nucl. Sci. NS-12 No. 1, 255

Tavendale A.J. 1966 I.E.E.E. Trans. Nucl. Sci. NS-13 No. 3,315

Verrall R.I., Hardy J.C. and Bell R.E. 1966 Nucl. Inst. and Methods 42 258

Van Wijngaarden W. and Connor R.D. 1964 Can. J. Phys. 42 504

de Waard H. 1955 Phys. Rev. 99 1045

Wanio K.M. 1965 Thesis - University of Michigan

Webb P.P. and Williams R.L. 1963 Nucl. Inst. and Methods 22 361

Wu C.S. and Moszkowski S.A. 1966 "Beta Decay" Published by Interscience Publishers

Zganjar E.F., Boyd H.W., Hamilton J.H., Newboldt W.B. and Herickhoff R.J. 1962 Bull. Am. Phys. Soc. Ser. II 7 566